QATAR UNIVERSITY

COLLEGE OF ENGINEERING

# INVESTIGATION OF THE SUITABILITY OF THE VIBRATION ACCEPTANCE CRITERIA FOR PROCESS PIPEWORK IN ASSESSING THE VIBRATION LEVELS OF THE FLOW-INDUCED FATIGUE FAILURE

BY

OMAR TWFIK SAAD MOHAMED SHADY

A Thesis Submitted to

the College of Engineering

in Partial Fulfillment of the Requirements for the Degree of

Master of Science in Mechanical Engineering

June 2021

# COMMITTEE PAGE

The members of the Committee approve the Thesis of
Omar Shady defended on 18/04/2021.

Dr. Jamil Renno
Thesis/Dissertation Supervisor

Professor Dr. Sadok Sassi
Committee Member

Approved:

Khalid Kamal Naji, Dean, College of Engineering

# ABSTRACT

SHADY, OMAR, T., Masters: June : [2021],

Masters of Science in Mechanical Engineering

Title: Investigation of the Suitability of the Vibration Acceptance Criteria for Process Pipework in Assessing the Vibration Levels of the Flow-Induced Fatigue Failure

Supervisor of Thesis: Jamil, Renno.

Process pipework is essential to the oil and gas industries. Usually, pipework is designed to satisfy static requirements. Often, vibration problems in process pipework are treated on an Adhoc basis. Pipework vibration can lead to the development of fatigue cracks/failures which lead to hydrocarbon leaks. The loss of containment of hydrocarbons could lead to environmental, human, or business disasters at best. A survey of all hydrocarbon leaks in the UK North Sea showed that the second reason (contributing around 25%) for all hydrocarbon leaks is fatigue failures. Fatigue usually happens on the branches welded to the main pipelines. It is impossible to avoid vibration-induced fatigue (VIF) in process pipework, but it can be minimized and monitored to avoid catastrophic failures and unplanned shutdowns which may negatively affect production and profits. The Vibration Acceptance Criteria, which were developed by the Energy Institute, have not been scientifically examined. It is therefore not possible to specifically determine appropriate vibration levels for all pipe geometries, configurations, and fittings by the Energy Institute criteria. In this thesis, the suitability of the Vibration Acceptance Criteria (VAC) in judging the vibration levels in process pipework is Investigated. This investigation was done using a random vibration Finite Element Analysis (FEA). This analysis was conducted on different

models with different geometric configurations to find the effect of geometrical changes on the suitability of the VAC. The output of this thesis shows that the length and the diameter of the run-pipe have a significant effect on the suitability is the VAC.

# DEDICATION

*This thesis is dedicated to my mother who is my greatest supporter and to my father who was and always will be my idol and motivation in this life. I also dedicate this thesis to my entire family.*

# ACKNOWLEDGMENTS

I would like to thank Dr. Jamil Renno for his tremendous support and engorgement which enabled me to gain a lot of experience in this area of science. I also acknowledge the financial support provided by the Qatar National Research Fund through the National Priorities Research Program under grant number NPRP 11S-1220-170112 and Qatar University Internal Grant QUCG-CENG-19/20-26.

# TABLE OF CONTENTS

LIST OF TABLES

LIST OF FIGURES

# CHAPTER 1: INTRODUCTION

This introductory section will present general information about some terms that will be used in this thesis which are important to know and understand before going through the thesis. The first term is hydrocarbons and their definition, composition, examples of hydrocarbons, and their impacts. The second term is metal fatigue where information about its history, the factors that affect fatigue behavior, the consequence of fatigue failure, the characteristics of low and high cycle fatigue, and its cycle phases will be presented. The third term is pipework and the standards used for it, pipework in the oil and gas industry, and pipe fatigue. Furthermore, the fourth term that is going to be introduced is weldolets, their manufacturing process, types, standards, benefits, and applications. Finally, this section concludes by presenting information about the most commonly used materials for process pipework in the O&G industry.

## 1.1.Hydrocarbons

A hydrocarbon is an organic compound made up of only atoms of hydrogen and carbon. Carbon requires four electrons to be intact, so it has precisely four bonds to create [1]. Another form of hydrocarbons is aromatic hydrocarbons, including alkanes, cycloalkanes, and alkyne-based compounds. Through bonding to themselves, hydrocarbons may create more complicated structures, such as cyclohexane. This is referred to as catenation. Nearly all hydrocarbons among crude oils, such as gasoline and natural gas, naturally occur. It is high in hydrogen and carbon atoms because crude oil is constructed from decomposed organic matter. These often exist in numerous trees and plants, producing a chemical dye called carotene, which can be contained in carrots and green leaves. Most of the natural raw rubber is composed of a hydrocarbon resin, 98 %; this is created when a chainlike molecule is shaped, comprising of many units that are joined together. Hydrocarbons are the most widely used organic compound on

the planet, and the main part of volatile organic compounds: they are perceived as the driving force of modern civilization because of the fossil fuels they make up. Such fuels are used for combustion, especially in applications for heating and engine fuel. Hydrocarbons such as butane and propane are used for internal combustion systems, in oil lamps, ovens, and lighters. Pentane is another hydrocarbon popular with all. Pentane becomes a liquid at room temperature when saturated; this liquid is used as an organic solvent, for transporting fuels and cleaning agents. The combustion properties of liquid hydrocarbons are relative to octane, i.e., petrol for internal combustion engines. Liquid hydrocarbons are classified as octane according to combustion properties, i.e., fuel for internal combustion engines in automobiles, buses, and lawnmowers. Examples of bigger hydrocarbon compounds are jet fuel, diesel fuel, and kerosene. The bigger the hydrocarbons, the denser the substance. Big hydrocarbons are often used for automotive lubrication and greases. Everything heavier than that, and they are like a wax or tar material, typically used in street or roofing. Thermal fracturing and fractional distillation of crude oils is the main cause of the above-mentioned hydrocarbons. However, the industrial refining of ethanol for the manufacturing of ethylene is another very common source. The produced ethylene is used in many hydrocarbons' chemical synthesis.

### *1.1.1. Impacts of Hydrocarbons Leaks and Spills*

A. Environmental Impact

Hydrocarbons do not pose a risk themselves. However, they undergo a chemical reaction when they are exposed to sunlight and/or nitrogen oxides. It is well known that in this industrial age the emissions and environmental damage by humans are harmful and a large part of these dangerous compounds is hydrocarbons. Crude oil, natural gas, and most chemicals are mainly made of hydrocarbons. The greenhouse

effect and degradation of the ozone layer are caused by all these substances. They also reduce plant photosynthesis and increase animal cancer rates. Oil spills are the most famous and hazardous type of hydrocarbon. Oil spills destroy the life of marine plants and kill and threaten hundreds, if not millions of animals every year.

B. Health Impact

There are many types of petroleum hydrocarbons such as natural gas, crude oil, tars, and asphalt [2]. The term "oil from the earth" or "rock oil" describes the word petroleum [3]. In our modern society, the oil employed in our daily lives plays a vital role. It is the primary source of energy for heating, transport, and processing. However, it is a raw material for plastic or synthetic rubber. Petroleum hydrocarbon (PHC) composition varies slightly depending on their source, but the toxic properties do hold. The greatest risk is with contaminants such as Benzene and Polycyclic Aromatic Hydrocarbons (PAHs). In compliance with the United States Environmental Protection Agency, the threat of leaking oil needs a combination of both hazard data and exposure details. The threat of contamination through skin contacts or digestion is related to a certain compound's ability to consume soil, and into vegetation by root absorption, which may lead it to eventually entering the food chain. These hydrocarbons contaminations increase human and animal cancer rates and the risk of respiratory disease. When poisonous contamination reaches the bloodstream, the results may be catastrophic. Benzene is a common oil and gas pollutant and has been linked to a blood cancer called leukemia in even small quantities. Studies have associated carbon monoxide, nitrogen oxides, and fluoride with arsenic, plum, and ozone with cardiac rates irregular, hypertension, allergic abnormal reactions, and heart disease [4].

## 1.2. Metal Fatigue

The most common and researched failure mechanisms since the last days of the industrial revolution have likely been fatigue. The mining and railways sectors have been responsible for modern fatigue science and the techniques and methodologies that we currently use. For example, the term "fatigue cycle" is analogous to cycles that are based on systems consisting of turning axels, gears, and chains. But the question of identifying what a cycle means in the sense of multiaxial charging is a challenge. Julius Albert (1829), the German mining director, is the first to document failure because of repeatedly small loads (compared with the ultimate tensile strength) [5]. He constructed the very first testing machine, figure 1: a crank connected to a waterwheel and a chain connecting the crank to a weight which was raised up and down until the chain had broken down. The test was conducted on an element at a constant amplitude, which determined the relation between loads and damage.

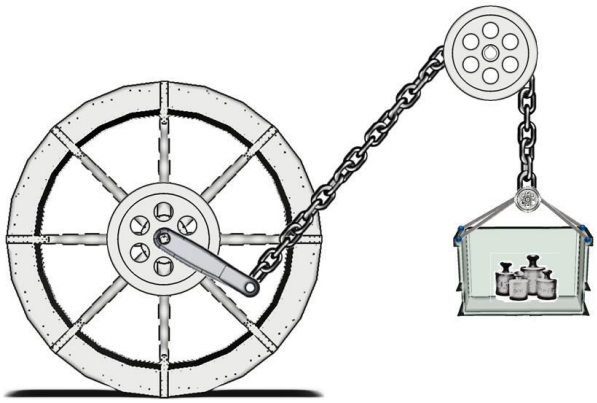

Figure 1. Albert's first fatigue test machine [5].

The Scottish engineer Rankine (1843) would note in the next decade that these failures started mostly on the notches of the railroad axes of where they perpetuated forward to another number of cycles, laying the foundation for [6], and [7], who developed the Theory of Critical Distance.

### *1.2.1. The Consequence of Fatigue Failure*

Fatigue costs can be calculated or estimated either directly or indirectly. The additional material that goes into the parts or the use of costlier methods and materials can be directly measured. For damage-tolerant models, costs for repair and maintenance of parts and assemblies may be measured directly. Nevertheless, loss of life, time, and competitiveness are not observable, they can only be felt. The costs of fatigue and fracture are always present in the production process, whether there is knowledge or not of the phenomenon of fatigue, whether fatigue problems are being approached and considered. The former President of the Structural Integrity Society of Europe, Ian Milne, says that the total cost of fracture-based events corresponds to 4% of the Gross Domestic Product (GDP) for the economies of advanced countries (2005). This is twice the amount spent on the military in the UK (defense 2% of GDP) [8].

### *1.2.2. Factors that Affect the Behavior of Fatigue*

The following variables impacting fatigue behavior:

- Loading type and nature.
- Frequency and rate of strain.
- Element volume and distribution of strain or stress.
- Environmental effects.
- Surface texture and directional characteristics.
- The concentration of stress or strain.
- Mean stress or strain.
- Material properties and metallurgical factors.

### *1.2.3. Low Cycle Fatigue Characteristics*

- Characterized by large loads and a small number of cycles before failure.
- Failures arise here in the plastic spectrum only with stress levels, i.e., during

each cycle, major plastic strain occurs.

- The peak stresses are the ones that trigger fatigue failure in the pipes.
- Many loading cycles would be of the low cycle kind.

### *1.2.4. High Cycle Fatigue Characteristics*

Low cycles Number (acceptable N>10 ^ 4) is defined by relatively low stresses and elastic deformation [9].

- When designing rotating machinery, this type of fatigue failure is usually used.
- This kind of fatigue is induced by elastic strain cycles.
- Stress level and endurance limit can be calculated without failure an infinite number of times.

### *1.2.5. Fatigue Cycle Phases*

The fatigue cycle comprises three phases: the initiation of crack from the constant processing of high-stress concentrations; the propagation of cracks to essential proportions and the unstable fracturing [10].

- Phase 1: Initiation of crack— Cracks of fatigue almost often begin on a free surface and in the vicinity of a pressure climb (e.g., the toe of a weld). At localized discontinuities in the metal structure, the initial development of the fatigue crack occurs. Ultimately, discontinuity generation and vibration strengthen the metal by plastic deformation. This is regarded as hardening work. As the metal hardens, it loses its ability to deform plastically in a location in which cyclical stresses are evident. When the stress exceeds its maximum, the discontinuity becomes a small crack.
- Phase 2: Propagation of the crack — Continued cyclic stress repeats the process once a crack occurs, increasing slowly into the microcrack which threatens the structural integrity of structures. In the case of containment of hydrocarbon, this

could be the beginning of a leak or loss-of-containment incident.

- Phase 3: Failure— Based on product, size, temperature, and pressure added, the final failure occurrence (i.e., severe fracture) may become ductile or brittle. Usually, fatigue failures happen suddenly. A fractured part typically has fatigue-induced crack surfaces that are flat, without evidence of plastic deformation.

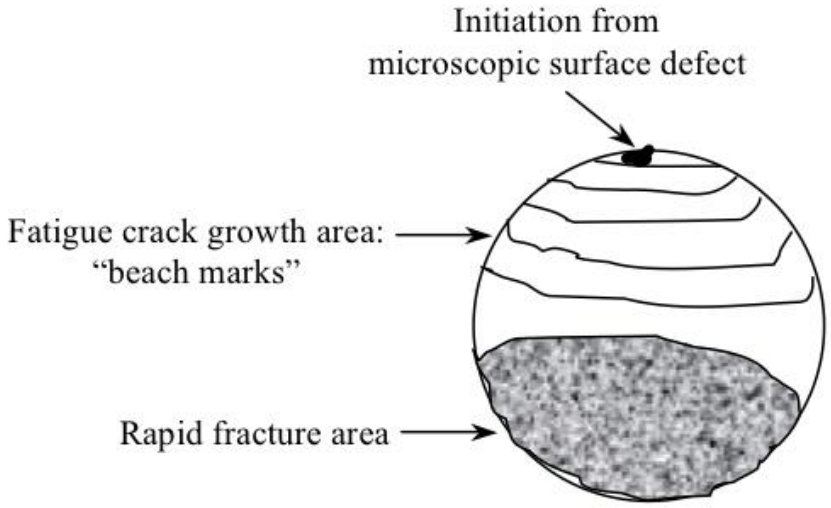


Figure 2. Fatigue failure stages [10].

## 1.3. Pipework

The first methods for manufacturing steel pipes were developed in the early 1800s, and they have continuously evolved into modern processes that we use today. Millions of tons of steel pipe are manufactured each year [11]. Its versatility makes it the most frequently used commodity produced by the steel industry. Because it is efficient, it is used underground in cities and towns to transport water and gas. They are also used to secure electrical cables in the building. They can also be lightweight, while steel pipes are strong. This makes them suitable for use in the manufacturing of bicycle frames.

They also find utilities in houses, ventilation units, heating and plumbing systems, flagpoles, street lighting, and medicines. For thousands of years, people have been using pipes. The first application was from ancient farmers who converted water into their fields from rivers and banks [11]. Archeological evidence shows that the Chinese used pipes as early as 2000 B.C. for water transport [12].

### *1.3.1. Standards, Codes, and Recommended Practices for pipework*

Standardization is the method of introducing and creating technical documents built on the agreement of various stakeholders that involve companies, consumers, community groups, standards organizations, and governments. The regularization of equipment, structures, components, and processes can or may minimize the expense, frustration, and uncertainty that emerges from the unwanted and undesired variations. In fields such as protection, inspection, and installation, guidelines should also register agreed industrial practices. The adoption of different guidelines, codes, and recommended procedures in process plant standardization is accomplished.

#### Standards

Standards are documents developed by a technical company or a commission that are thought to be effective engineering standards and that contain compulsory specifications. The users would be liable for implementing it correctly. Compliance with the standard does not itself grant a civil responsibility exemption.

#### Code

Code is a collection of general laws or systemic design, production, construction, and testing processes that are made lawful and implemented under legal authority. Engineering specifications considered necessary for proper construction and design of piping installations are to be set out by the Codes. Unlike voluntarily agreed standards which are only obligatory when implemented into a business arrangement, a code is of

legal force.

## Recommended Practices

Professional associations and committees prepared papers with sound engineering practices, but optional. Companies are now creating their own recommended practices to ensure continuity in development and prevent dramatically varying from one project and another.

Each country has its Codes and Standards [16]. The major organizations for standards are shown in Table 1.

Table 1. Major Organizations for Standards and Their Countries [16].

| S. No. | Abbreviation | Organization | Country |
|---|---|---|---|
| 1 | ANSI | American National Standard Institute | United States |
| 2 | SCC | Standard Council of Canada | Canada |
| 3 | AFNOR | Association Française de Normalisation | France |
| 4 | BSI | British Standard Institute | United Kingdom |
| 5 | CEN | Committee of European Normalization | Europe |
| 6 | DIN | Deutsches Institute for Normung | Germany |
| 7 | JISC | Japanese Industrial Standards Committee | Japan |
| 8 | BIS | Bureau of Indian Standards | India |
| 9 | ISO | International Organizations for Standards | Worldwide |

Few generally referred standards by Piping Engineers are listed in appendix A.

### *1.3.2. Pipe Fatigue*

Fatigue of pipes occurs in piping systems when dynamic stress combinations in the pipe's components surpass permissible levels. A combination of pressure and thermal expansion is the main source of static stress in the pipe. In general, thermal stress can be very high when support is not properly installed or maintained [17]. Vibrations transmitted through connected machines or forces generated by hammer or pressure pulsations inside pipes or by fluids or other external loads can cause dynamic stress. When a pipe fails due to fatigue, the containment of the system fluid is usually released. This may lead to dangerous releases and threaten workers from high pressure and/or temperature steam and other liquids. In some instances, failures can manifest very rapidly or occur due to an aggregation of dynamic stress cycles after long-term periods. For a machine that operates at 3,600 rpm, usually, fatigue failure requires ten hours or less to occur when the pressures of high cycle fatigue surpass acceptable levels due to the high vibration caused by the device [17].

## 1.4.Weldolets

The most popular pipe olet is the weldolet. It is suitable for the application of high-pressure weight and is welded to the outlet of the running pipe. The end is beveled to pro-mote this operation, and hence the weld is known to be a butt weld fitting. Weldolet is an extension of a branch butt weld that is connected to a release pipe to mitigate stress concentrations. In general, it has the same or higher schedule than running pipes and provides different forged materials, such as ASTM A105, A350, A182, which supplies essential reinforcements. The measurements of the Weldolet are between 1/4 inch and 36 inches in diameter for running pipes and between 1/4 "and 2" in diameter for the branch. Although it is possible to customize a big brand diameter [18].

Figure 3. Weldolet [18].

## 1.5. Characteristics of Carbon Steels (CSs), Stainless Steels (SSs), and Duplex stainless steels (DSSs)

The most commonly used materials for piping systems in the oil and gas industry are (CS), (SS), and (DSS).

### *1.5.1. General Information*

#### A. Carbon steel

The alloying elements of (CS) do not surpass the following limits:

Table 2. Alloying Elements of (CS) [19].

| Element | Max weight % |
|---|---|
| C | 1.00 |
| Cu | 0.60 |
| Mn | 1.65 |
| P | 0.40 |
| Si | 0.60 |
| S | 0.05 |

Carbon steels may be categorized into three major groups: low (sometimes referred to as mild steels), Medium, and High carbon steel.

- Low Carbon Steels (Mild Steels): this is one of Carbon Steel's largest groups. Usually, it contains 0.04% to 0.30% of carbon [19]. It covers a wide range of forms, from plain sheets to Beams. Furthermore, Additional elements are added or augmented according to the desired properties. For example, carbon levels are higher, and the content of manganese is increased for structural steel, on the other hand, carbon levels are kept low, and aluminum is added for Drawing Quality (DQ).
- Medium Carbon Steels (MCSs): is typically between 0.31% and 0.60% of carbon, and between 0.60% and 1.65% of manganese [19]. This product is harder to shape, weld and trim, than low-carbon steel. heat treatment is used to harden and temper medium carbon steels quite often.
- High Carbon Steels (HCSs): Usually famous as “carbon tool steel” it normally has a carbon limit range of 0.61% and 1.50% [19]. It is very hard to bend, cut, and weld (HCS). It becomes extremely hard and brittle once heat treated.

## B. Stainless steels

Stainless steels are steels with a strong composition resistant to rust compared to other steels due to their large quantities of chromium content. Stainless steels could include 4-30% chromium anywhere, but most hold around 10% [19]. Depending on its crystal structure, stainless steel can be categorized into three main categories: austenitic, ferritic, and martensitic. A mixture of martensitic and austenitic steels is also known as precipitation-hardened steels. The general compositions of these groups are described below.

- Ferritic grades: Magnetic, un-heat treatable metals that comprise chromium and

no nickel. They have good resistance to heat and rust, especially seawater, and good endurance to cracking due to stress corrosion. Their mechanical properties are not as strong as those of the austenitic grades, but they have a better appeal for decoration.

- Martensitic grades: The martensitic grades are heat treatable and magnetic, they can be treated by tempering or quenching. They comprise chromium but usually do not include nickel except for 2 grades. Martensitic steels are not as prone to rust as austenitic or ferritic types, but they are amongst the hardest of all stainless steels.
- Austenitic grades: Non-magnetic non-heat-treatable steels, typically annealed and cold-drawn. After the cold drawing, some austenitic steels appear to be magnetic. Austenitic steels have good mechanical characteristics over a large-ranging temperature, in addition to having excellent corrosion and heat resistance. Austenitic stainless steels have two sub-classes: chromium-manganese-low nickel and chromium-nickel steels. The most commonly used steels of chromium-nickel are 18-8 (Cr-Ni) steels. To increase the formability, the chromium-nickel ratio can be adjusted, and carbon content lowered to enhance the intergranular corrosion resistance. Molybdenum could also be added to increase corrosion resistance. Furthermore, Cr-Ni content can be increased.

### C. Duplex stainless steels (DSSs)

(DSSs) are chromium-nickel-molybdenum-iron bi-phased alloys in which the proportions of the constituent elements enable the optimization of the balance of the volume fractions of austenite and ferrite [20]. Thanks to their pi-phase ferritic austenitic microstructure, they have a higher mechanical strength and a greater tolerance to

corrosion than normal austenitic stainless steels. Currently, thanks to their outstanding assets and their reasonably low prices, the DSS applications and sales tend to be growing. The usage of DSSs in oil and gas, pulp and paper, and chemical industries has grown significantly over the past ten years. Figure 7 Microstructure of austenite and ferrite grains are available in double stainless steel. depicts the yellow austenitic process as the blue ferritic process "Is-lands." Once stainless steel is cooled, it solidifies to a fully ferritic form from the liquid process. With a room temperature cooling medium, roughly half of the ferritic grains turn into austenitic grains ("îles"). This ended in an estimated 50% austenite and 50% ferrite microstructure.

The family of DSSs consist of four types with different compositions [20]:

- Lean DSS: lower nickel and no molybdenum, such as 2101, 2102, 2202, 2304 grades.
- Duplex SS: higher nickel and molybdenum, such as 2205, 2003, 2404 grades.
- Super DSS: 25% Chromium and higher nickel and molybdenum “plus”, such as 2507, 255, and Z100 grades.
- Hyper DSS: More Cr, Ni, Mo, and N, such as 2707 grade.

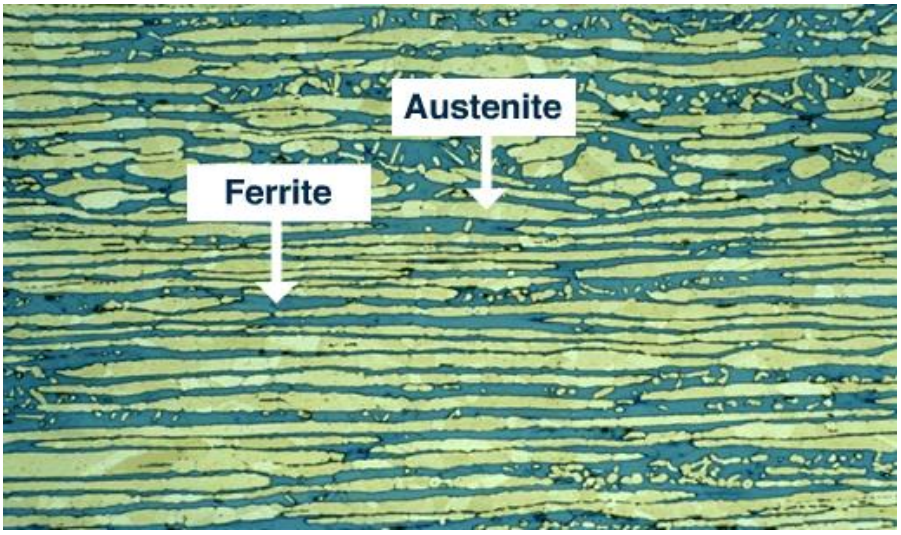


Figure 4. The microstructure of austenite and ferrite grains is available in double stainless steel [20].

The duplex arrangement gives a range of desirable properties to this family of stainless steels [20]:

- Robustness: duplex steels are almost twice as robust as standard austenitic or ferritic steels.
- Toughness and ductility: stainless steels are far more durable and ductile than ferritic types, but they do not reach outstanding austenitic qualities.
- Robustness: Corrosion tolerance, as is the case with other stainless steels, relies mainly on the stainless-steel composition. Their chromium, molybdenum, and nitrogen content are most essential for chloride pitting and crevice resistance to corrosion. Similar to the variety of austenite stainless steel grades (e.g., LDX 2101) from 304 or 316 to 6 percent molybdenum (e.g., SAF 2507 ©) stainless steel was corrosion-resistant to double-gauge stainless steel grades.
- Crack resistance to stress corrosion: Duplex stainless steels display very high resistance to stress corrosion (SCC), which is a feature they have "inherited" on

the ferritic side. In certain conditions, SCC can be an issue for typical austenitic goods such as Types 304 and 316 (chloride, dust, elevated temperature).

- Cost: Duplex stainless steels produce less nickel and molybdenum than their austenitic equivalents, with greater corrosion resistance. Dual stainless steels can, due to the lesser alloying material, be cheaper, especially when high alloy surcharges are added. Furthermore, owing to the improved yield strength compared with austenitic stainless steel, the section thickness of duplex stainless steel may also be decreased. In contrast with a solution in austenitic stainless steel, it will result in substantial cost and weight savings.

### *1.5.2. General Properties of Steels*

The table below shows the typical characteristics of steels at room temperature (25 ° C) [21]. The wide ranges of some properties are mostly due to diverse heat treatment conditions and/or grades.

Table 3. Carbon Steel vs Stainless Steel vs Duplex Stainless Steels [21].

| Properties | Carbon Steels | Stainless Steels | Duplex Stainless Steels |
|---|---|---|---|
| Density (1000 kg/m$^3$) | 7.85 | 7.75-8.1 | 7.75-8 |
| Elastic Modulus (GPa) | 190-210 | 190-210 | 190-220 |
| Poisson's Ratio | 0.27-0.3 | 0.27-0.3 | 0.2-0.35 |
| Thermal Expansion ($10^{-6}$/K) | 11-16.6 | 9.0-20.7 | 10-18 |
| Melting Point (°C) | 1425 – 1540 | 1371-1454 | - |
| Thermal Conductivity (W/m-K) | 24.3-65.2 | 11.2-36.7 | 12-25 |
| Specific Heat (J/kg-K) | 450-2081 | 420-500 | 450-502 |
| Electrical Resistivity ($10^{-9}$W-m) | 130-1250 | 75.7-1020 | 60-85 |
| Tensile Strength (MPa) | 276-1882 | 515-827 | 600-1200 |
| Yield Strength (MPa) | 186-758 | 207-552 | 400-1000 |
| Percent Elongation (%) | 10-32 | 12-40 | 20-51 |
| Hardness (Brinell 3000 kg) | 86-388 | 137-595 | - |

### *1.5.3. Carbon Steel vs Stainless Steel vs Duplex stainless steel*

The discussion around carbon steel, stainless steel duplex stainless steels is a little harder than initially thought. Carbon steel could relate to two different kinds of steel: traditional carbon steel and low alloy steel. The strength, hardness, and, most significantly, corrosion resistance is improved by stainless steel in comparison with low carbon steel [22]. High carbon steel has the toughness that equals and sometimes exceeds stainless steel but is mainly a production niche product. In comparison to carbon steel, stainless steel can survive and flourish without corrosion in corrosive and humid conditions. Carbon steel is far less expensive than stainless steel and more suitable for large components such as tubing, beams, and rolling sheet steel. Low-alloy steel in most ways is supreme to carbon steel, yet still lacks corrosion resistance. It also can easily match stainless steel's material characteristics. Alloys such as 4140 and 4340 are of-ten machined and used in many applications where a little oxidation does not affect. Stainless steel is a better material used in industries where the quality of the part cannot be jeopardized [23]. Compared to austenitic stainless steel, the major distinction in the composition is that duplex steels have a higher concentration of chromium, 20%-28%, higher molybdenum, up to 5%, and less nickel, up to 9% [23]. Two major advantages are the low nickel content and high strength (allowing the use of thinner parts). Therefore, in the offshore oil and gas industry, they are used widely in piping, manifolds, levitations, and other applications as pipelines and pressure vessels in the petrochemical industry. In comparison to 300 series stainless steel, duplex steels still have higher strength, in addition to the increased corrosion resistance [20].

## 1.6. Aim and objectives

The overreaching aim of this thesis is to investigate the suitability of the Vibration Acceptance Criteria (VAC). This will be achieved by realizing the following objectives:

1) To understand the bases of the Vibration Acceptance Criteria (VAC).
2) To create different models of pipework to be used for the investigation.
3) To conduct Finite Element Analysis (FEA) on the models to find the vibration and stress values.
4) To compare the results of the FEA with the VAC and stress limits to judge the vibration and stress levels.
5) To find the suitability and confidence levels of the VAC.

## 1.7. Thesis outline

This thesis has five chapters, the first chapter is the introductory chapter. It provides general information about the topic and some of the most important definitions and terminologies related to this topic. This includes the definition of Hydrocarbons and their impact, metal fatigue, pipework, welds, and material characteristics of commonly used materials in the O&G industry. The second chapter "Literature Review" will explain pipe fatigue and vibration, major hydrocarbon leak accidents due to VIF, Vibration Acceptance Criteria (VAC), stress limits used for pipework, and the Literature gap of knowledge. Chapter three covers the methodology used for the investigation of the suitability of the VAC. This includes the CAD models, software packages used for the analysis, the Finite Element Analysis (FEA) that will be used for this investigation, and the inputs and outputs of the FEA, and what variables will be used to generate the cases of the analysis. Result analysis and discussion will be presented in chapter 4. And finally, conclusions and recommendations will be presented in chapter five.

# CHAPTER 2: LITERATURE REVIEW

## 2.1. Pipe Fatigue and Vibration

This section will address the sources of pipe fatigue and why these issues arise in piping networks. Furthermore, the main causes of the vibration and its effects on piping systems will also be addressed.

### *2.1.1. Sources*

Due to the failure to address the vibration issues in detail in most piping design codes (ASME B 31.3, B31.1, B31.4, B 31.8, etc.), the damaging effect is usually ignored during the design phase and merely vibration-free static analysis is conducted on piping systems [24]. In the same period, because of enhanced processes industries flow rate through pipes and the use of thin (flexible) wall piping high-strength material during development, the vibration tendency of the tubing network is through to a significant degree. Vibration in running plants can be seen to trigger most issues and the issue should be addressed during the design phase. When the correct development approach is followed while developing the system, the most damaging effects of vibrations can be mitigated. The main causes of the vibration and its effects are highlighted below. Movement from an equilibrium position can be described as continuous backward and forwards motion [25]. In a piping system, there are many explanations for vibrations. Various excitation mechanisms can manifest in a pipe system and can cause vibrations and ultimately fatigue failure. The following are a few major reasons for the vibration [25]:

- Vibration induced by the moving stream turbulence.
- Pressure Reciprocal device pulsations.
- A small pressure drop induces cavitation or a gas bubble to collapse.

- Periodic stress fluctuations over the dead end of branch / instrumental objects during discharge.
- Fluid pulse suddenly.
- Changes to the Water Hammer or Momentum due to the sudden closure of the valve.
- Acoustic excitations are created by shutoff valves, regulation valves, or orifice plates.
- Machinery mechanical forces are attributable to the effects of excitation of reciprocating and revolving machinery, such as motors, compressors, etc.
- Laps between SBC layout and site production in particular local support/bracing.

### *2.1.2. Effect of Vibration*

Statistics have shown that about 10-15 percent of all losses and downtimes in every single plant have vibration-induced fatigue. The most significant results of vibration are:

- Vibration in a piping system induces dynamic pressure (fatigue). If these stresses are more than a critical value, a crack will start propagating, until the item in question fails. The more vulnerable places of fatigue are the connections between the branch and the header [26].
- Besides dynamic stresses, vibration results in the wear of contact surface by cyclical relative movement between them. This phenomenon is defined as Fretting [27].

## 2.2. Major Hydrocarbon Leaks Accidents due to Vibration Induced Fatigue (VIF)

A famous example of Vibration Induced Fatigue (VIF) failure that was possibly a major accident of injuries, substantial damage to the plant, and consequent environmental

damage is the Gudrun incident in the Norwegian North Sea region. This occurred directly because of a leak in a 2-inch pipe in a bypass line, directly downstream of the separator in the first phase. Statoil estimated an initial eight kilograms of leakage per second. The first stage separator condensate was spilled into the open air. The total condensate emissions/discharges are estimated at 2,800 kilograms / 4 cubic meters, and it is estimated that more than 1 cubic meter has been discharged to the sea [28]. Gudrun leak has been considered one of the largest hydrocarbon leaks registered over the last decade on Norway's continental shelf (NCS). The incident caused no personal injury. However, the incident could have led to a major accident, loss of life, significant damage to material assents, and marine ecosystems in somewhat different circumstances.

Another critical case, according to the Petroleum Safety Authority (PSA) investigation was the hydrocarbon leak in the Hammerfest LNG plant in Northern Norway on 5 January 2014, which had a high potential explosion and life-loss [29]. This occurred in the evening when the Melkøya processing plant was operating normally outside of Hammerfest. It is estimated that the leak rate is 0.1-0.3 kg per second and the amount of escaping natural gas at 250-750 kg. There was no personal injury but property harm to the accident. Production was shut down for three days at Hammerfest LNG. Nevertheless, if the hydrocarbon leak had sparked, an explosion would have led to two deaths. One worker was close to the leak, and another individual in the factory could have been harmed. An explosion could have also damaged the equipment and structures, and the plant would have been long shutdown.

### 2.3. Vibration Acceptance Criteria (VAC)

To quantify the risk of vibration-induced fatigue (VIF) measurements must be carried out. Ideally, a strain measurement, stress calculation, and fatigue life assessment would

evaluate the risks of VIF. However, it is not always possible to install strain gauges (for example with hot piping) and, if possible, they can take time (need to remove the paint, surface preparation, etc.). To determine the risk of VIF, the industry has thus taken measures for the vibration velocity. The motivation to follow this approach is to make it feasible and easy to implement. The vibrometer can be calibrated with a hand-held, single-channel frequency analyzer and an accelerometer. Measurement is investigated against vibration identification curves that provide the foundation for the vibration acceptance criteria defined in the majority of cases by the Southwest Gas Association (SWGA). The Energy Institute has implemented these curves and approval criteria in [30]. High-stress levels correspond often to vibration levels PROBLEM (and sometimes CONCERN) (as illustrated in Figure 8).

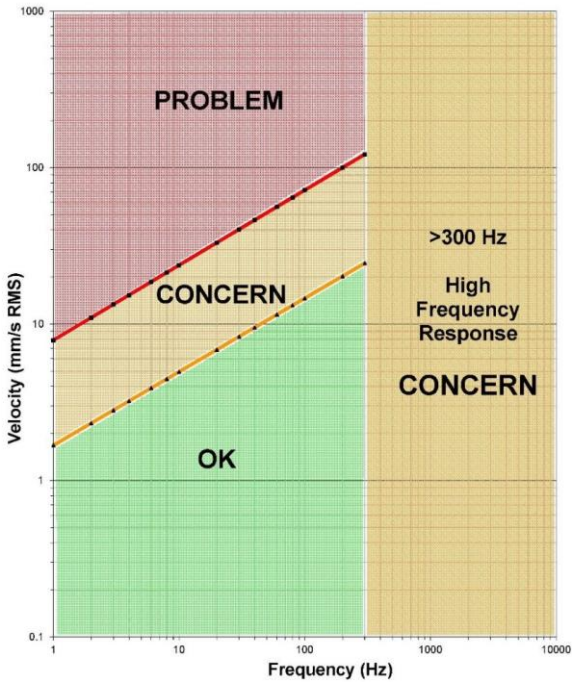


Figure 5. Vibration acceptance criteria were adopted by the Energy Institute in [30].

## 2.4. Stress limits used for pipework

The Dynamic stress (DS) in process pipework is usually compared to the allowable stress ranges developed and reported in BS 7608 [31]. In BS 7608 [31], they generally evaluate the stress levels based on the assumption of the classification of the F2 weld class to be complete penetration, one-sided butt weld, or fillet irrespective of the type of fitting. The permissible peak-to-peak stress (PTP) for this weld rating is 35 N/mm$^2$ with a fatigue limit of 107 cycles (based on average minus two standard deviation rates, 2.3% durability curve). It is also advised that this stress should be lowered to 17.5 N/mm$^2$ in accordance with [31] and the guidelines set out in [30] to decrease the likelihood of failure to an acceptable hydrocarbon piping. The following table shows the recommended DS ranges.

Table 4. Stress Limits for Hydrocarbon Processing Pipework [31]

| Stress level | Stress Range (N/mm$^2$ PTP) |
|---|---|
| | Stress < 17.5 |
| CONCERN | 17.5< Stress < 35 |
| PROBLEM | Stress >35 |

## 2.5. The Gap in the Literature

Although design guidance is provided in standards for the nuclear industry and reciprocating gas compressors such as ASME OM-3 [32] and API618 [33] respectively, there are no API/ASME standards for vibration fatigue evaluation of in-service pipes. The conceptual foundations for the current screening criteria available in the literature and the level of conservatism implanted in these criteria are not well understood. Although the existing screening procedures are warranted by practice, the evaluations are open for interpretation by the user. There exist two screening criteria: Velocity RMS Based Screening and Peak-to-Peak Displacement Based Screening. The Energy Institute (EI) "Guidelines for Avoidance of Vibration Induced Fatigue Failure in Process Pipework" [30] points out the most widely used velocity limit methods based on root-mean-square (RMS) velocity estimation. The permissible velocity amplitudes (0-pk) are divided into units of RMS velocity by a crest factor (CF) of 1.4142, which is only relevant to sinusoidal amplitude vibration. In addition, a constant amplitude fatigue limit has been set which may not be satisfactory in cases of Gaussian vibration or strong kurtosis (non-Gaussian) vibration. The EI limits are based on a stress amplitude of 2.5 ksi (kilopound per square inch) corresponding to the BS7608 [31] Class F2 welded Joint Fatigue curves and the Safety Factor (SF) of 2.0. The 'CONCERN' limit is the lower bound of a range of FEA models relating to the vibration velocity and frequency resulting in a 2.5 ksi constant amplitude fatigue limit. The EI limits consist of 10 rigorously tested classes of small-bore cantilever FEA models and 1 class of mainline pipes, as referred to in Appendix A of reference [30]. The precise number of geometry variants analyzed within each class is unclear. In addition, the basis of the upper 'PROBLEM' line is unclear but is roughly a factor of 4.9 greater than the ‘CONCERN’ line. Using these curves for random (variable amplitude) vibrations

can be troublesome for two reasons. First, the presumed CF of 1.414 was possibly used to cast the produced FEA velocity from 0-pk units to RMS units, which is unconservative for most random vibrations. Second, a constant amplitude fatigue limit has been developed which may not be satisfactory in cases of Gaussian vibration or high kurtosis (non-Gaussian) vibration. The EI proposed using the VAC of Figure 8 based on the work of the Southwest Gas Association [34]. There is, however, no agreement on pipework vibration acceptance criteria. Beta Machinery Ltd., for instance, has altered the curves in [34]. The resulting criteria are contained in [35] and are more conservative than those provided by the Energy Institute [30]. Other operators, for example, Norwegian operators use an aggregate of the Energy Institute [30] curves and standards established by the European Forum of Reciprocating Compressors [36]. The recommendations in [36] are more specific for machine-induced excitations and gas pulse movement, flow-induced vibrations are not included in [36].

Alternatively, Nimitz/SWRI Displacement Criterion includes the estimation of peak-to-peak displacement and 5 choices of screening restrictions. Reference [37] suggests that these standards are for average piping structures designed in compliance with sound engineering practices and that additional provision for sensitive applications or unreinforced branch connections should be given. These comments, along with numerous choices of acceptability limits and lack of usable technological foundation, put an enormous amount of pressure on the user.

Because of the above variations in the assessment of pipework vibrations severity, important dynamic stress locations may be missed which results in VIF risks not being managed properly. Besides, the permissible vibrational rates may rely on variables including pipe length, the support structure (and condition), fittings, and deflection types. Therefore, in all piping geometries, arrangements, and fittings the criteria in

Figure 8 might not be suitable to accurately specify the levels of vibration.

This gap in the literature will be addressed using FEA to investigate the suitability of the VAC and how different dimensions of the run-pipe will affect the suitability of the VAC. This will be realized using random vibration analysis which will be conducted on different models. In the following chapter further explanation will be provided on how this gap of knowledge will be addressed.

# CHAPTER 3: METHODOLOGY

This chapter will introduce the steps that shall be taken to investigate the suitability of the VAC. The first section will explain how this investigation will be carried out. The second section will introduce the software which will be used for modeling and simulation. After that, the third section will illustrate the models that will be used for this investigation and how they were modeled. In the fourth section, the Finite Element Analysis (FEA) will be used to find the suitability of the VAC and the inputs and output of this analysis will be presented. Lastly, the fifth section will highlight the variables and the boundary conditions to generate the cases that will be used in this investigation.

## 3.1 General Procedure for the Investigation of the VAC

To assess the suitability of the VAC, 3 models will be created using 3D modeling software. These models will be subject to different excitations and boundary conditions. The excitations will be obtained using MATLAB as will be shown in section 3.5. After that, these excitations will be used along with different supporting conditions to generate different cases. These cases will be applied to all the models which will be created to find the vibration and stress of each model. Two types of results for the vibration and stress will be obtained which are the 1 and 3 sigma results. These results will indicate how much confidence can be put in these results. For instance, if a 100-vibration measurement is taken how many of these measurements are close to the average value at that location where the measurements are taken. The 1-sigma confidence results which are also known as the RMS gives a confidence interval of 68.27%. Meaning that out of 100-measurements for example, 68.27% of these measurements are 1-standard deviation above or below the average measurement at the location and the remaining 32% are out of this interval. Similarly, the 3-sigma results

give a confidence interval of 99.73%. This means that 99.73% of the measurements are 3-standard deviation above or below the average. Following that, these results will be compared with the VAC and the stress curves to find the vibration and stress levels. Then the cases of each model will be categorized based on their vibration and stress levels. These categories will be defined by 2 letters, the first letter indicates the vibration level, and the second letter will indicate the stress level. The categorization will be as follows, the first category will hold all the cases with OK vibration and stress levels and this category will be appointed the letters (OO). The second category which will be referred to by the letters (OC) will hold all the cases with OK vibration levels and 'CONCERN' stress levels. Furthermore, the third category will hold all the cases with OK vibration levels and problem stress levels, and it will be assigned the letters (OP). The matrix in Table 5 shows all the possible category combinations based on the stress and vibration levels.

Table 5. Possible Category Combinations Based on Vibration and Stress Levels.

| Stress Level | Vibration Level: OK | Vibration Level: CONCERN | Vibration Level: PROBLEM | Category Combinations |
|---|---|---|---|---|
| OK | OO | OC | OP | |
| CONCERN | CO | CC | CP | |
| PROBLEM | PO | PC | PP | |

After categorizing all the cases the suitability of the VAC will be calculated using the following equation.

$$VAC\ Suitability = \frac{No.of\ correctly\ judged\ cases\ by\ the\ VAC}{Total\ No.of\ cases} \times 100 \qquad (1)$$

3.2 Software packages used

Three software packages will be used for this investigation of the suitability of the VAC.

1) The first software is SolidWorks®. It is a solid modeling computer-aided design and computer-aided engineering computer program. This software will be used to create the models that will be used to investigate the suitability of the VAC as will be explained in the next section.
2) The second software is ANSYS®. It is an engineering simulation and 3D design

program that provides product modeling solutions with unparalleled scalability and robust Multiphysics. ANSYS® offers an extensive software package covering all physics, which provides access to practically any engineering simulation area required by a design process. Two plat-forms of the ANSYS® software will be used, ANSYS Workbench®, and ANSYS Mechanical APDL®. Workbench® is the backbone for providing a completed integrated simulation. It is used for structural, thermal, fluid, and electromagnetic studies of different kinds. The complete simulation process is linked by a project diagram, which enables you to communicate with ANSYS-native apps or launch applications that are incorporated with ANSYS Work-bench®. It incorporates CAD connectivity, automatic meshing, updating process at a project level, tools for optimization, DOE. APDL stands for ANSYS Parametric Design Language, it is the basis of all advanced features, many of which do not appear on the Workbench Mechanical User Interface. It provides a wide range of conveniences including parameterization, macros, branching, looping, and complex math. All these advantages are available in-side the Ansys Mechanical APDL user interface. These platforms will be used to conduct the Random Vibration Analysis on the models created in the SolidWorks® which will be shown in the coming sections.

3) The third software is MATLAB®, it is a programming platform for the analysis and design of the systems and devices that transform our world. It is developed specially for engineers and scientists. The MATLAB® is built on the MATLAB language, which is a matrix-based language that allows for natural computational mathematics. This software will be used to find different cases of excitations which will be applied to the models created by Solid-Works® in

ANSYS Workbench® using a Mechanical APDL® code as will be shown in the following sections.

## 3.3 CAD models

Three main models will be used for this investigation, each model has 3 sub-models. The models consist of Small-Bore Connections (SBCs) connected to run pipes (mainlines) which were modeled using SolidWorks®. Each model consists of a carbon steel run-pipe with 3 different lengths connected to an SBC which consists of a branch pipe of the same material and a weldolet that acts as a reducer between the run-pipe and the branch-pipe. The three parts were modeled separately and afterward, they were assembled by a means of welds using the same software to form the final model as shown in Figure 9 and Figure 10. Later, these models were exported to a finite element software to be prepared for the analysis. Table 6 below lists all the model configurations used in this thesis. Schematics of all these models are shown in the appendix sections.

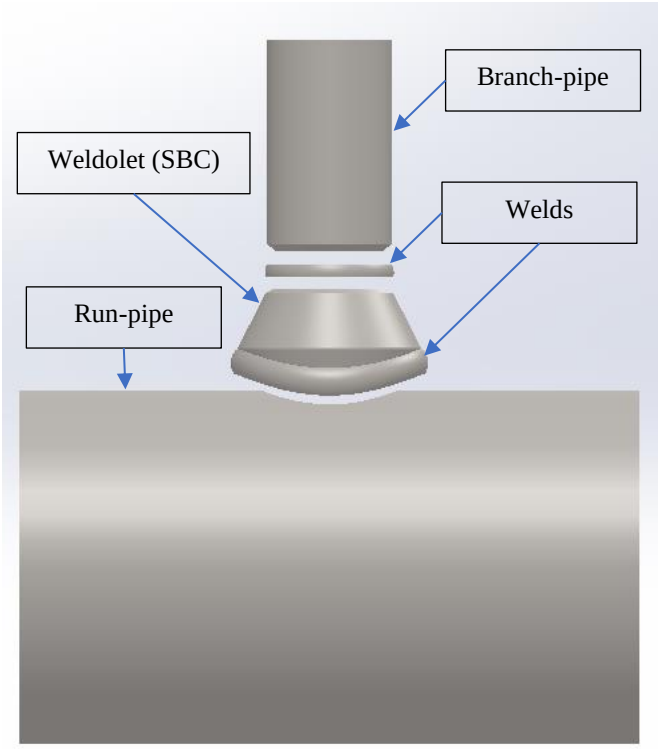


Figure 6. Exploded view of one of the models that will be used for the analysis.

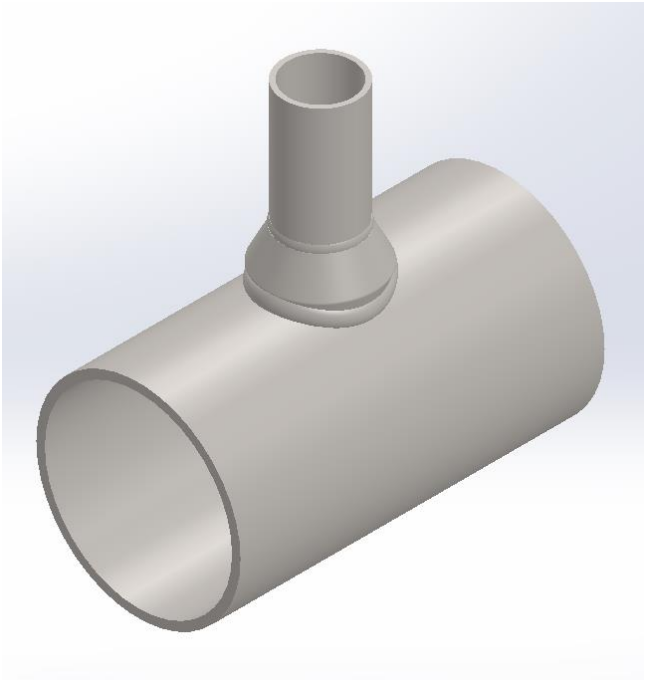

Figure 7. Isometric view of the same model in figure 9.

Table 6. List of All the Models That Will Be Used for The Analysis

| Model Number | Sub-Models | Configuration |
|---|---|---|
| 1 | 1.1 | This model consists of a 0.3-m, 6-inches, SCH 40 carbon steel run-pipe connected to a 2-inch, 0.1-m, SCH 40 branch-pipe of the same material, a 2x6 inch SCH 40 weldolet (SBC), and a 5-kg valve represented by a point load on the branch-pipe. |
| | 1.2 | This model consists of a 1-m, 6-inches, SCH 40 carbon steel run-pipe connected to a 2-inch, 0.1-m, SCH 40 branch-pipe of the same material, a 2x6 inch SCH 40 weldolet (SBC), and a 5-kg valve represented by a point load on the branch-pipe. |
| | 1.3 | This model consists of a 1.5-m, 6-inches, SCH 40 carbon steel run-pipe connected to a 2-inch, 0.1-m, SCH 40 branch-pipe of the same material, a 2x6 inch SCH 40 weldolet (SBC), and a 5-kg valve represented by a point load on the branch-pipe. |
| 2 | 2.1 | This model consists of a 0.3-m, 5-inches, SCH 40 carbon steel run-pipe connected to a 2-inch, 0.1-m, SCH 40 branch-pipe of the same material, a 2x5 inch SCH 40 weldolet (SBC), and a 5-kg valve represented by a point load on the branch-pipe. |
| | 2.2 | This model consists of a 1-m, 5-inches, SCH 40 carbon steel run-pipe connected to a 2-inch, 0.1-m, SCH 40 branch-pipe of the same material, a 2x5 inch SCH 40 weldolet (SBC), and a 5-kg valve represented by a point load on the branch-pipe. |
| | 2.3 | This model consists of a 1.5-m, 5-inches, SCH 40 carbon steel run-pipe connected to a 2-inch, 0.1-m, SCH 40 branch-pipe of the same material, a 2x5 inch SCH 40 weldolet (SBC), and a 5-kg valve represented by a point load on the branch-pipe. |
| 3 | 3.1 | This model consists of a 0.3-m, 4-inches, SCH 40 carbon steel run-pipe connected to a 2-inch, 0.1-m, 0.1-m, SCH 40 branch pipe of the same material, a 2x4 inch SCH 40 weldolet (SBC), and a 5-kg valve represented by a point load on the branch-pipe. |
| | 3.2 | This model consists of a 1-m, 4-inches, SCH 40 carbon steel run-pipe connected to a 2-inch, 0.1-m, SCH 40 branch-pipe of the same material, a 2x4 inch SCH 40 weldolet (SBC), and a 5-kg valve represented by a point load on the branch-pipe. |
| | 3.3 | This model consists of a 1.5-m, 4-inches, SCH 40 carbon steel run-pipe connected to a 2-inch, 0.1-m, SCH 40 branch-pipe of the same material, a 2x4 inch SCH 40 weldolet (SBC), and a 5-kg valve represented by a point load on the branch-pipe. |

## 3.4 Finite Element Analysis (FEA)

In this thesis, a random vibration analysis will be conducted for each model with multiple cases. Random vibration is an indeterminate motion, which means that potential behavior cannot be accurately predicted. Also, the randomness is an excitation or input attribute, and not a characteristic of the mode shapes or natural frequencies. An example of random vibration is flow-induced vibration which is common in process pipework in the Oil and Gas industry. This flow-induced vibration is due to the high flow velocity inside the pipes that causes the flow to be turbulent. This is the reason why random vibration analysis is essential for this investigation to be able to simulate such randomness. This randomness will be simulated by a mean of a Power Spectral Density (PSD) force which will be applied to the models using ANSYS Workbench®. The FEA model in the Workbench® consists of five components.

- The first component is Geometry which will be used to import the models from Solid-Works® to the Workbench®.
- The second component is the mechanical model which is going to be used to configure the engineering data. This includes the material properties and the unit system (metric) that will be used through the analysis. In addition, it includes the material assignment to each part, meshing and its properties, connections such as contact areas between the components and the springs connecting the model to the ground, and assigning names to the surfaces and remote attachment points that will be used to connect the springs.
- The third component of the system which is the Modal analysis will be utilized to find the mode shapes of the models which will be required for the random vibration analysis.
- The fourth component and the most important one is the random vibration

analysis. In this component, an APDL code will be used to define the input PSD force which will be used for the analysis as will be explained later. This component will be also used to set the inputs and outputs of the analysis.

- The fifth and last component of the system was the Microsoft excel component which was used to connect the excel file that was containing the input data for the different cases to the random vibration component.

### *3.4.1 Inputs and Outputs of FE Model*

Different inputs will be used to simulate flow-induced vibrations in this analysis. The first input is the rotational and translational support stiffnesses which will simulate different supporting conditions for the run pipe. The second input is the Excitation Forces which will be applied as Power Spectral Density (PSD) to simulate different flow conditions with its randomness. This certain input is challenging to apply as the Workbench allows the user to a PSD Displacement, PSD Velocity, or PSD Acceleration only. Hence, the only way to apply a PSD force was to use ANSYS Parametric Design Language (APDL) to create a code that allows the input of a PSD force. The PSD force was obtained using the variables discussed in Section 3.5.

Using the above-mentioned inputs, the simulation will provide the necessary outputs which will be used to evaluate the suitability of the VAC. The first output is the vibration velocity of the SBCs where 1 and 3 sigma results will be obtained. These results will show how much confidence the VAC can provide when judging the vibration levels as explained in section 3.1. The second output is the stress levels which will be evaluated with the vibration velocity against the VAC in Figure 8 and the stress curves to see how appropriate the VAC is when judging random vibrations as will be shown in chapter 4.

3.5 Excitation force and variables used to generate different cases

In [38] the excitation mechanism regulating in-plan vibrations on a U-shaped pipe component was investigated in a series of experiments. This was done to characterize the in-plane fluctuating forces and to understand the related vibrational phenomena. Their study concluded that in the context of the internal two-phase flow and pipe natural frequency conditions the excitation process is likely to cause vibrations in pipe systems consisting of elbows or other flow-turning pipe components. Hereafter, the characterization of the excitation force due to two-phase flow based on the experiments done in [38] are explained.

Two parameters have been used to describe the flow conditions: superficial velocity (in this thesis simply referred to as velocity), $V$, and volumetric quality (or homogeneous fraction of the void), $\beta$, designated as:

$$\beta = \frac{Q_g}{Q_g + Q_l} \qquad (2)$$

$$V = \frac{Q_g + Q_l}{A} \qquad (3)$$

where $Q_g$ and $Q_l$ are the volumetric flow rates of the mixture correspondingly, and A is the total flow area of the mixture. For this simulation, a velocity varying from 5 to 20 m/s is used, these values are considered as typical values in pipework flow. The upper limit of hydrocarbon flow by many engineers in the industry is regarded as 20 m/s. In addition, a variety of different volumetric qualities ($\beta$ =25, 50, 75, and 95%) have been used. To correlate the data, normalized or dimensionless variables were also used. Therefore, two of these variables are described as the dimensionless frequency, $\bar{f}$, and the normalized PSD of force, $\overline{PSD}$ [38]:

$$\overline{PSD(\bar{f})} = \frac{PSD}{(GD)^2} \qquad (4)$$

$$\bar{f} = \frac{fD}{V} \qquad (5)$$

where $f$, is the dimensionless frequency, $D$, is the diameter of the run pipe in (m), and $G$ is the mass flux of the mixture, described as:

$$G = \left[\rho_g \beta + \rho_l (1-\beta)\right] V \qquad (6)$$

Equations (3) and (4) comply with the established terminology by [39]. The units of PSD are $m^4 s^{-1}$.

$$\overline{PSD(\bar{f})} = \left[\frac{\overline{PSD(f_0)}}{(\bar{f}_0)^{m_2}}\right](\bar{f})^{m_1},\ \bar{f} \le \bar{f}_0 \qquad (7a)$$

$$\overline{PSD(\bar{f})} = \left[\frac{\overline{PSD(f_0)}}{(\bar{f}_0)^{m_2}}\right](\bar{f})^{m_2},\ \bar{f} \ge \bar{f}_0 \qquad (7b)$$

The coefficients $\bar{f}_0$ , $\overline{PSD(f_0)}$, $m_1$, and $m_2$ are presented in the following table, which was established based on the experiments done in [38].

Table 7. Coefficients of Eq. (6) [38].

| $\beta$ | $\bar{f}_0$ | $\overline{PSD(f_0)}\ (m^4 s^{-1})$ | $m_1$ | $m_2$ |
|---|---|---|---|---|
| 25 | 0.064 | 1.88E-05 | 1.9 | -2.5 |
| 50 | 0.059 | 8.58E-04 | 3.2 | -3.5 |
| 75 | 0.035 | 1.97E-03 | 3.5 | -2.5 |
| 95 | 0.018 | 1.99E-03 | 3.5 | -2 |

The interpretation of vibration, according to the random vibration theorem [40], is the mean square value of a system response subjected to random PSD excitation $S(f)$ is as follows:

$$\overline{y^2} = \int_0^\infty |H(f)|^2 S_x(f) df, \qquad (8)$$

where $H(f)$ is the system transfer function given by:

$$H(f) = \frac{1/k}{[1-(f/f_n)^2]-i[2\zeta(f/f_n)]} \qquad (8)$$

The transfer function can be acquired experimentally, by determining the natural frequency ($f_n$), the equivalent stiffness (k), and the damping ratio ($\zeta$).

Replacing the next relation to Eq. (7):

$$S_x(f) = PSD(f) = \overline{PSD(f)}(GD)^2 \qquad (9)$$

and applying Eq. (6) to evaluate PSD(f), the vibration response can be approximate via numerical integration [38]. However, in this thesis, the PSD will not be evaluated using the transfer function method discussed above. It is rather indirectly implemented in ANSYS Workbench®. A MATLAB code was generated to find the PSD(f) curves which were obtained by employing the above equations and the data presented in Table 7. Next, the code was run and the PSD versus frequency curves were attained as shown in Figure 11.

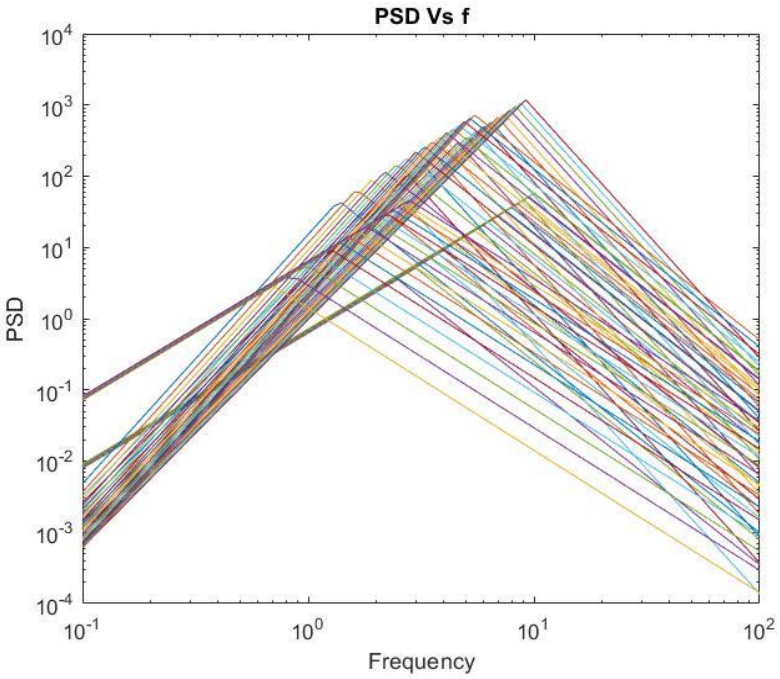


Figure 8. PSD curves generated by MATLAB for different cases.

To simulate different supporting conditions different translational and rotational support stiffnesses were used. Table 8 shows typical values of translational and rotational support stiffnesses that can be found in pipe supports. These values were obtained from [41] where they introduced a new screening method based on the experiment that was conducted.

Table 8. Translational and Rotational Support Stiffness [41].

| Translational Support Stiffness | | Rotational Support Stiffness | |
|---|---|---|---|
| (N/m) | (lb./in) | (N-m/rad) | (lb.-in/rad) |
| 112.9848293 | 1x103 | 1129.848293 | 1x104 |
| 5705.73388 | 5.05x104 | 57057.3388 | 5.05x105 |
| 11298.48293 | 1x105 | 112984.8293 | 1x106 |
| 570573.388 | 5.05x106 | 5705733.88 | 5.05x107 |
| 1129848.293 | 1x107 | 11298482.93 | 1x108 |

The following table summarizes all the parameters and variables used in the analysis.

Table 9. Varied Parameters and Parameter Ranges for FEA Pipe Models

| Variable | Variable Options/Ranges | Assumption |
|---|---|---|
| Pipe OD | NPS 4-6 inches SCH 40 | Random Choice |
| Translational Support Stiffness | Table 4 | Based on the FEA done in [41] |
| Rotational Support Stiffness | Table 4 | Based on the FEA done in [41] |
| Volumetric quality (or homogeneous void fraction), $\beta$ | 25, 50, 75, and 95% | Based on the experiment done in [38] |
| Superficial velocity, V | 5, 6, 7, …, 20 m/s | Typical values of velocity in pipework for hydrocarbons |
| Coefficients: $\bar{f}_0$ , $\overline{PSD(f_0)}$, $m_1$, and $m_2$ | Table 3 | Based on the experiment done in [38] |
| $f$ | 0.1-100 | Uniform Distribution |

# CHAPTER 4: RESULTS ANALYSIS

In this chapter, the results of the models with different cases will be presented. The first section will represent the first main model and its 3 sub-models which were listed in Section 3.3. The second section will show the results of the second main model with its 3 sub-models. And the results of the third model will be presented in the third section.

## 4.1 Models 1

For this model, 3 sub-models with different lengths of run-pipe were considered for analysis. The 3 sub-models consist of a 2-inch, 0.1-meter branch pipe, a 2x6-inch weldolet (SBC), a 5-kg point mass that is connected to the tip of the branch pipe as a representation of a valve, and 3 different run-pipes with 3 different lengths as mentioned in Section. The purpose of this variation is to study the effect of the run-pipe length on the suitability of the VAC when judging the vibration levels. Two different types of results were obtained for this model which are the 1 and 3 sigma results. The 1-sigma results provide a confidence level of 68.27% in the judgment of the VAC. Whereas the 3-sigma results provide a 99.73% confidence level as was explained in Section 3.1. In the following sub-sections, the 1 and 3 sigma results are illustrated for the 3 sub-models.

### *4.1.1 Sub-model 1.1*

1-Sigma confidence results

A total of 1600 cases were simulated for this sub-model. These cases were simulated under different excitations and stiffnesses as mentioned in subsection 3.5. After running the simulation, the obtained results were compared with the (VAC) explained in section 2.3 to find the vibration levels resulting from this random vibration analysis. The results were also compared with the stress limits shown in section 2.4 to check the

stress levels associated with each case. Ideally, the vibration and stress levels for each case should match. For instance, if the vibration level is OK then the stress level should be OK as well. To check whether they match or not, the cases were categorized based on the vibration and stress levels as prescribed in section 3.1 after they were compared with the vibration and stress limits. The categories are appointed by two letters. The first letter stands for the vibration level, if it is Ok, it is denoted as (O), (C) designates the Concern levels, and Problem levels are denoted as (P). The second letter represents the stress levels, and the letter designation is the same as the vibration levels. After comparing all the cases with the criteria, it was found that a total of 1092 cases out of the 1600 cases have Ok vibration levels. 1046 cases out of the 1092 cases have an Ok level of stress, these cases form the first category which is denoted as (OO), 40 cases have concern (C) level of stress which were referred to by (OC), and 6 cases have problem stress levels forming the (OP) category. Furthermore, 323 cases were found to have concern (C) vibration levels. Out of these 323 cases, there are 234 cases with Ok stress level designated by (CO), 51 cases with concern (C) stress level denoted by (CC), and 38 cases with a problem (P) stress level designated by (CP). In addition, 185 cases were found to have a problem (P) vibration level, 10 cases of which, have (OK) stress level and they were denoted by (PO), 21 cases have a concern (C) stress level referred to by (PC), and 154 cases have a problem (P) stress level and those were denoted by (PP). Table 9 summarizes the categories and the number of cases in each category. After categorizing the cases, as shown above, it is noticed that only 1251 cases out of 1600 are matching. Therefore, these results show that the Vibration Acceptance Criteria (VAC) are not 100% accurate when judging the vibration levels in process pipework. So, the question now is how suitable the (VAC) are? Using the above-illustrated results, it can be shown that the (VAC) has a suitability of 78.1875%. This suitability level

means that the vibration acceptance criteria for this sub-model will give correct judgment of the vibration levels 78% of the time with a confidence of 68% only. Table 10 below summarizes all the categories and the number of cases in each category.

Table 10. Classification of Case Categories and the Number of Cases in Each Category for Sub-Model 1.1 (1-Sigma Confidence)

| # | Category | No. of Cases |
|---|---|---|
| 1 | OO | 1046 |
| 2 | OC | 40 |
| 3 | OP | 6 |
| 4 | CO | 234 |
| 5 | CC | 51 |
| 6 | CP | 38 |
| 7 | PO | 10 |
| 8 | PC | 21 |
| 9 | PP | 154 |
| Total | - | 1600 |

Figures 9 through 17 show the above-prescribed categories which are illustrated with respect to the VAC curves. In these graphs, the Orange line (upper line) corresponds to Problem vibration levels, and the blue line (lower line) corresponds to the concern vibration levels. The gray dots represent the cases which were described above. In the graphs below the horizontal axis represent the frequency of vibration in (Hz). Where the left vertical axis represents the RMS vibration velocity of the VAC in (mm/s). And the right vertical axis represents the vibration velocity of the sub-model in (mm/s). It is important to mention that all the graphs are of a logarithmic scale.

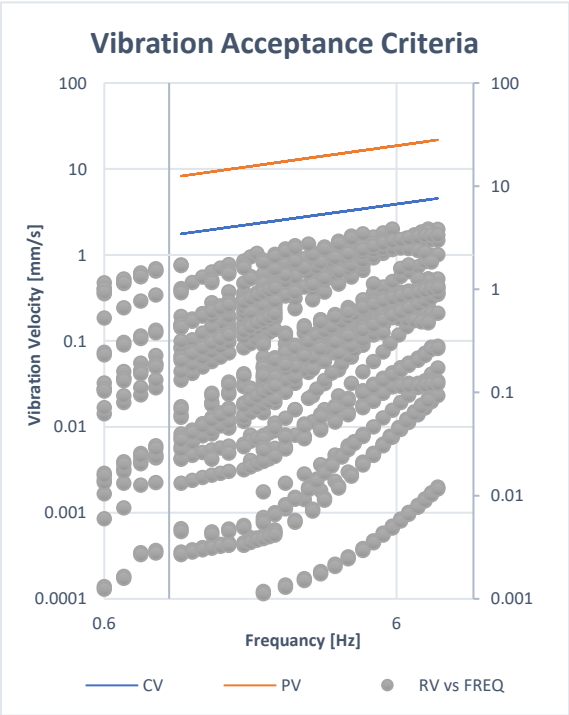


Figure 9. Graph of (OO) category with respect to the VAC lines for sub-model 1.1 (1-Sigma Confidence Results).

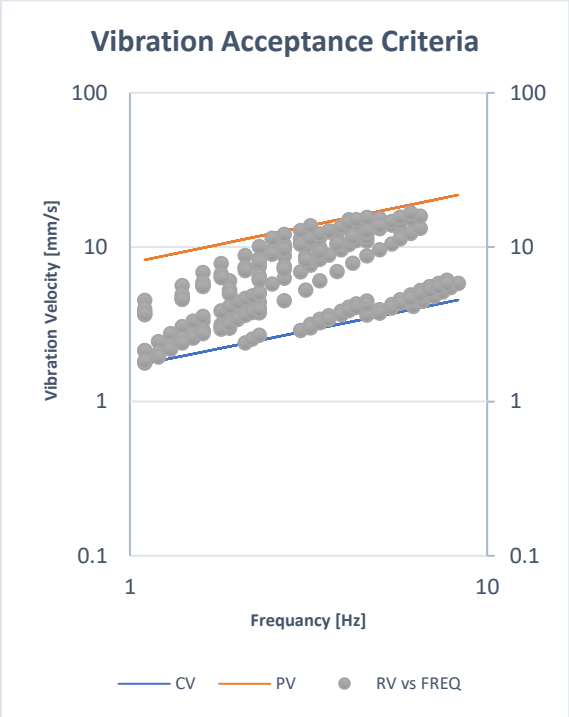


Figure 10. Graph of (CO) category with respect to the VAC lines for sub-model 1.1 (1-Sigma Confidence Results).

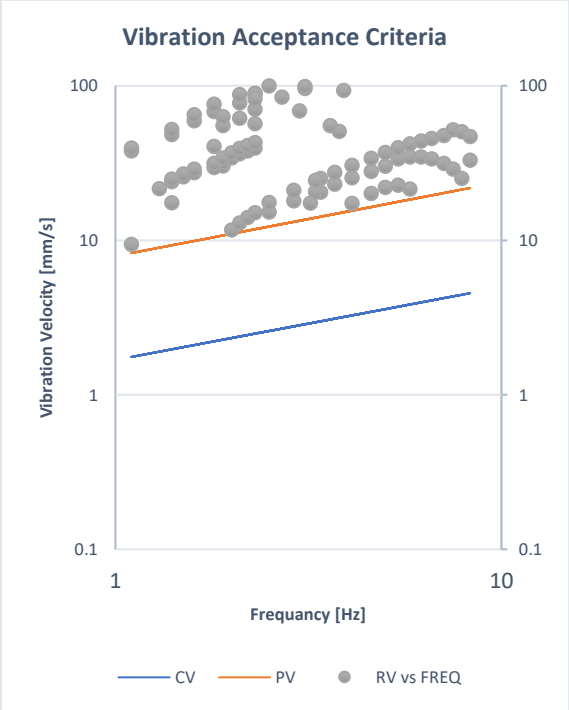


Figure 11. Graph of (PP) category with respect to the VAC lines for sub-model 1.1 (1-Sigma Confidence Results).

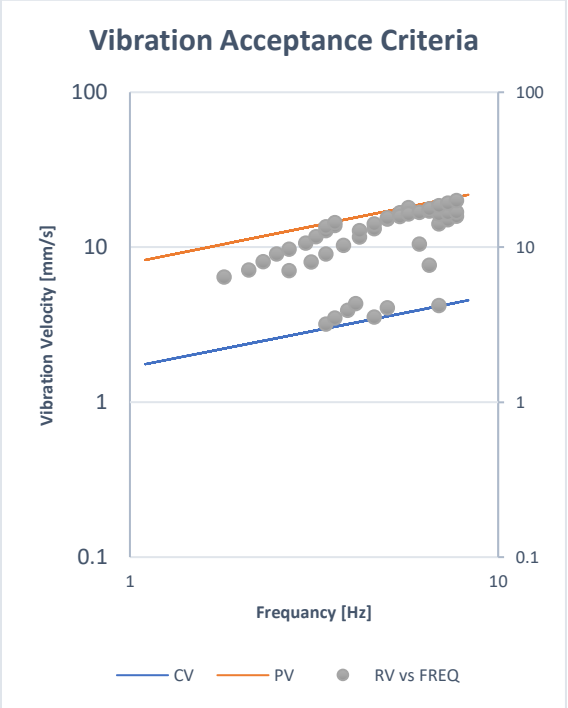


Figure 12. Graph of (CC) category with respect to the VAC lines for sub-model 1.1 (1-Sigma Confidence Results).

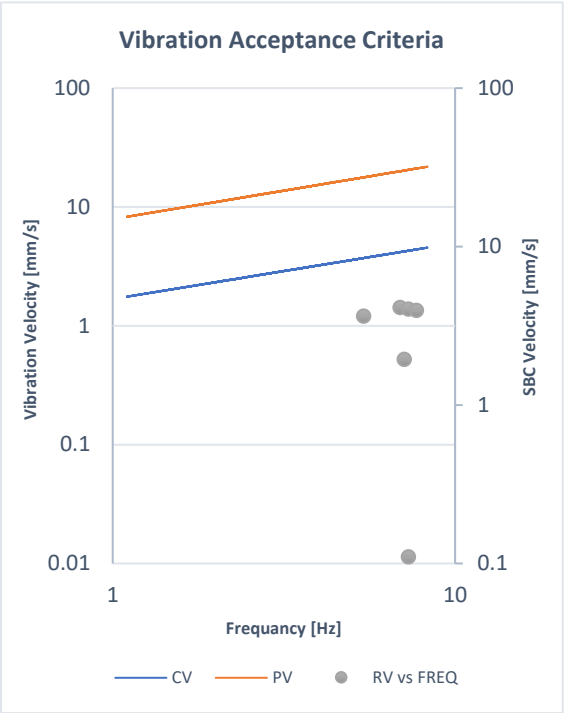


Figure 13. Graph of (OP) category with respect to the VAC lines for sub-model 1.1 (1-Sigma Confidence Results).

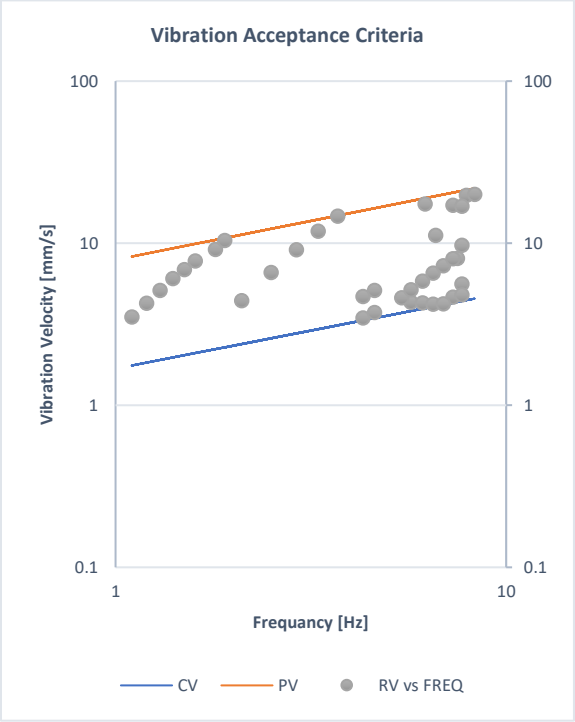


Figure 14. Graph of (CP) category with respect to the VAC lines for sub-model 1.1 (1-Sigma Confidence Results).

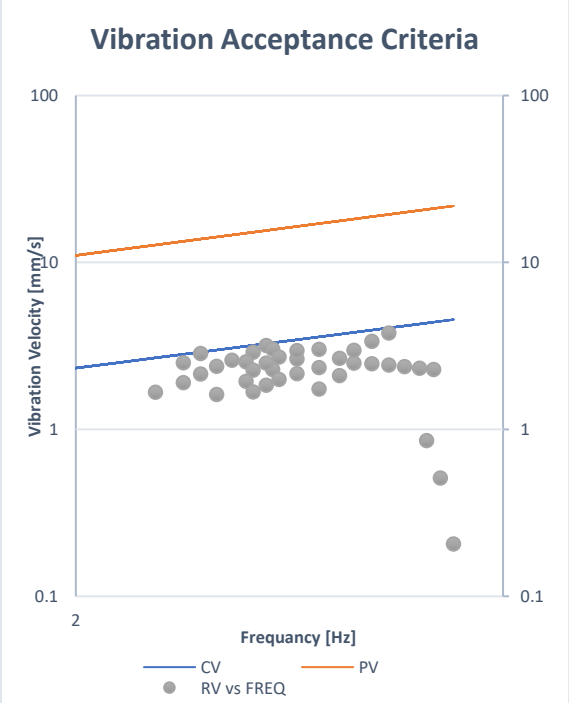


Figure 15. Graph of (OC) category with respect to the VAC lines for sub-model 1.1 (1-Sigma Confidence Results).

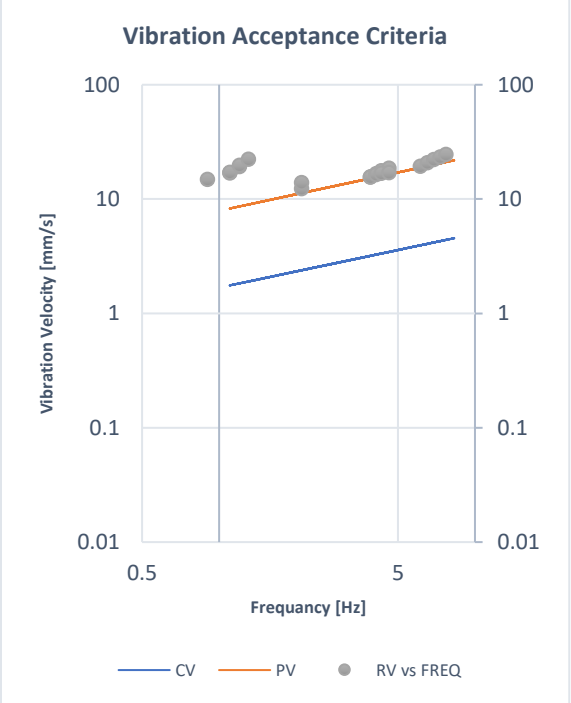


Figure 16. Graph of (PC) category with respect to the VAC lines for sub-model 1.1 (1-Sigma Confidence Results).

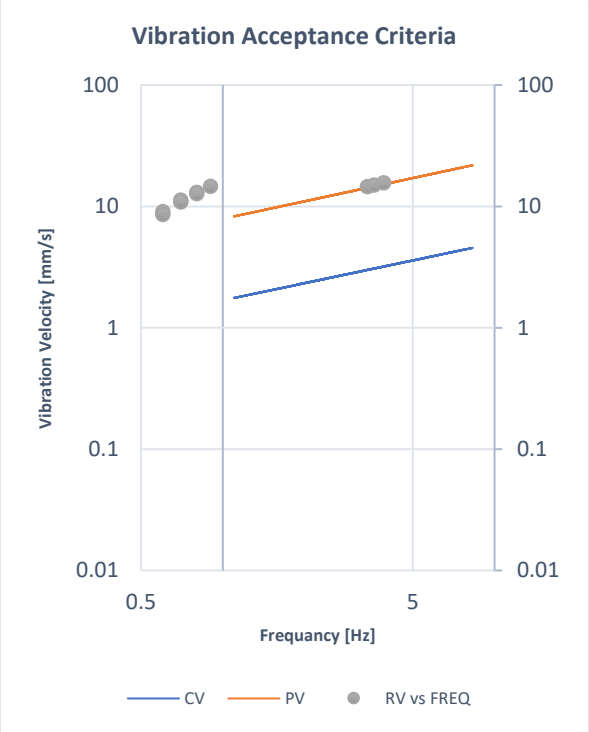


Figure 17 Graph of (PO) category with respect to the VAC lines for sub-model 1.1 (1-Sigma Confidence Results).

3-Sigma confidence results

The same categorization was done on the 3-Sigma results, which were obtained by multiplying the vibration velocity by a factor of 3, and the stress was multiplied by a factor of 6. The distribution of cases in each category has changed and the new distribution of cases is shown in the below table.

From Table 11 it can be shown that the suitability of the VAC in judging the vibration levels have dropped and it is now 65.0625% only. Although, the suitability of the VAC has dropped from 78% for the 1-sigma confidence results to 65% for the 3-sigma confidence results; the confidence has increased from 68.27% for the 1-sigma to 99.73% for the 3-sigma. This means that the VAC almost 100% confidently judges the vibration levels only 65% of the time. In other words, if an operator took a 100-vibration reading of a pipe and compared it with VAC, only 65 of those readings are most likely

to be correctly judged by the VAC. The following figures 18 to 26 show the 3-sigma confidence results with respect to the VAC.

Table 11. Classification of Case Categories and the Number of Cases in Each Category for Sub-Model 1.1 (3-Sigma Confidence).

| # | Category | No. of Cases |
|---|---|---|
| 1 | OO | 560 |
| 2 | OC | 122 |
| 3 | OP | 103 |
| 4 | CO | 146 |
| 5 | CC | 121 |
| 6 | CP | 154 |
| 7 | PO | 10 |
| 8 | PC | 24 |
| 9 | PP | 360 |
| Total | - | 1600 |

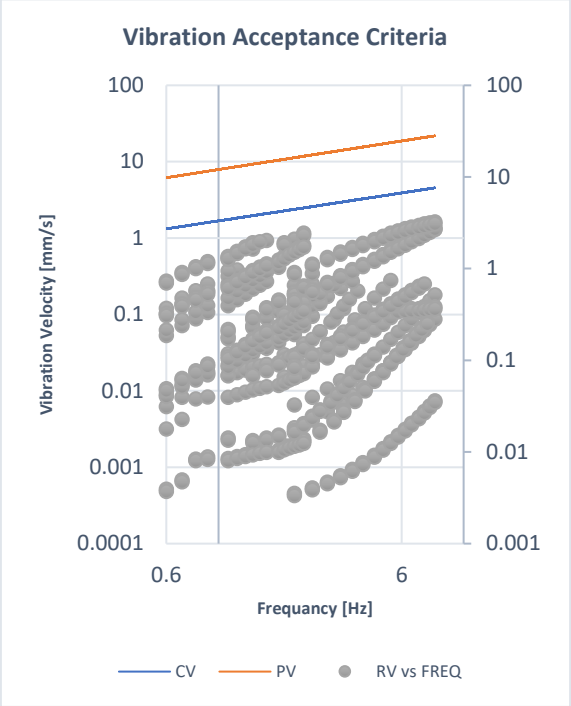


Figure 18. Graph of (OO) category with respect to the VAC lines for sub-model 1.1 (3-Sigma Confidence Results).

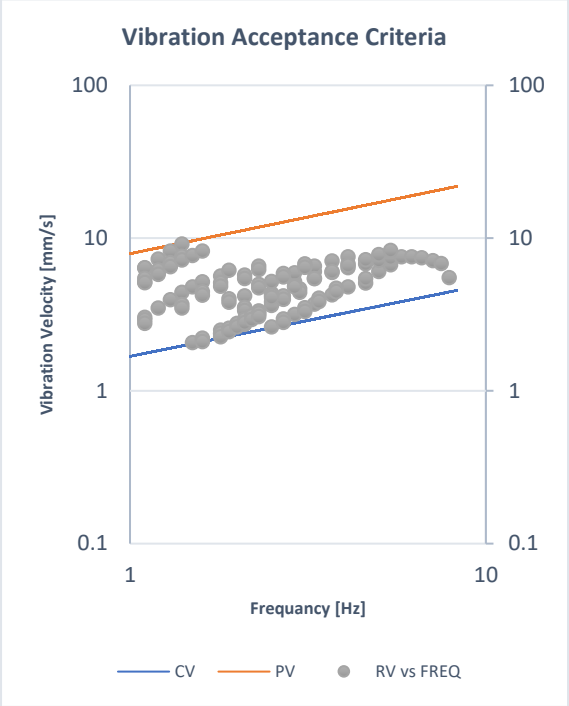


Figure 19. Graph of (CO) category with respect to the VAC lines for sub-model 1.1 (3-Sigma Confidence Results).

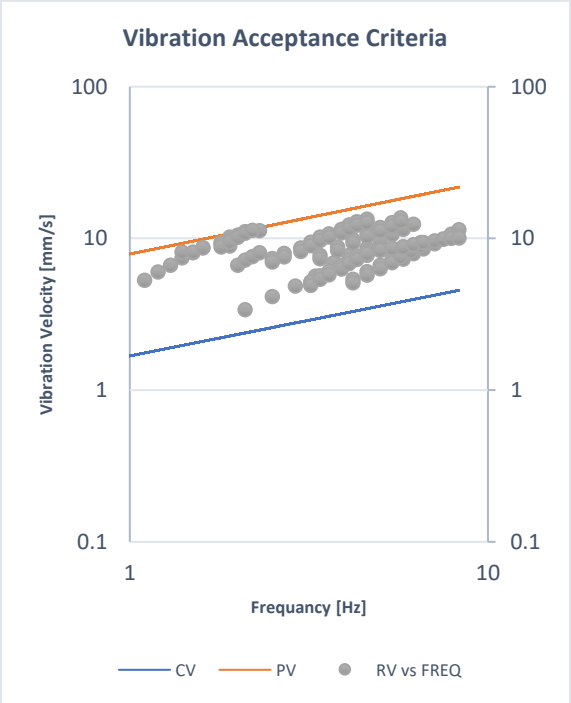


Figure 20. Graph of (CC) category with respect to the VAC lines for sub-model 1.1 (3-Sigma Confidence Results).

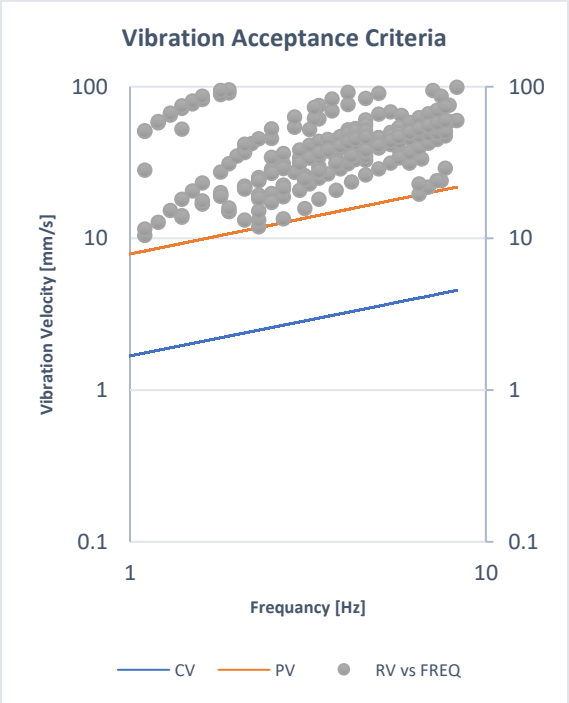


Figure 21. Graph of (PP) category with respect to the VAC lines for sub-model 1.1 (3-Sigma Confidence Results).

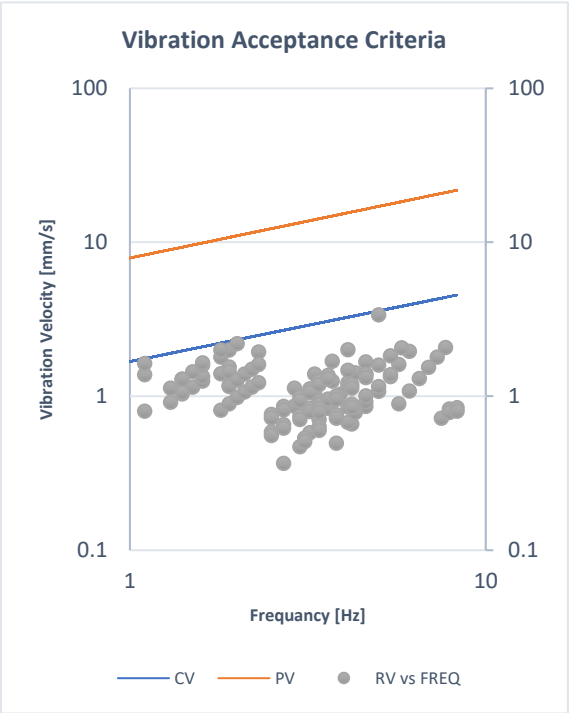


Figure 22. Graph of (OC) category with respect to the VAC lines for sub-model 1.1 (3-Sigma Confidence Results).

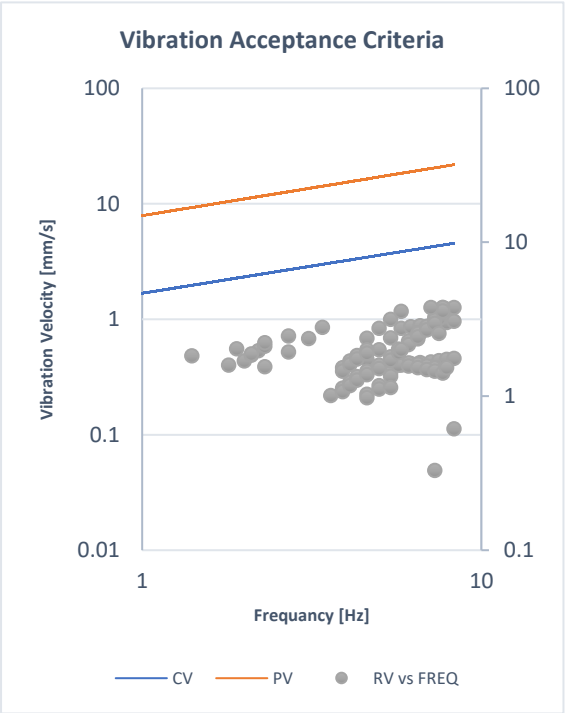


Figure 23. Graph of (OP) category with respect to the VAC lines for sub-model 1.1 (3-Sigma Confidence Results).

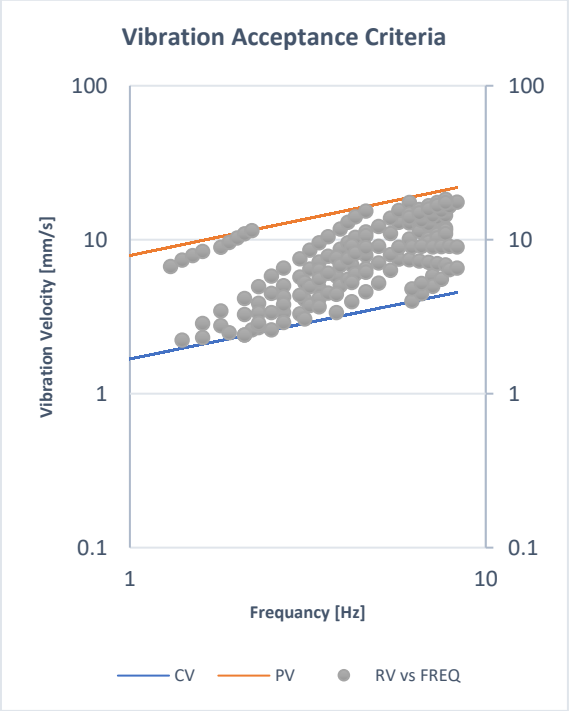


Figure 24. Graph of (CP) category with respect to the VAC lines for sub-model 1.1 (3-Sigma Confidence Results).

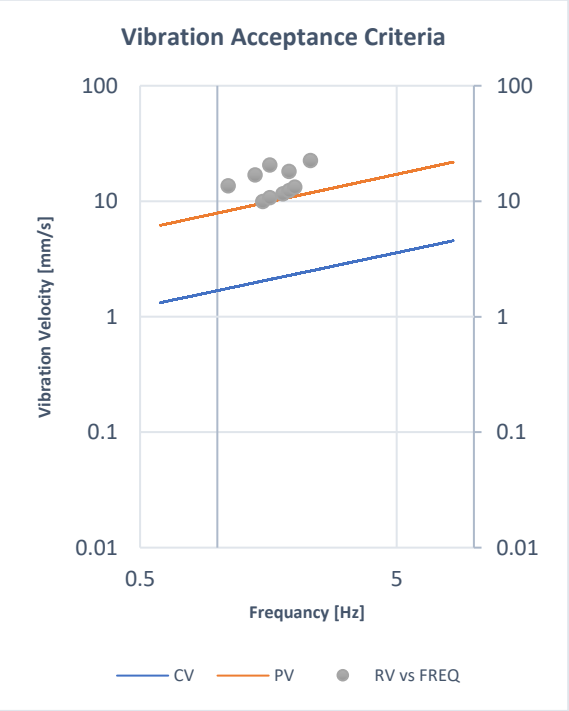


Figure 25. Graph of (PO) category with respect to the VAC lines for sub-model 1.1 (3-Sigma Confidence Results).

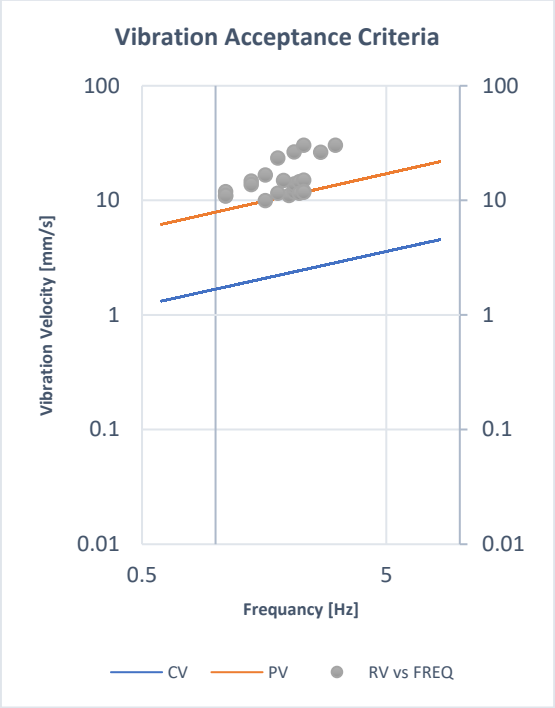


Figure 26. Graph of (PC) category with respect to the VAC lines for sub-model 1.1 (3-Sigma Confidence Results).

### *4.1.2 Sub-model 1.2*

1-Sigma confidence results

For this sub-model, the same 1600 cases were simulated. The results were obtained and compared with the VAC and the stress limits as was done for the previous sub-model 1.1. As expected, the case distribution among the categories has changed. The first category which is (OO) contains 943 cases compared to 1046 cases in the same category for sub-model 1.1. The second category (OC) has 29 cases which were 40 in sub-model 1.1. Furthermore, the third category (OP) consists of 3 cases that were 6 in sub-model 1.1. The (CO), (CC), and (CP) categories have 264, 58, and 25 cases respectively where sub-model 1.1 had 234, 51, and 38 for the same categories representatively. The categories which have problem vibration levels (PO), (PC), and (PP) had 45, 44, 189

cases correspondingly, where the previous sub-model had 10, 21, 154 cases for the same categories. Table 12 shows a summary of the categories and the number of cases in each category. Using these results, it was found that the VAC suitability is 74.375% with a confidence level of 68.27% compared to 82.1875% for sub-model 1.1. This 6% drop proves that the suitability of the VAC is sensitive to the change in the run-pipe length. The below-summarized cases in Table 12 are shown in figures 27 to 35 with respect to the VAC.

Table 12. Classification of Case Categories and the Number of Cases in Each Category for Sub-Model 1.2 (1-Sigma Confidence).

| # | Category | No. of Cases |
|---|---|---|
| 1 | OO | 943 |
| 2 | OC | 29 |
| 3 | OP | 3 |
| 4 | CO | 264 |
| 5 | CC | 58 |
| 6 | CP | 25 |
| 7 | PO | 45 |
| 8 | PC | 44 |
| 9 | PP | 189 |
| Total | - | 1600 |

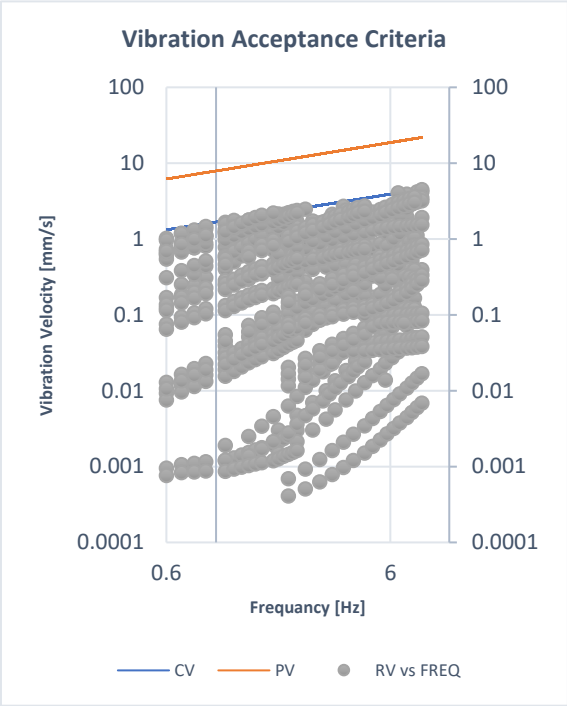


Figure 27. Graph of (OO) category with respect to the VAC lines for sub-model 1.2 (1-Sigma Confidence Results).

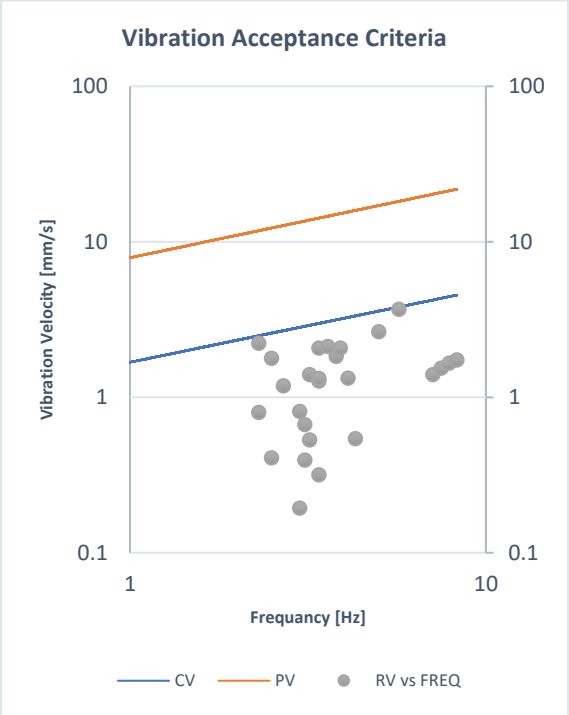


Figure 28. Graph of (OC) category with respect to the VAC lines for sub-model 1.2 (1-Sigma Confidence Results).

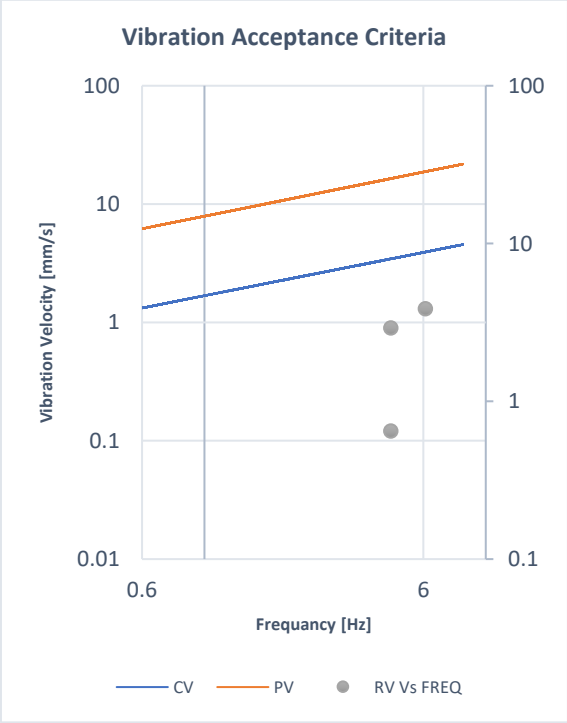


Figure 29. Graph of (OP) category with respect to the VAC lines for sub-model 1.2 (1-Sigma Confidence Results).

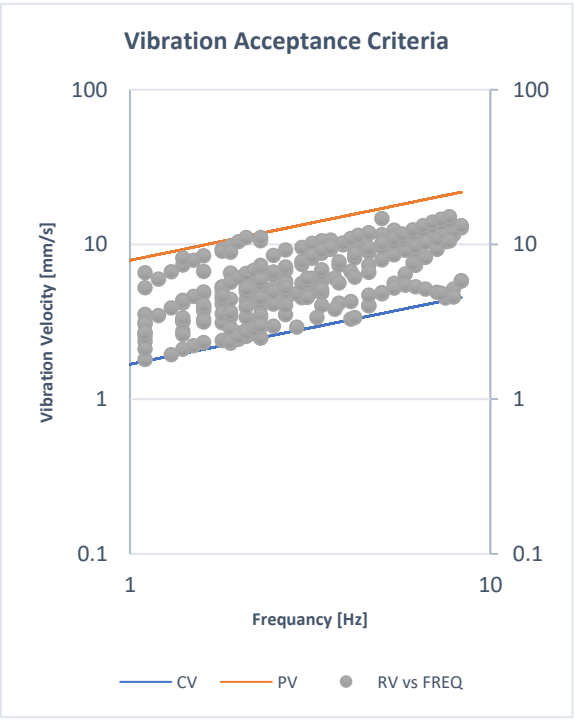


Figure 30. Graph of (CO) category with respect to the VAC lines for sub-model 1.2 (1-Sigma Confidence Results).

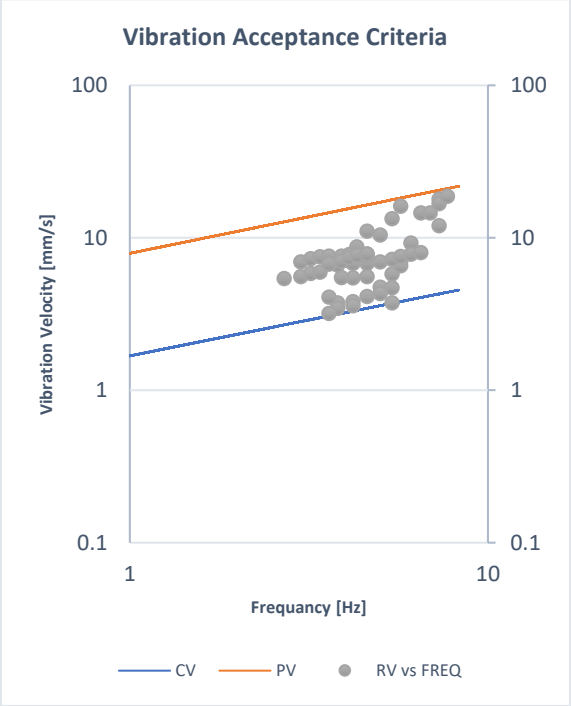


Figure 31. Graph of (CC) category with respect to the VAC lines for sub-model 1.2 (1-Sigma Confidence Results).

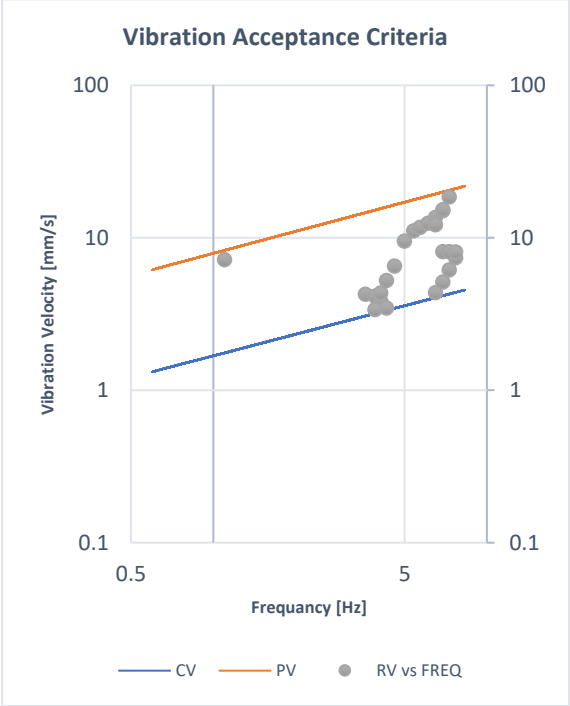


Figure 32. Graph of (CP) category with respect to the VAC lines for sub-model 1.2 (1-Sigma Confidence Results).

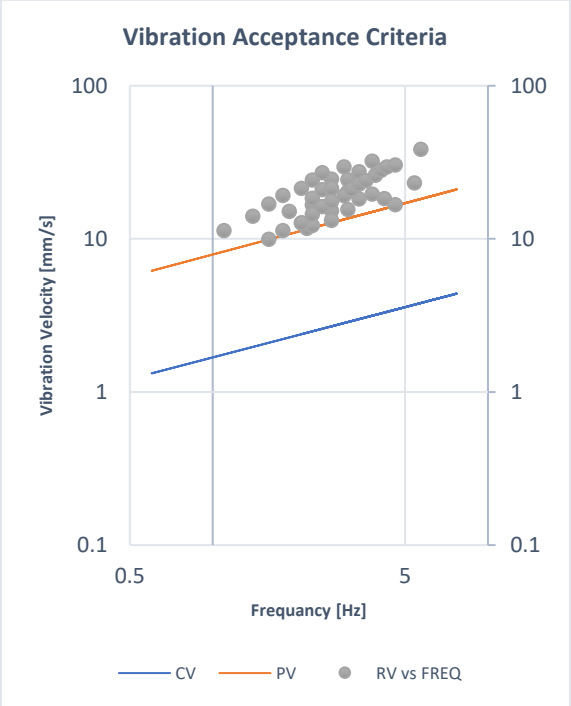


Figure 33. Graph of (PO) category with respect to the VAC lines for sub-model 1.2 (1-Sigma Confidence Results).

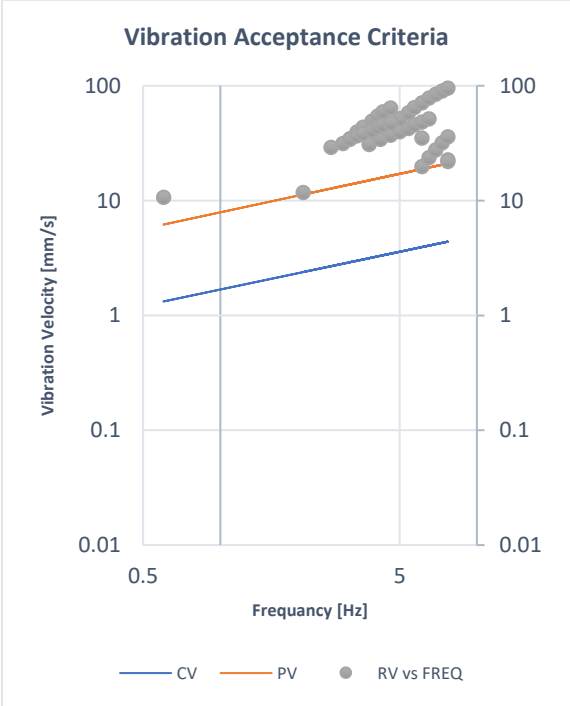


Figure 34. Graph of (PC) category with respect to the VAC lines for sub-model 1.2 (1-Sigma Confidence Results).

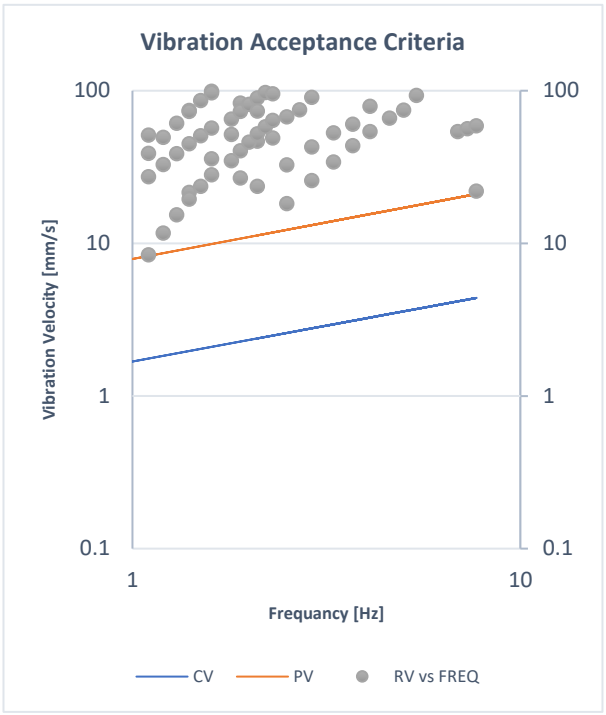


Figure 35. Graph of (PP) category with respect to the VAC lines for sub-model 1.2 (1-Sigma Confidence Results).

3-Sigma confidence results

The three Sigma results of this sub-model show similar behavior to that of sub-model 1.1. For instance, the distribution of cases among the categories has decreased similarly to the first model. For example, the number of cases in the first category (OO) of this model has dropped from 943 cases to 589 cases, while the number of cases in the first sub-model for the same category dropped from 1046 cases to 560 cases. The classification of the cases among the categories of this sub-model is summarized in Table 13. Using the data in this table the suitability of the VAC was found to be 64.375% with a confidence of 99.73%. This value is very close to the value obtained from sub-model 1.1 which was 65.0625%. These results show that the suitability of the VAC at high levels of confidence is not as sensitive to the change in the length of the

run-pipe as it is at lower confidence levels. Although, it only gives a correct judgment of the vibration level 64.375% of the time. In the following figure 36 to 44, the cases of each category are presented with respect to the VAC.

Table 13. Classification of Case Categories and the Number of Cases in Each Category for Sub-Model 1.2 (3-Sigma Confidence).

| # | Category | No. of Cases |
|---|---|---|
| 1 | OO | 589 |
| 2 | OC | 79 |
| 3 | OP | 19 |
| 4 | CO | 238 |
| 5 | CC | 96 |
| 6 | CP | 54 |
| 7 | PO | 86 |
| 8 | PC | 94 |
| 9 | PP | 345 |
| Total | - | 1600 |

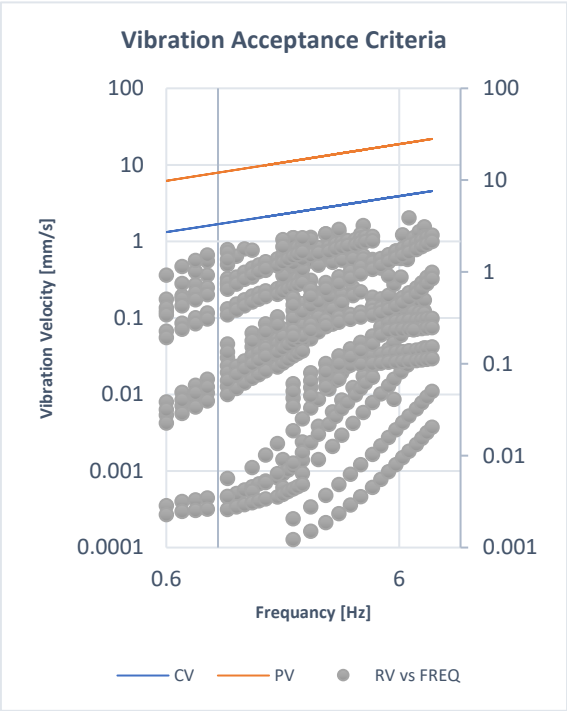


Figure 36. Graph of (OO) category with respect to the VAC lines for sub-model 1.2 (3-Sigma Confidence Results).

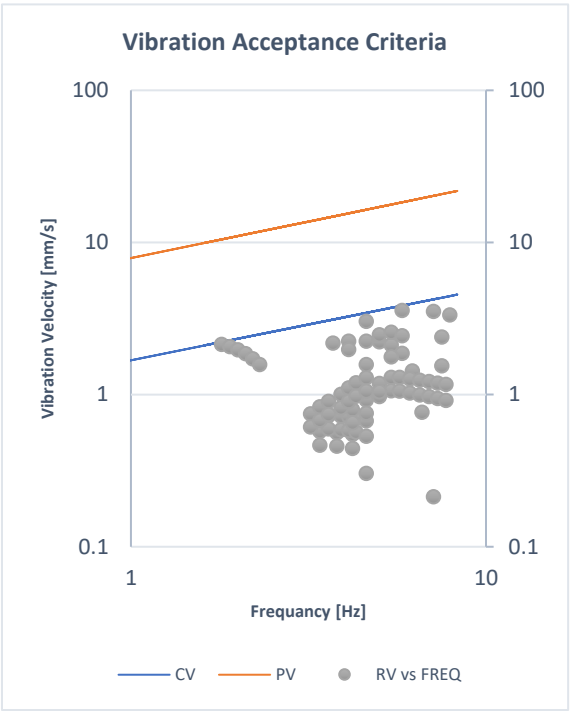


Figure 37. Graph of (OC) category with respect to the VAC lines for sub-model 1.2 (3-Sigma Confidence Results).

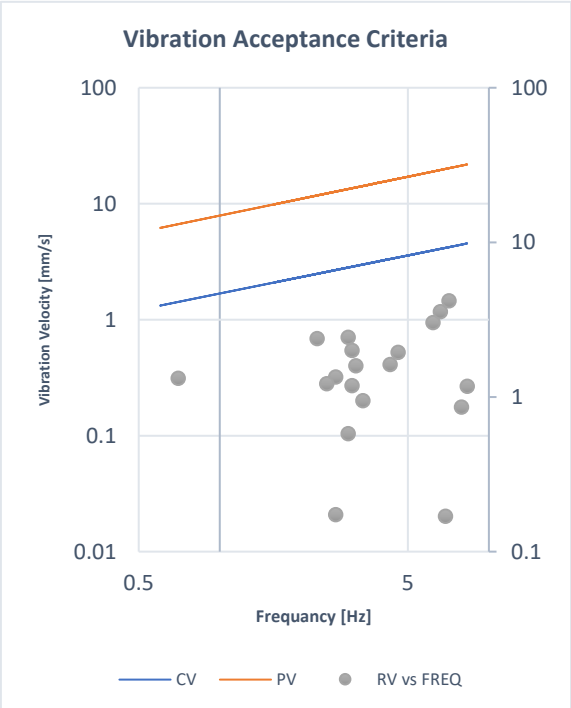


Figure 38. Graph of (OP) category with respect to the VAC lines for sub-model 1.2 (3-Sigma Confidence Results).

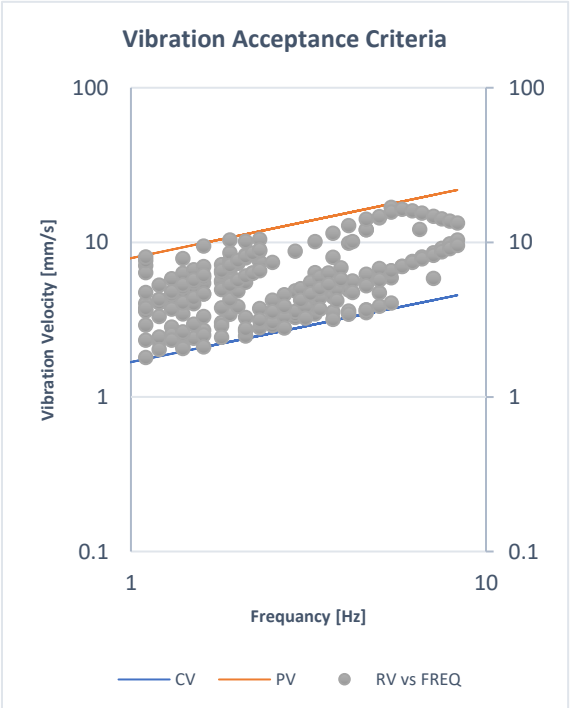


Figure 39. Graph of (CO) category with respect to the VAC lines for sub-model 1.2 (3-Sigma Confidence Results).

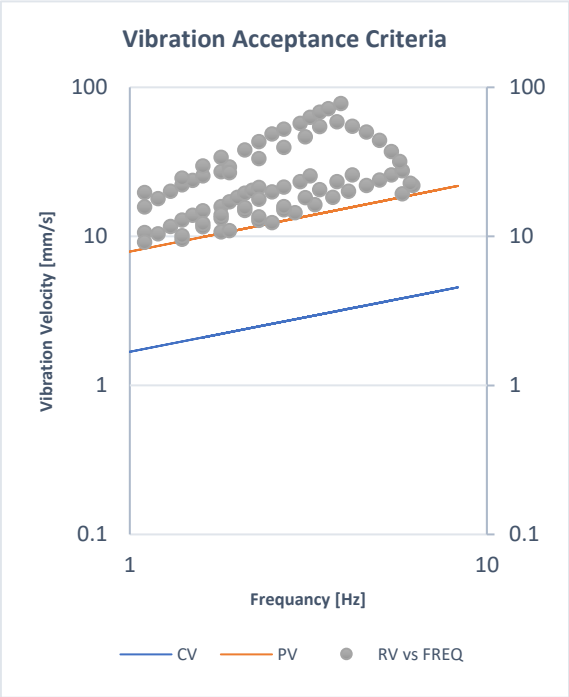


Figure 40. Graph of (CC) category with respect to the VAC lines for sub-model 1.2 (3-Sigma Confidence Results).

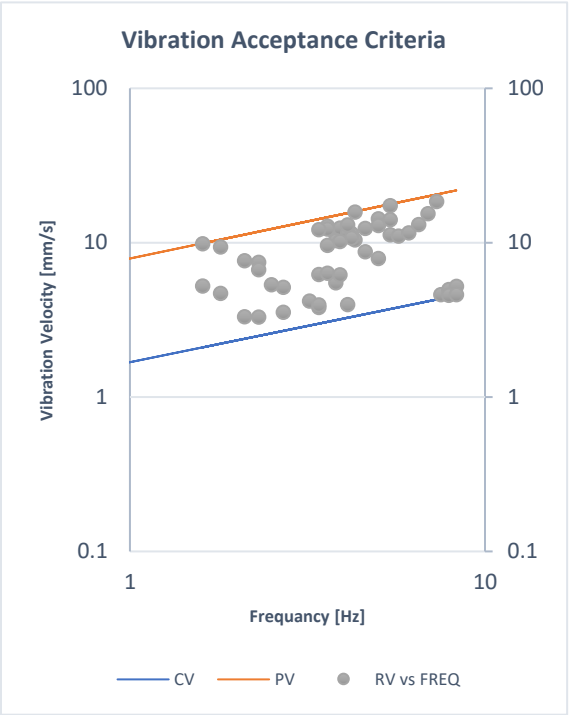


Figure 41. Graph of (CP) category with respect to the VAC lines for sub-model 1.2 (3-Sigma Confidence Results).

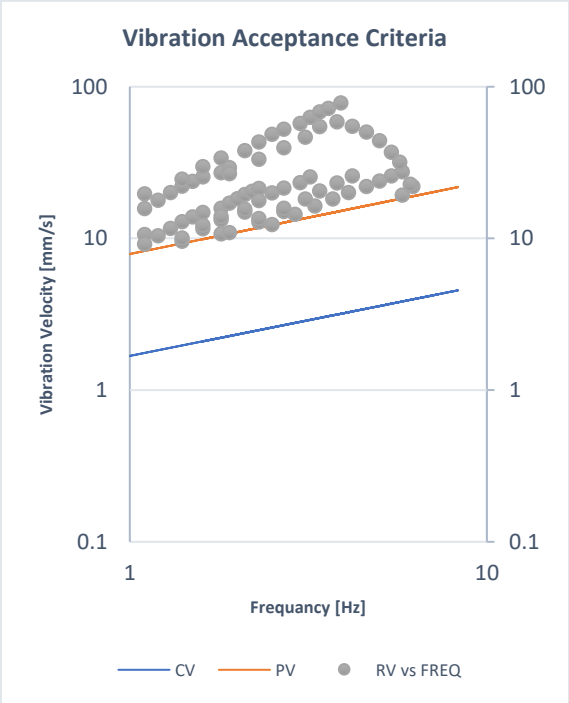


Figure 42. Graph of (PO) category with respect to the VAC lines for sub-model 1.2 (3-Sigma Confidence Results).

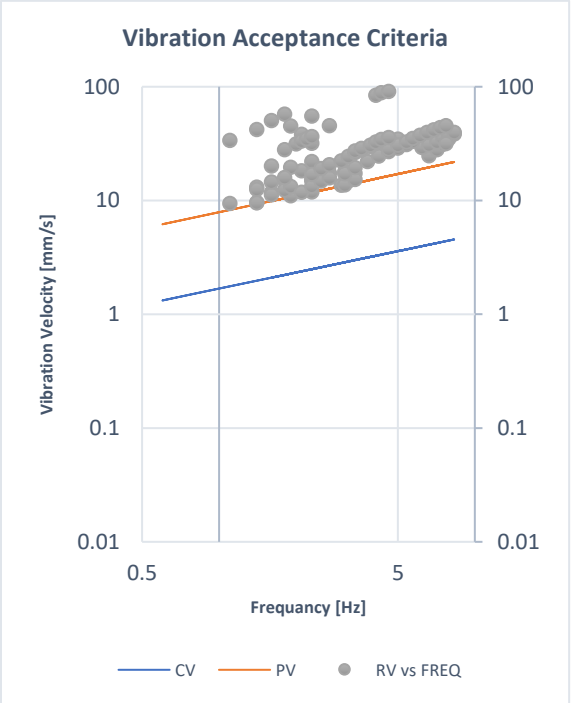


Figure 43. Graph of (PC) category with respect to the VAC lines for sub-model 1.2 (3-Sigma Confidence Results).

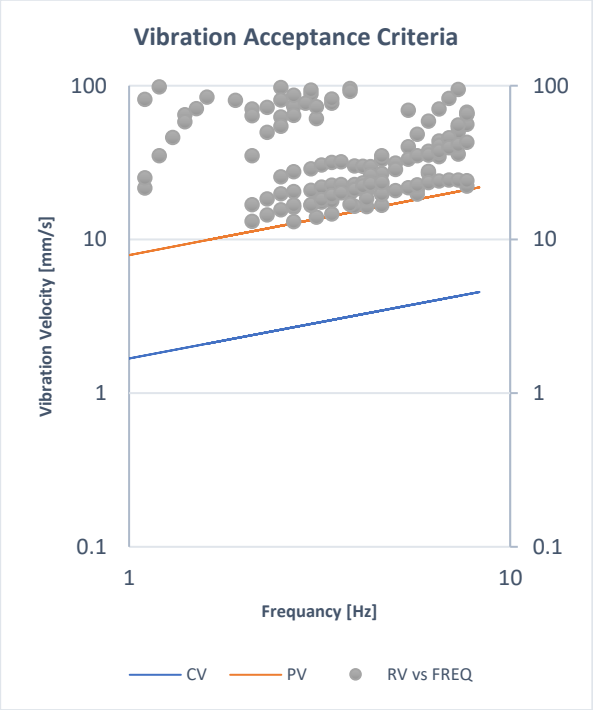


Figure 44. Graph of (PP) category with respect to the VAC lines for sub-model 1.2 (3-Sigma Confidence Results).

### *4.1.3 Sub-model 1.3*

1-Sigma confidence results

This sub-model is the last of three with a run-pipe of 6-inches. It was also simulated with the same 1600 cases that were used for the previous sub-models. Like the 2 sub-models before this one has a different classification of cases among the categories. For instance, the first category (OO) has 929 cases, while the (OC) category has 14 cases, and the (OP) category has 4 cases. The number of cases for each of the concern vibration velocity categories (CO), (CC), and (CP) are 245, 15, and 2, respectively. Moreover, the (PO) category contains 63 cases, whilst the (PC) category has 126 cases, and the (PP) categories have 202 cases. These classifications are summarized in Table 14. Using the below-summarized cases the suitability of the VAC was found to be

71.625% with a confidence of 68% compared to 74% for sub-model 1.2 and 82% for sub-model 1.1. Figures 45 to 53 present the graphs of each of these categories with respect to the VAC.

Table 14. Classification of Case Categories and the Number of Cases in Each Category for Sub-Model 1.3 (1-Sigma Confidence)

| # | Category | No. of Cases |
|---|---|---|
| 1 | OO | 929 |
| 2 | OC | 14 |
| 3 | OP | 4 |
| 4 | CO | 245 |
| 5 | CC | 15 |
| 6 | CP | 2 |
| 7 | PO | 63 |
| 8 | PC | 126 |
| 9 | PP | 202 |
| Total | - | 1600 |

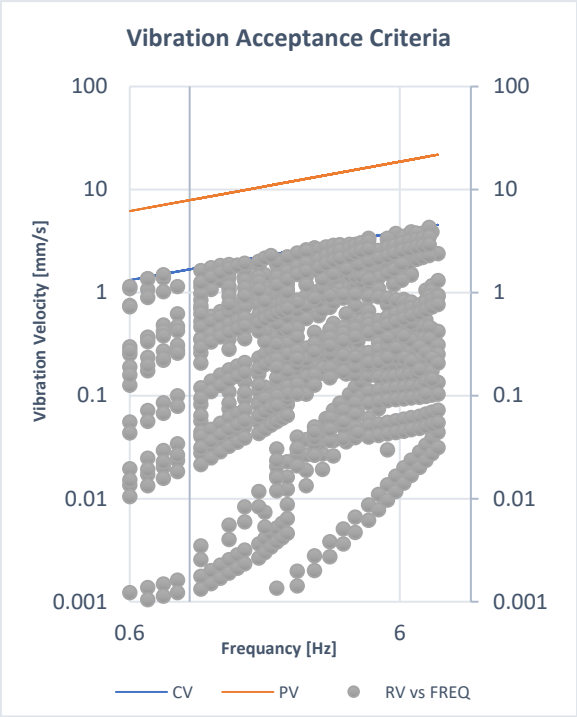


Figure 45. Graph of (OO) category with respect to the VAC lines for sub-model 1.3 (1-Sigma Confidence Results).

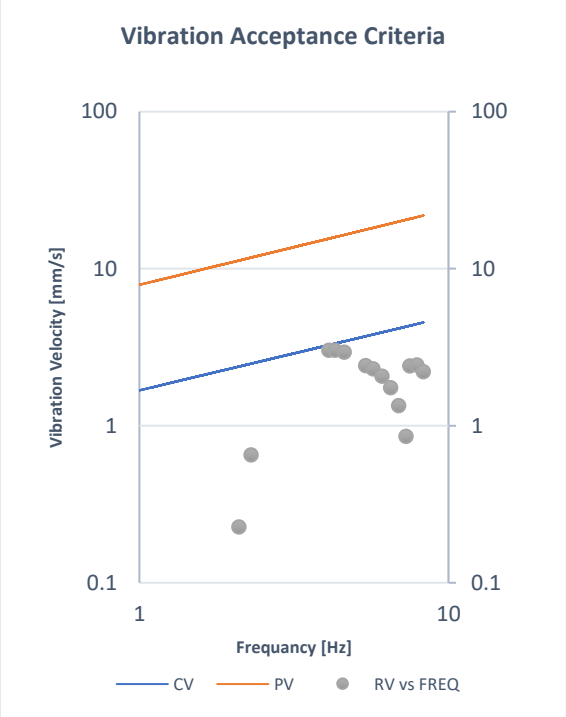


Figure 46. Graph of (OC) category with respect to the VAC lines for sub-model 1.3 (1-Sigma Confidence Results).

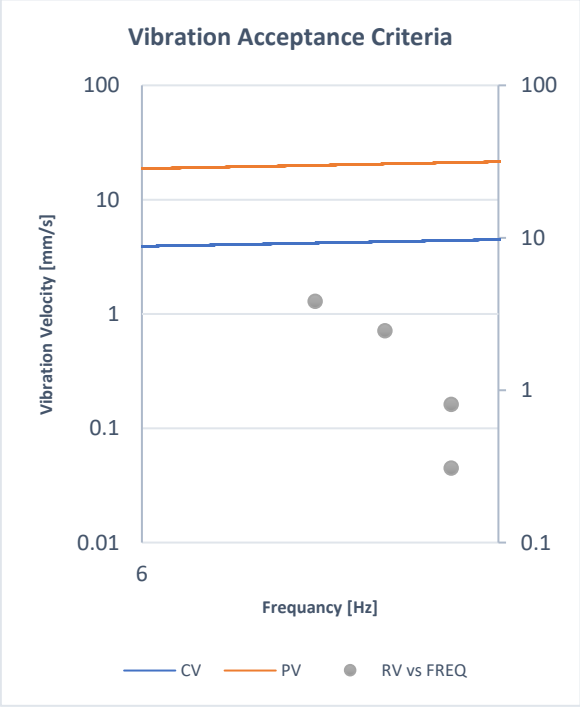


Figure 47. Graph of (OP) category with respect to the VAC lines for sub-model 1.3 (1-Sigma Confidence Results).

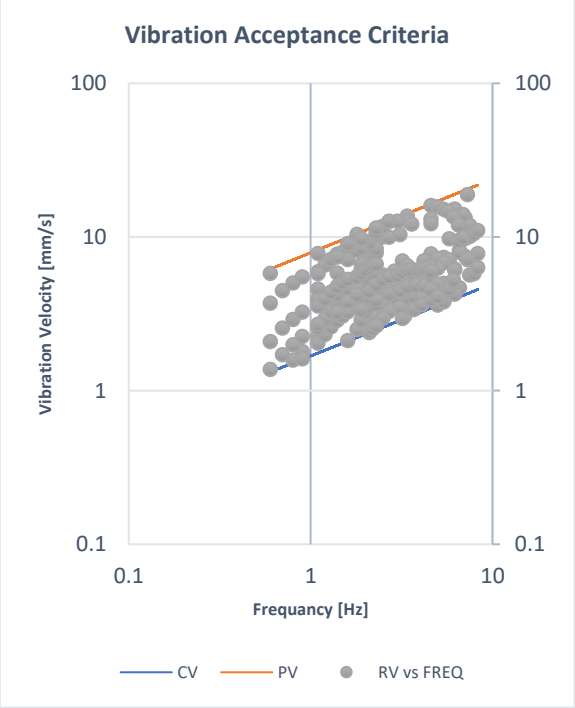


Figure 48. Graph of (CO) category with respect to the VAC lines for sub-model 1.3 (1-Sigma Confidence Results).

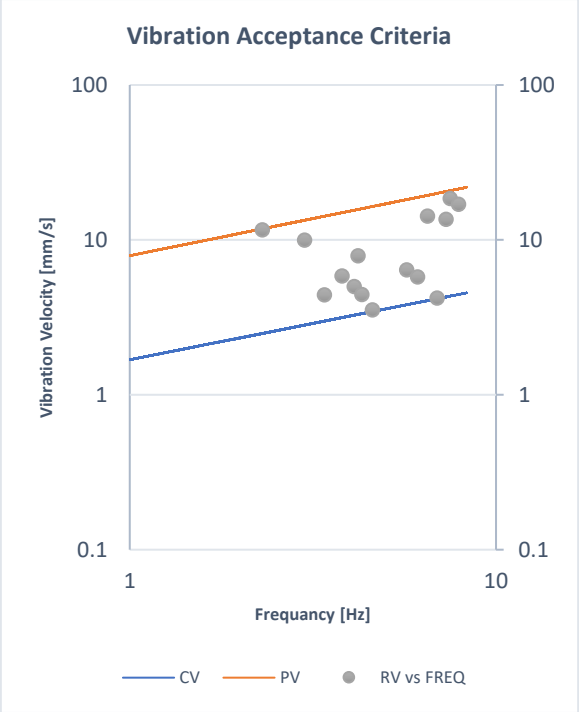


Figure 49. Graph of (CC) category with respect to the VAC lines for sub-model 1.3 (1-Sigma Confidence Results).

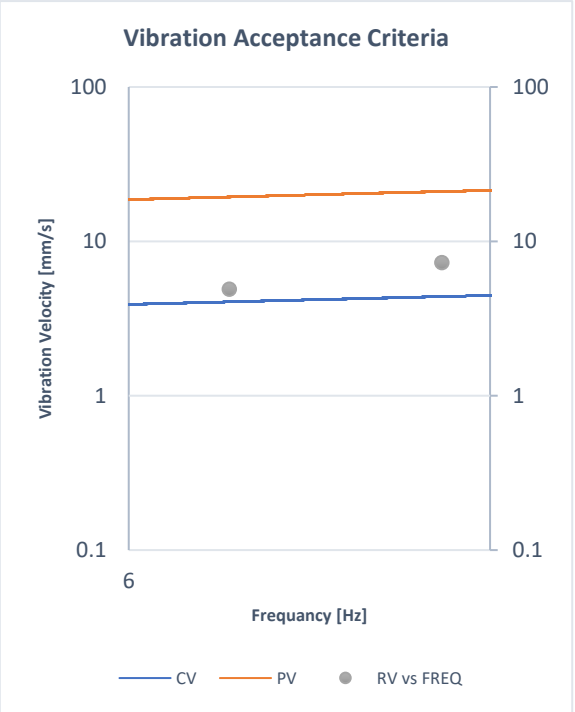


Figure 50. Graph of (CP) category with respect to the VAC lines for sub-model 1.3 (1-Sigma Confidence Results).

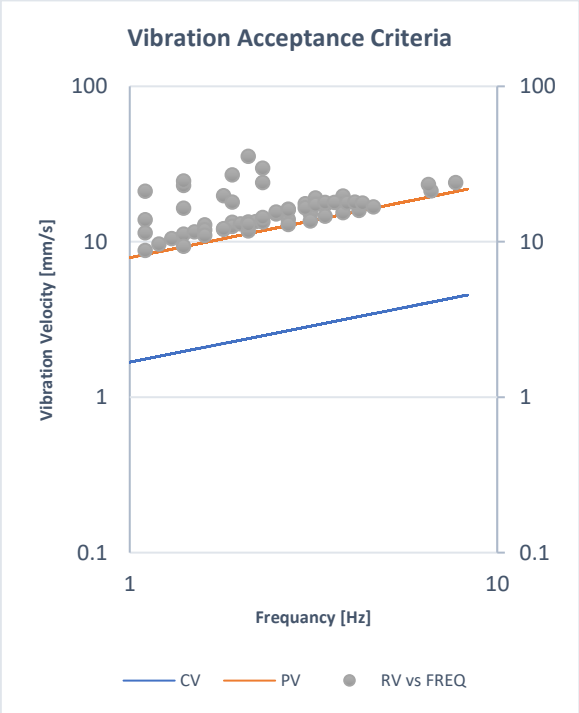


Figure 51. Graph of (PO) category with respect to the VAC lines for sub-model 1.3 (1-Sigma Confidence Results).

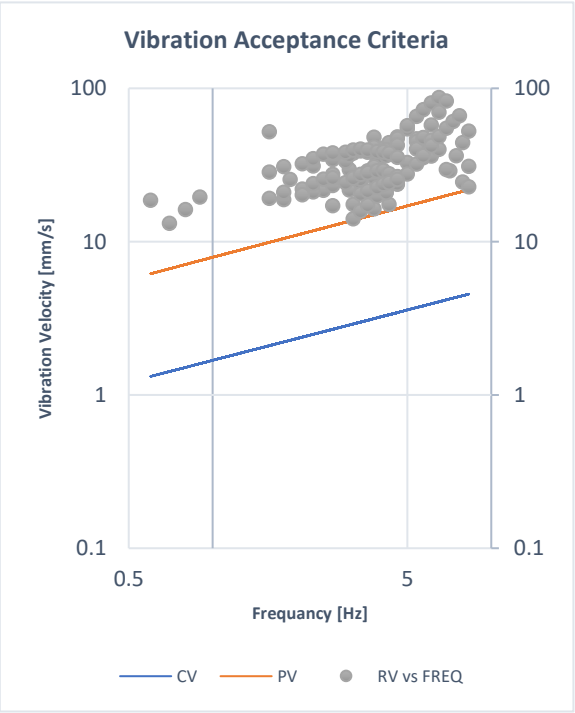


Figure 52. Graph of (PP) category with respect to the VAC lines for sub-model 1.3 (1-Sigma Confidence Results).

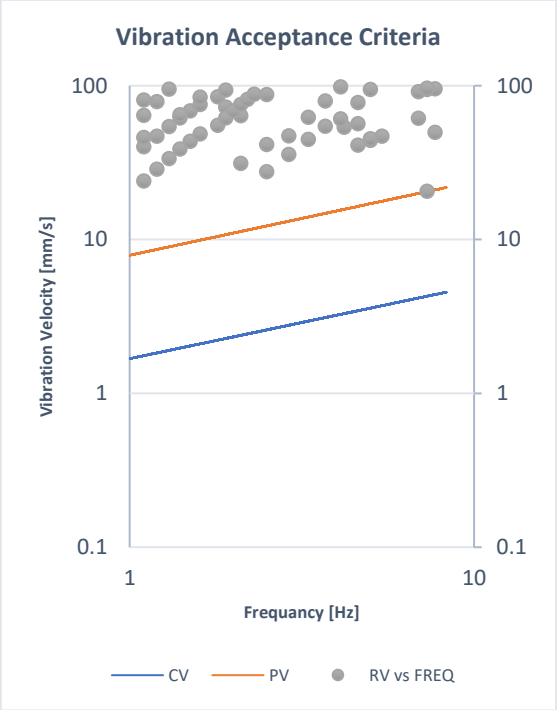


Figure 53. Graph of (PP) category with respect to the VAC lines for sub-model 1.3 (1-Sigma Confidence Results).

3- Sigma confidence results

The 3-sigma results of this sub-model were analyzed and compared with the VAC. After that, the cases were distributed among their respective categories. The Ok vibration level categories which are (OO), (OC), and (OP) consisted of 623, 25, and 8 cases representatively. Furthermore, the concern vibration level categories (CO), (CC), and (CP) had 294 cases, 37 cases, and 43 cases, respectively. The last 3 categories which have problem vibration levels appointed as (PO), (PC), and (PP) have 126 cases, 62 cases, and 382 cases correspondingly. Below Table 15 shows a summary of the categories and the number of cases in each category. The data in the table was used to find the suitability of the VAC considering this model. The suitability of the VAC was found to be 65.125% at a confidence of 99.73% which is almost the same as that of

sub-model 1.1 and sub-model 1.2. Below figures, 54 to 62 are illustrating the graphs of the cases in each category compared with the VAC.

Table 15. Classification of Case Categories and the Number of Cases in Each Category for Sub-Model 1.3 (3-Sigma Confidence)

| # | Category | No. of Cases |
|---|---|---|
| 1 | OO | 623 |
| 2 | OC | 25 |
| 3 | OP | 8 |
| 4 | CO | 294 |
| 5 | CC | 37 |
| 6 | CP | 43 |
| 7 | PO | 126 |
| 8 | PC | 62 |
| 9 | PP | 382 |
| Total | - | 1600 |

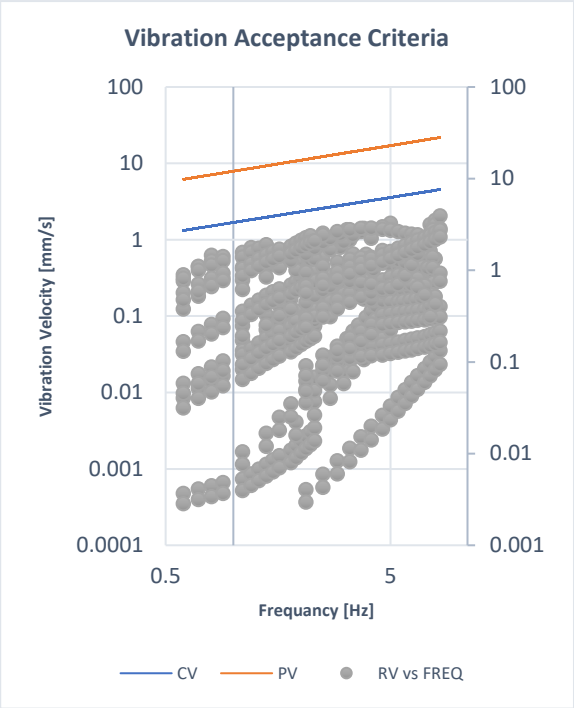


Figure 54. Graph of (OO) category with respect to the VAC lines for sub-model 1.3 (3-Sigma Confidence Results).

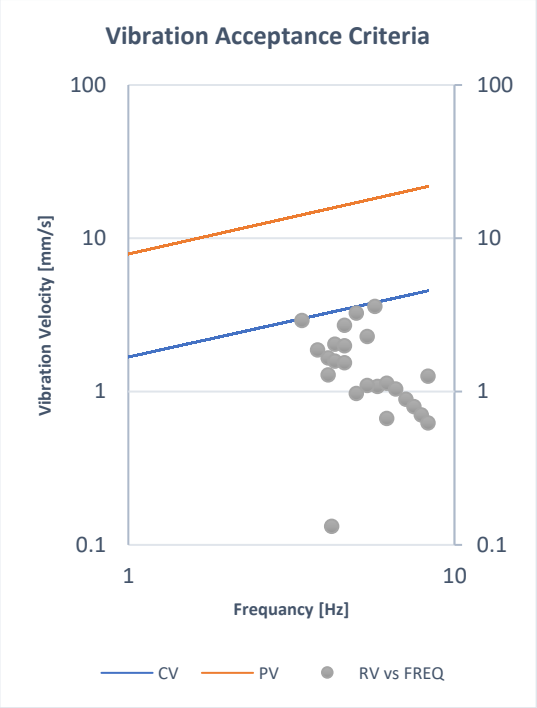


Figure 55. Graph of (OC) category with respect to the VAC lines for sub-model 1.3 (3-Sigma Confidence Results).

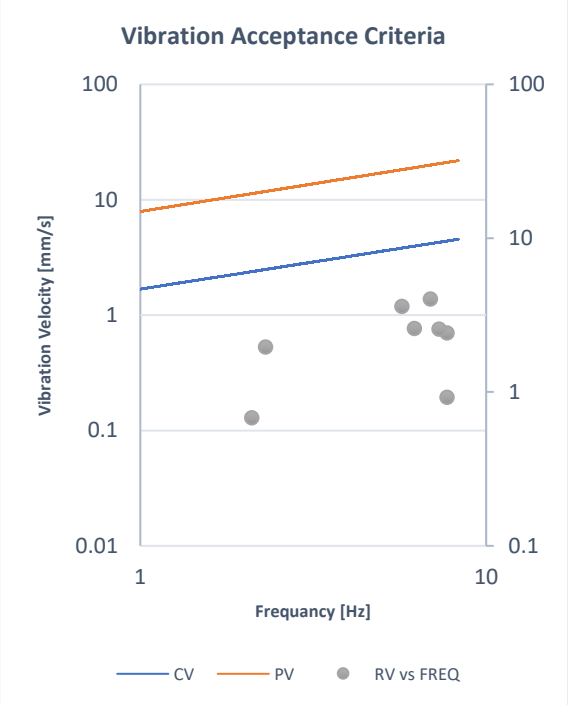


Figure 56. Graph of (OP) category with respect to the VAC lines for sub-model 1.3 (3-Sigma Confidence Results).

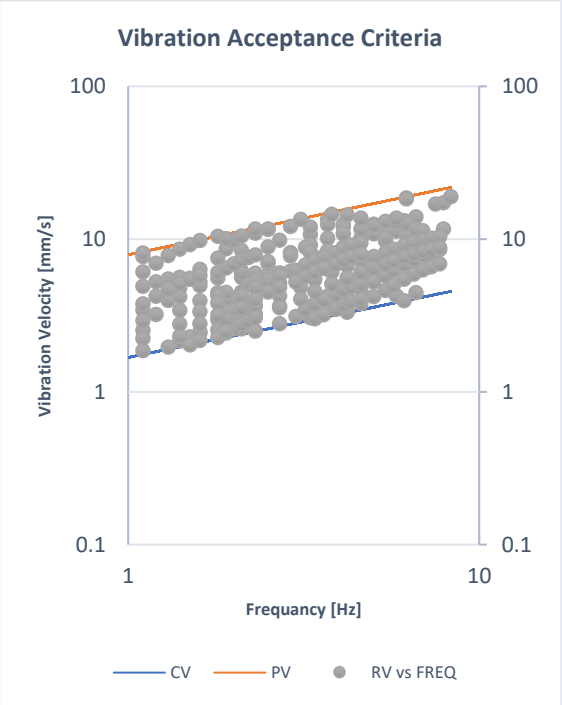


Figure 57. Graph of (CO) category with respect to the VAC lines for sub-model 1.3 (3-Sigma Confidence Results).

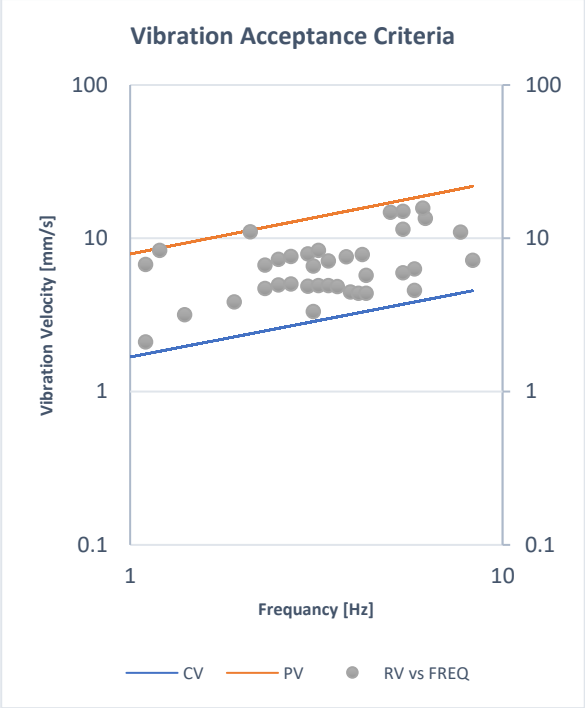


Figure 58. Graph of (CC) category with respect to the VAC lines for sub-model 1.3 (3-Sigma Confidence Results).

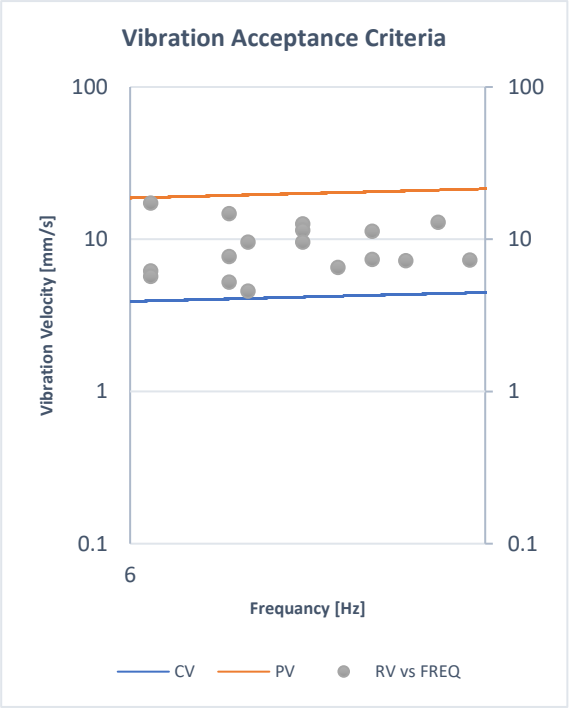


Figure 59. Graph of (CP) category with respect to the VAC lines for sub-model 1.3 (3-Sigma Confidence Results).

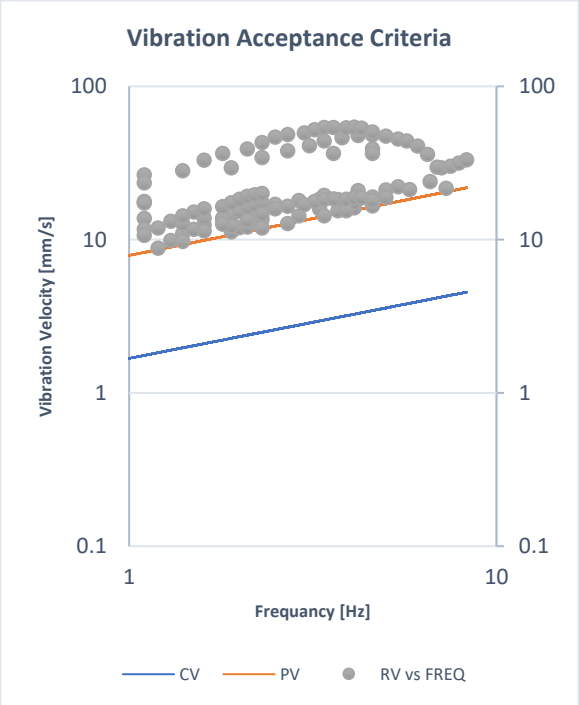


Figure 60. Graph of (PO) category with respect to the VAC lines for sub-model 1.3 (3-Sigma Confidence Results).

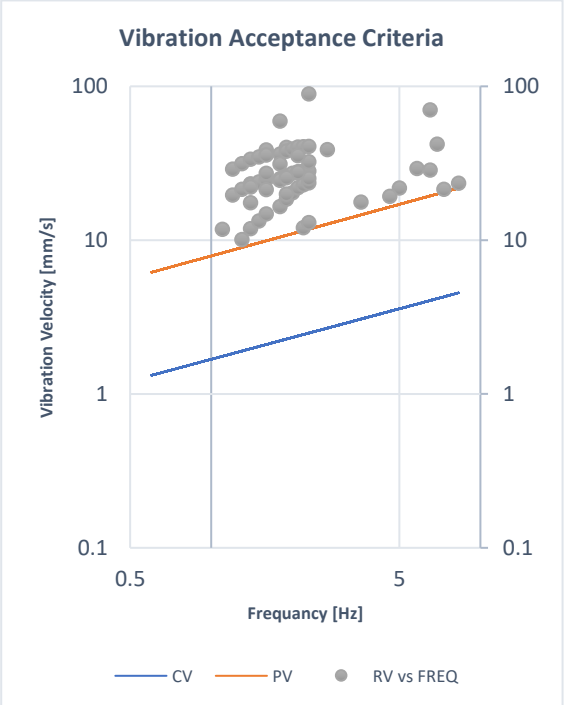


Figure 61. Graph of (PP) category with respect to the VAC lines for sub-model 1.3 (3-Sigma Confidence Results).

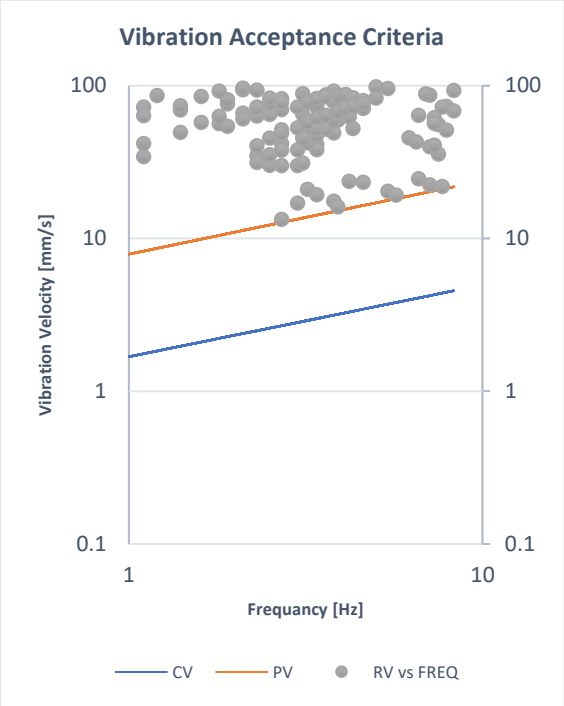


Figure 62. Graph of (PP) category with respect to the VAC lines for sub-model 1.3 (3-Sigma Confidence Results).

*4.1.4 Discussion of model 1*

For this model, 3 different sub-models were investigated to find the effect of the run-pipe length on the suitability of the VAC. The first sub-model has a 0.3-meter-long run-pipe which was excited with 1600 different cases of excitation. The 1-sigma confidence results of this model yielded an 78.1875% suitability level, while the 3-sigma results showed only 65.0625%. These results mean that out of 100 vibration velocity measurements on a 0.3-meter run- pipe the VAC correctly judge 78 of the measured reading with a confidence of 68.27% and 65 readings out of the 100 with 99.73% confidence. The second sub-model has a 1-meter-long run-pipe which was also excited with the same 1600 cases of excitation. The suitability level of the VAC for this model was found to be 74.375% with 68.27% confidence and 64.375% with a 99.73%

confidence. The increase of the length of the run-pipe has decreased the suitability level of the VAC from 78% to 74% for the 1-Sigma confidence, meaning that the VAC only indicates a correct vibration level 74 times out of a 100-vibration reading. Meanwhile, the 3-sigma confidence level has not changed much, as it dropped from 65.0625% for sub-model 1.1 to 64.375% sub-model 1.3. The third and last sub-model has a 1.5-meter run-pipe. This model was investigated with the same excitations and the resulting suitability level was obtained as follows. For the 1-sigma confidence, the suitability level was found to be 71.625%, and the 3-sigma confidence level was 65.125%. this model shows a decrease in the 1-sigma confidence level by about 3% compared to sub-model 1.2 and around 10% compared to sub-model 1.1. Interestingly, the 3-sigma confidence for the 3 sub-models is almost the same, but the problem is that the suitability level is only 65%. This means that the VAC will only give a correct judgment of the vibration velocity measurements 65 % of the time. From the above results, it is advised to use the VAC to judge the vibration velocity of this model when the span of the run-pipe is short to get higher reliability of the VAC.

### 4.2 Model 2

Three different sub-models were investigated for this model. The 3 sub-models consist of a 2-inch, 0.1-meter branch pipe, a 2x5-inch weldolet (SBC), a 5-kg point mass that is connected to the tip of the branch pipe as a representation of a valve mass, and 3 different run-pipes with 3 different lengths. This variation intends to study the effect of the run-pipe length on the suitability of the VAC when judging the vibration levels. Two different types of results were obtained for this model which are the 1 and 3 sigma results. The 1-sigma results provide a confidence level of 68.27% in the judgment of the VAC. Whereas the 3-sigma results provide a 99.73% confidence level as prescribed in Section 3.1.

*4.2.1 Sub-model 2.1*

1-Sigma confidence results

A total of 1600 cases were simulated for this sub-model. These cases consist of a variety of supporting stiffnesses, flow velocities, and volumetric quality (or homogeneous fraction of the void) which are explained in section 3.5. After obtaining the results for these cases they were compared with the Vibration Acceptance Criteria (VAC) to find out the vibration levels resulting from this random vibration analysis. The results were also compared with the stress limits to check the stress levels for each case to verify whether the judgment of the VAC is correct or not. After comparing all cases with vibration velocity and stress limits they were categorized based on the vibration and stress levels as follows. The categories are denoted by two letters, the first one refers to the vibration level, and the second one refers to the stress level. The first category contains all the cases with ok levels of vibration velocity and stress. This category has a total of 1048 cases out of the 1600 cases and is denoted by (OO). The second category which is referred to by (OC) contains 72 cases that have ok (O) levels of vibration velocity and concern (C) levels of stress. 88 cases were found to have ok (O) levels of vibration and problem (P) stress levels, and these cases form the third category which was referred to by (OP). Furthermore, 269 cases were found to have concern (C) vibration levels. Out of these 269 cases, there are 87 cases with ok (O) stress levels, which shape the fourth category designated by (CO). the fifth category has 54 cases with concern (C) stress level and is de-noted by (CC). The remaining 128 cases out of the 269 cases are having a problem (P) stress levels creating the sixth category designated by (CP). In addition, the seventh category which is referred to by (PO) has no cases and the eighth category has only 1 case which has problem vibration level and concern (C) stress level and was denoted by (PC). The last category is referred to by

(PP) and it contains 122 cases that have a problem (P) vibration and stress levels. The following table shows a summary of all the categories and the number of cases in each category. From Table 16, it can be seen that a total of 1224 cases were correctly judged by the VAC. For instance, the stress levels were found to be ok when the vibration levels were ok, the stress levels were a concern when the vibration levels were a concern, and the stress levels were a problem when the vibration levels were a problem. These 1224 cases represent 76.5% of the 1600 cases that were used for the simulation. The results presented in Table 16 and Figure 63 to Figure 70 below are having confidence of 68.27 %. This means that 76.5 % of the time the VAC can be used to correctly judge the vibration levels with a confidence of 68.27%.

Table 16. Classification of Cases Categories and the Number of Cases in Each Category for Sub-Model 2.1 (1-Sigma Confidence)

| # | Category | No. of Cases |
|---|---|---|
| 1 | OO | 1048 |
| 2 | OC | 72 |
| 3 | OP | 88 |
| 4 | CO | 87 |
| 5 | CC | 54 |
| 6 | CP | 128 |
| 7 | PO | 0 |
| 8 | PC | 1 |
| 9 | PP | 122 |
| Total | - | 1600 |

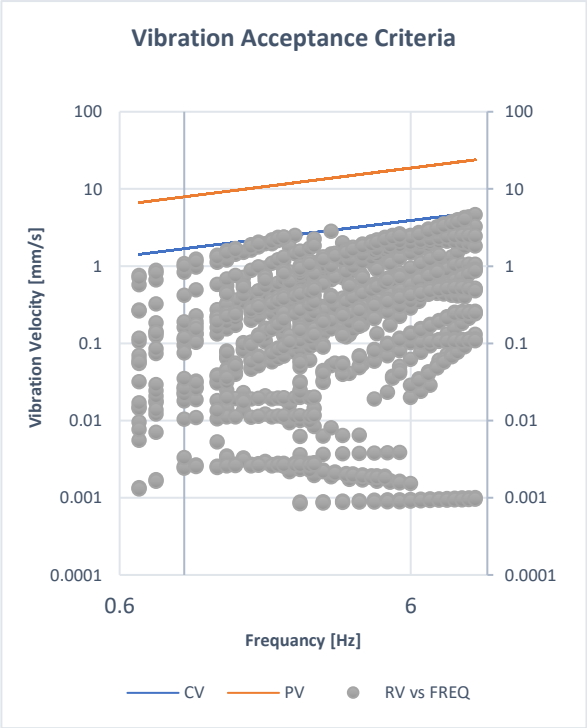


Figure 63. Graph of (OO) category with respect to the VAC lines for sub-model 2.1 (1-Sigma Confidence Results).

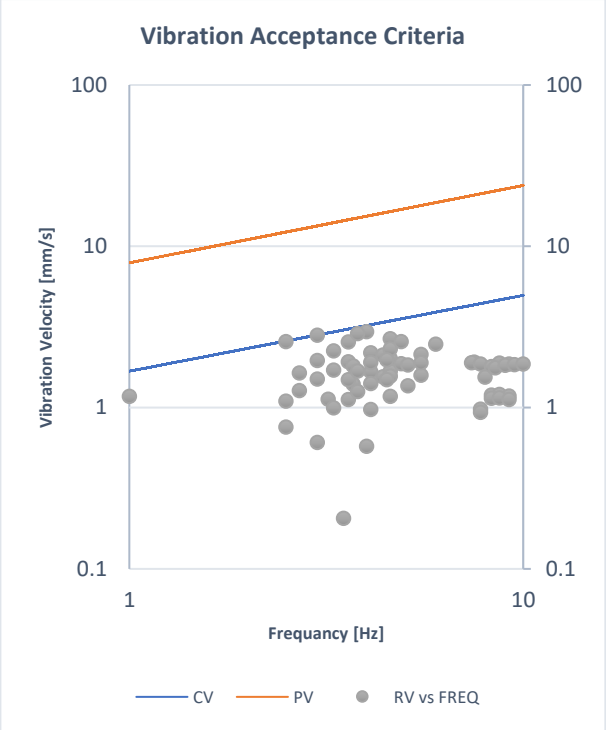


Figure 64. Graph of (OC) category with respect to the VAC lines for sub-model 2.1 (1-Sigma Confidence Results).

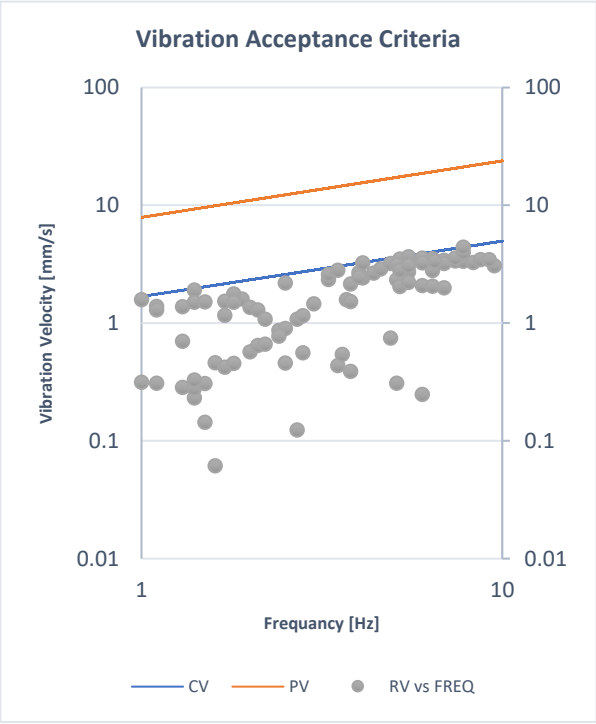


Figure 65. Graph of (OP) category with respect to the VAC lines for sub-model 2.1 (1-Sigma Confidence Results).

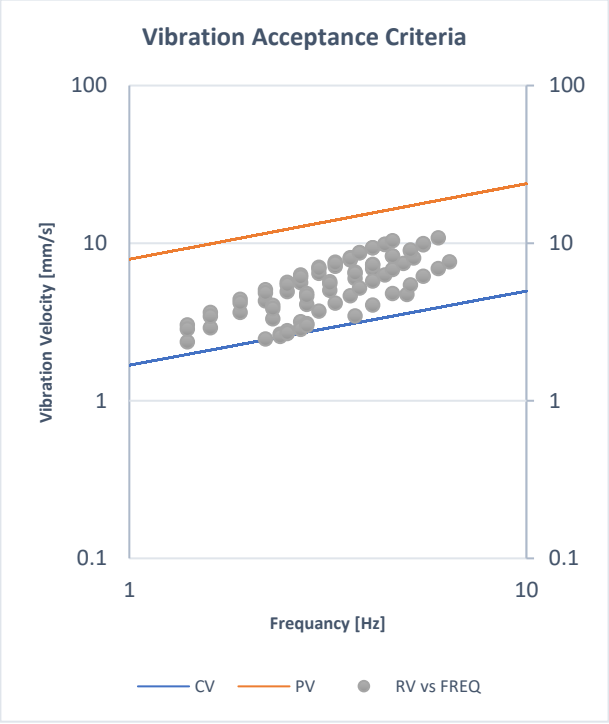


Figure 66. Graph of (CO) category with respect to the VAC lines for sub-model 2.1 (1-Sigma Confidence Results).

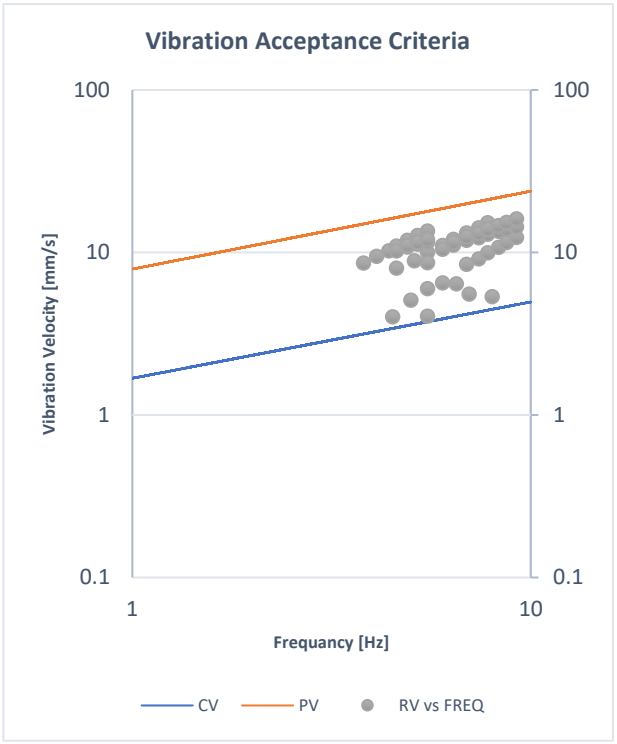


Figure 67. Graph of (CC) category with respect to the VAC lines for sub-model 2.1 (1-Sigma Confidence Results).

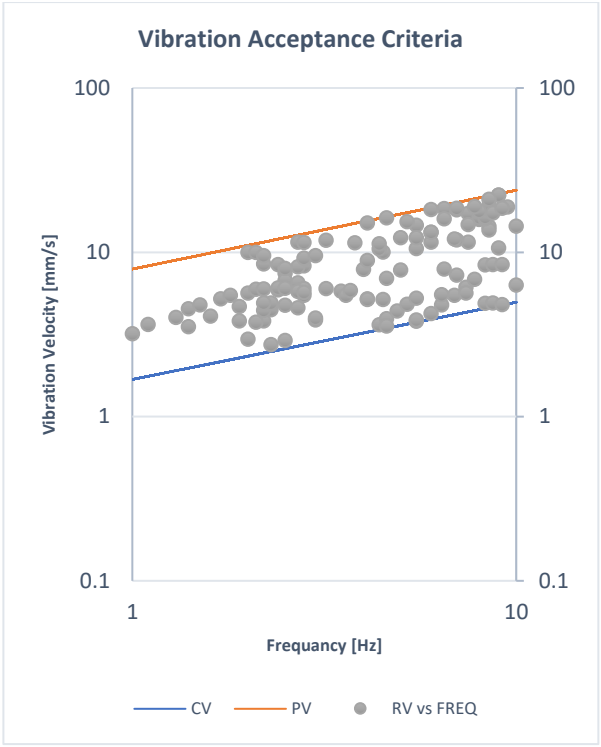


Figure 68. Graph of (CP) category with respect to the VAC lines for sub-model 2.1 (1-Sigma Confidence Results).

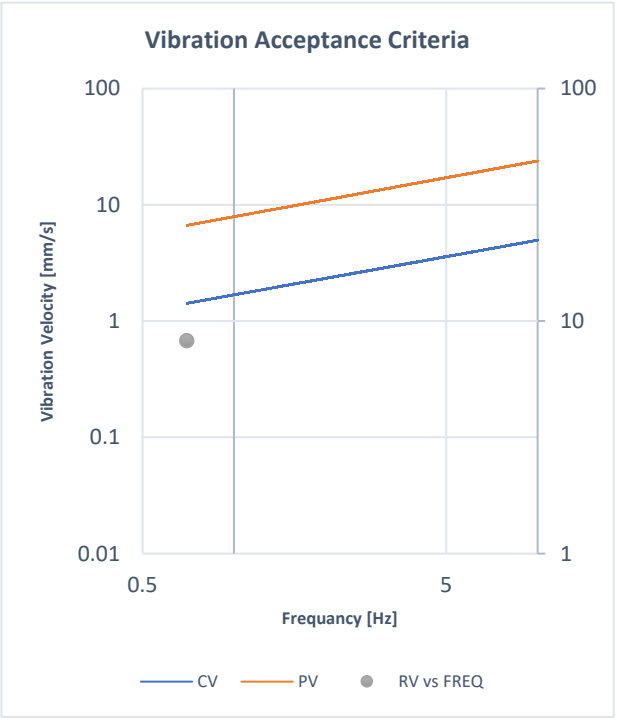


Figure 69. Graph of (PC) category with respect to the VAC lines for sub-model 2.1 (1-Sigma Confidence Results).

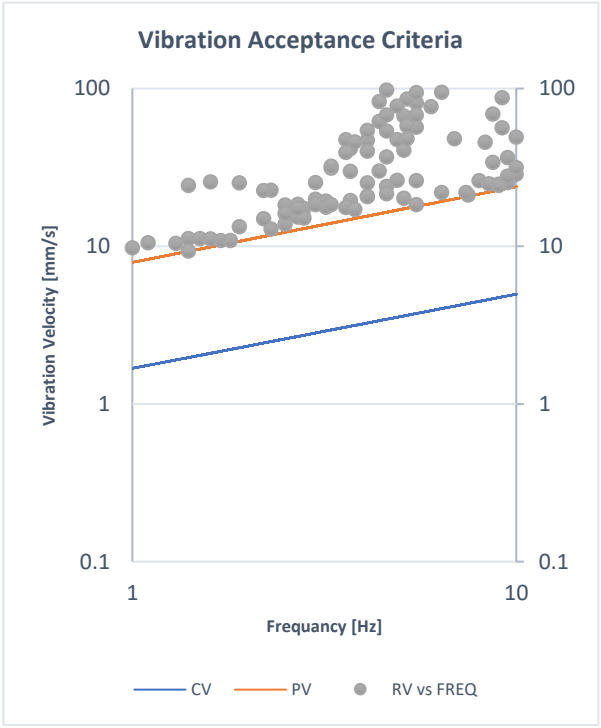


Figure 70. Graph of (PP) category with respect to the VAC lines for sub-model 2.1 (1-Sigma Confidence Results).

### 3-Sigma Results

For some applications, a 68 % confidence is not sufficient, hence, further analysis was done to find how reliable the VAC will be with a confidence of 99.73 %. The 3-sigma results were obtained by multiplying the vibration and stress by 3. Following that the cases were categorized as was done for the 1-sigma results. Table 17 below illustrates a summary of the categories and the number of cases in each category with a 99.73 % confidence. From this table, it can be found that 1029 cases out of the 1600 cases were judged correctly by the VAC. These cases represent 64.3125% of the 1600 cases. which means that 64.3125% of the time the VAC can be used to correctly judge the vibration level with a confidence of 99.73 %. Figures 71 to 79 illustrate the 3-sigma results with respect to the VAC for all the categories.

Table 17. Classification of Case Categories and The Number of Cases in Each Category for Sub-Model 2.1 (3-Sigma Confidence)

| # | Category | No. of Cases |
|---|---|---|
| 1 | OO | 676 |
| 2 | OC | 109 |
| 3 | OP | 91 |
| 4 | CO | 178 |
| 5 | CC | 50 |
| 6 | CP | 169 |
| 7 | PO | 1 |
| 8 | PC | 23 |
| 9 | PP | 303 |
| Total | - | 1600 |

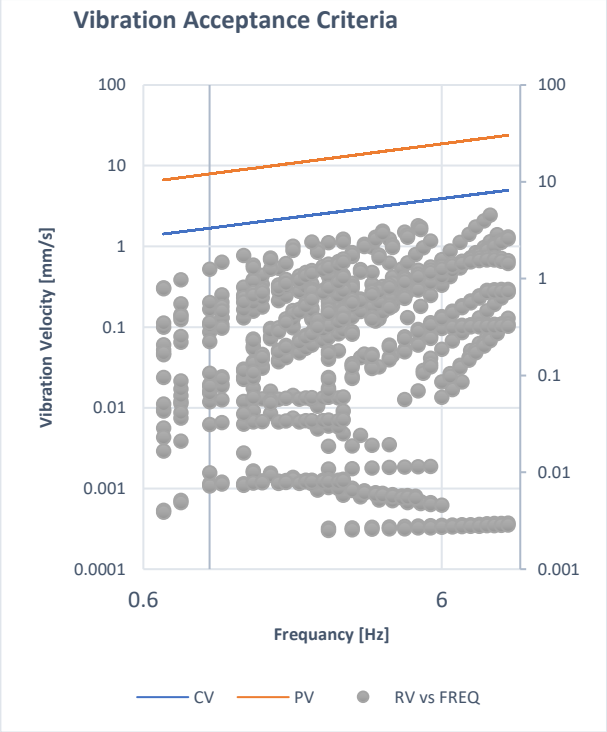


Figure 71. Graph of (OO) category with respect to the VAC lines for sub-model 2.1 (3-Sigma Confidence Results).

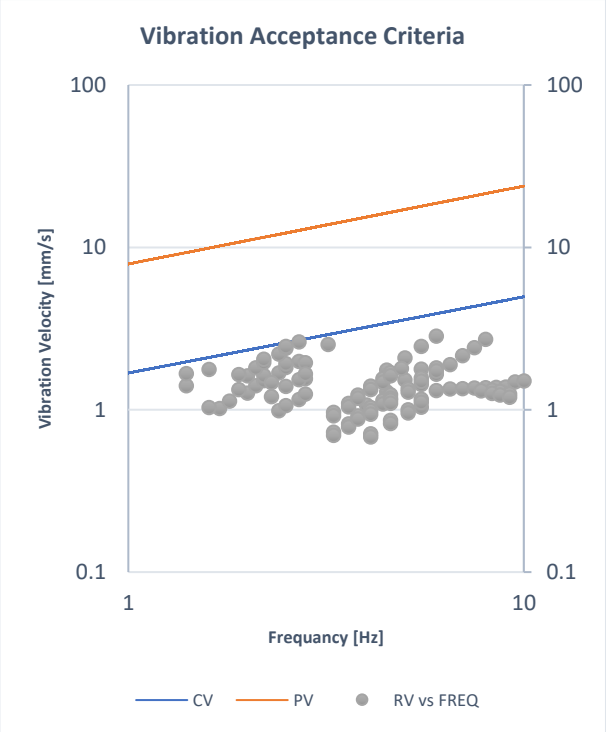


Figure 72. Graph of (OC) category with respect to the VAC lines for sub-model 2.1 (3-Sigma Confidence Results).

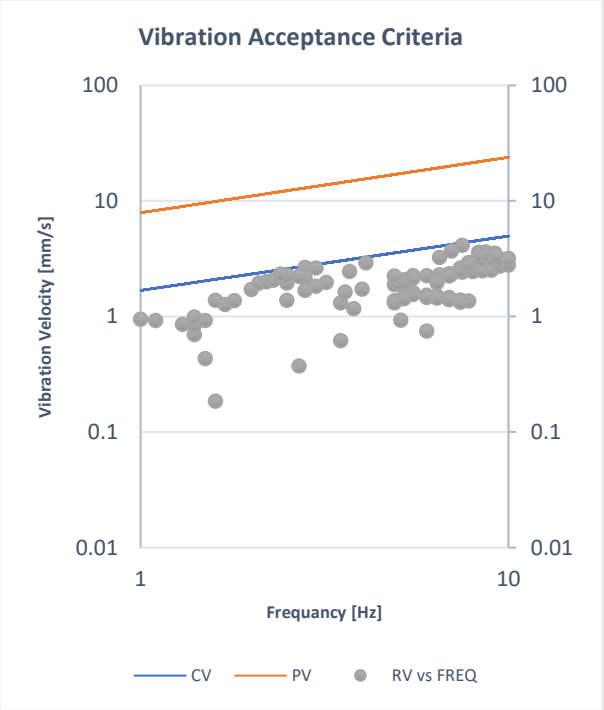


Figure 73. Graph of (OP) category with respect to the VAC lines for sub-model 2.1 (3-Sigma Confidence Results).

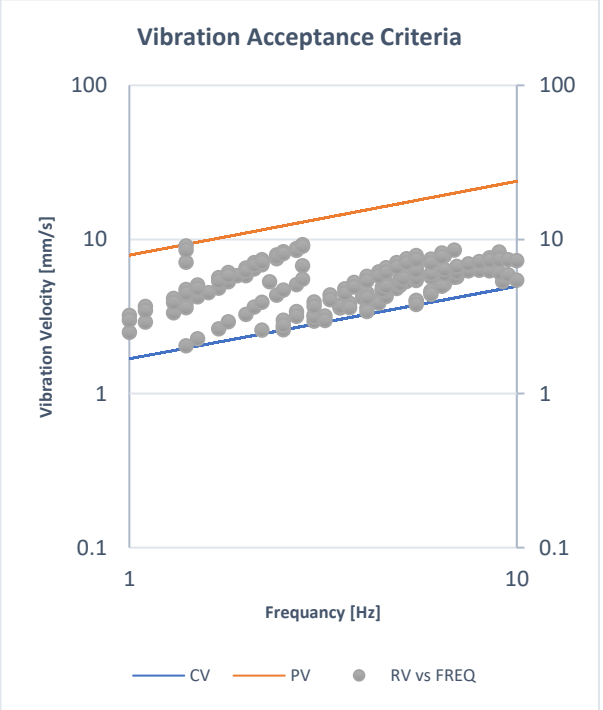


Figure 74. Graph of (CO) category with respect to the VAC lines for sub-model 2.1 (3-Sigma Confidence Results).

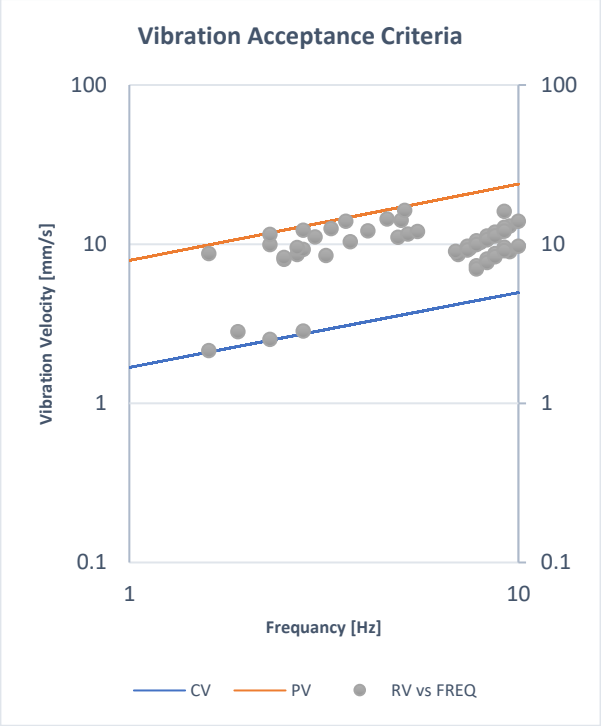


Figure 75. Graph of (CC) category with respect to the VAC lines for sub-model 2.1 (3-Sigma Confidence Results).

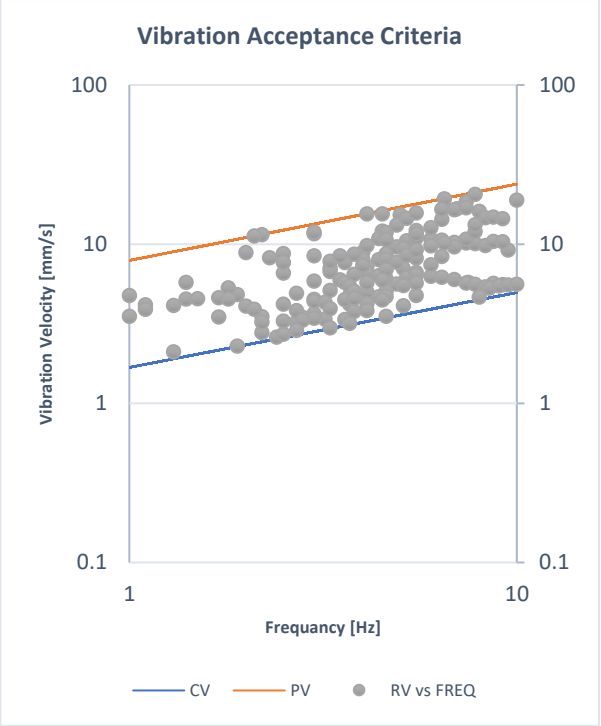


Figure 76. Graph of (CP) category with respect to the VAC lines for sub-model 2.1 (3-Sigma Confidence Results).

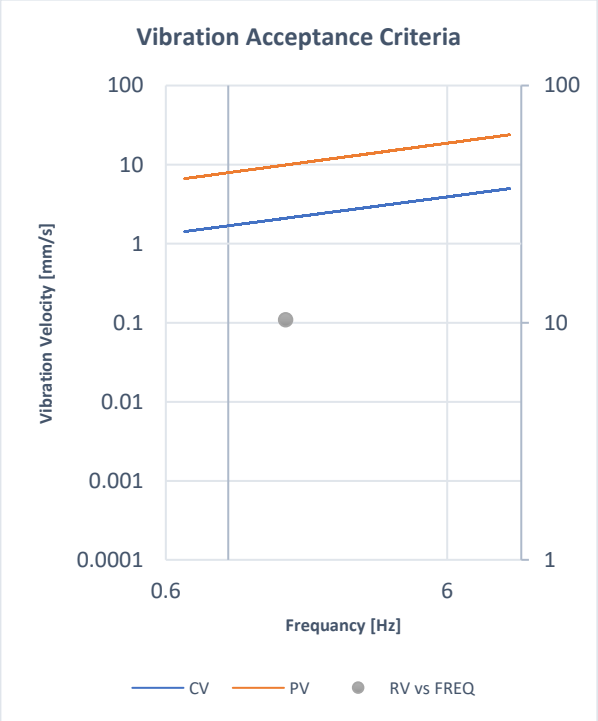


Figure 77. Graph of (PO) category with respect to the VAC lines for sub-model 2.1 (3-Sigma Confidence Results).

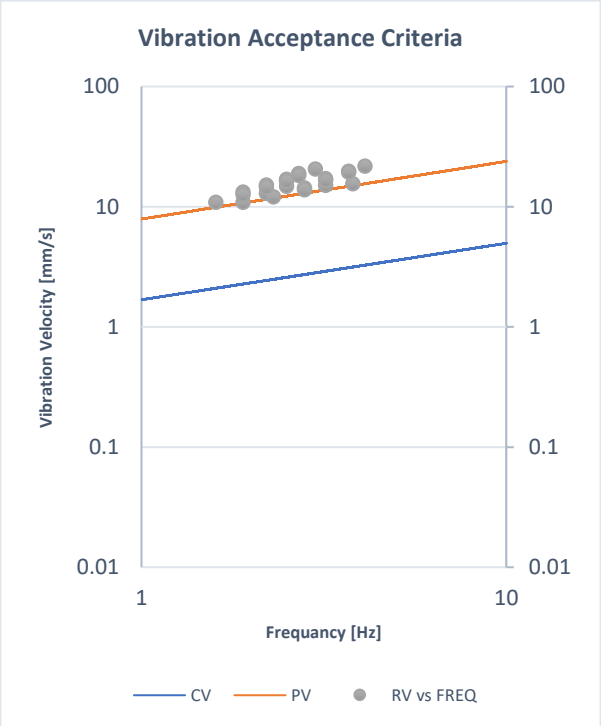


Figure 78. Graph of (PC) category with respect to the VAC lines for sub-model 2.1 (3-Sigma Confidence Results).

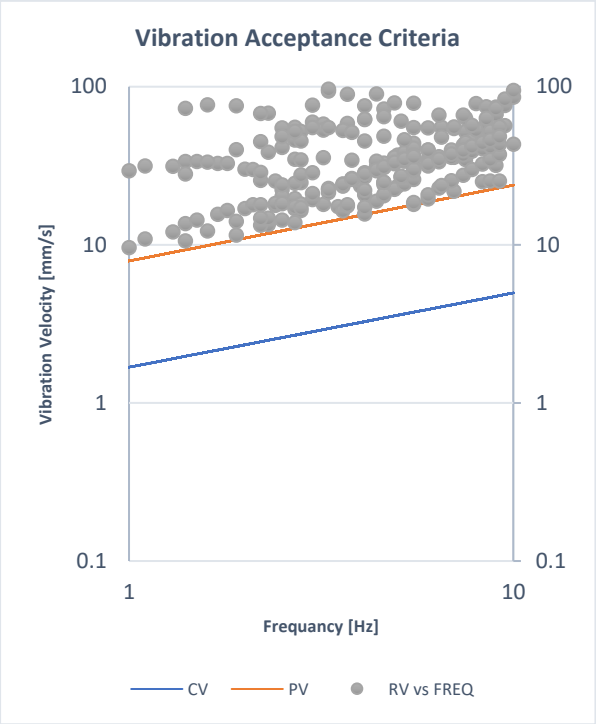


Figure 79. Graph of (PP) category with respect to the VAC lines for sub-model 2.1 (3-Sigma Confidence Results).

### 4.2.2. Sub-model 2.2

#### 1-Sigma Results

For this sub-model, the same 1600 cases were investigated. The software did not calculate the results of 64 cases out of these 1600 cases. The reason for that is the low values of the rotational and translational support stiffnesses which were not sufficient enough to hold the model. The other 1536 cases were successfully simulated, and the results were obtained and compared with the VAC and the stress curves as was done for the earlier sub-model. Unexpectedly, all the cases of this sub-model have ok (O) vibration levels and ok (O) stress levels. This means that the VAC has suitability of 100% with a confidence level of 68.27%. Figure 80 shows the cases compared to the VAC.

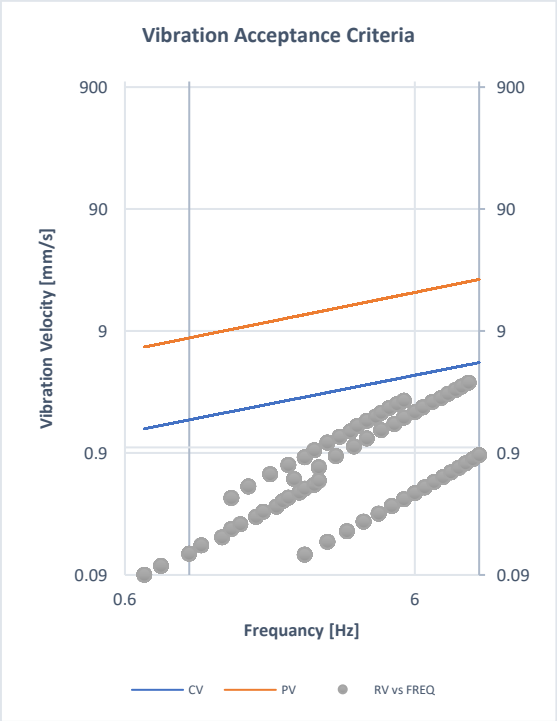


Figure 80. Graph of (OO) category with respect to the VAC lines for sub-model 2.2 (1-Sigma Confidence Results).

3-Sigma Results

For the 3-sigma results of this sub-model, only 1536 cases out of the 1600 cases were considered as explained in the 1-sigma results above. The 3-sigma results were calculated by multiplying the 1-sigma results by 3 as discussed in the earlier models. Then the VAC was used to find the vibration levels and the stress limits were used to find the stress levels for all cases. Following that, the cases were distributed among their respective categories. The first category has 984 cases that have ok (O) vibration levels and ok (O) stress levels. This category is referred to by (OO). The second category is the (CO) category which holds the remaining 552 cases that are having concern (C) vibration levels and ok (O) stress levels. The suitability of the VAC using the results of this model is 64.0625%. This suitability percentage shows a 35.9375% drop compared to the 1-sigma result of the same sub-model which was 100%. The

following figures 81-82 show the graph of the two categories with respect to the VAC.

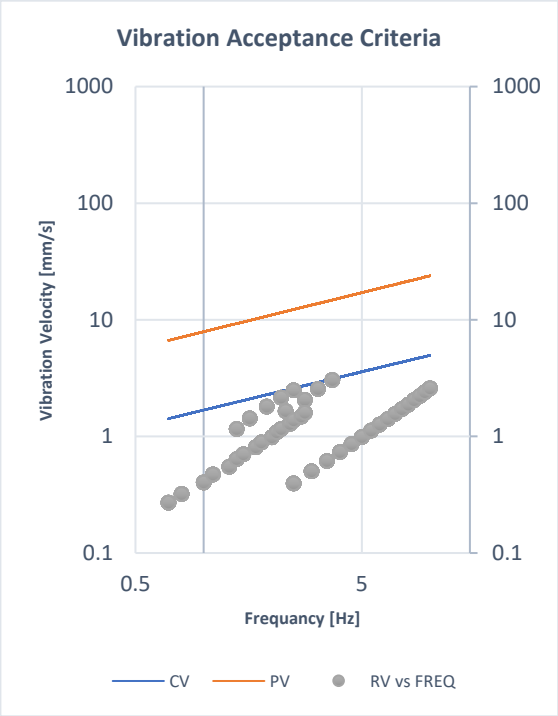


Figure 81. Graph of (OO) category with respect to the VAC lines for sub-model 2.2 (3-Sigma Confidence Results).

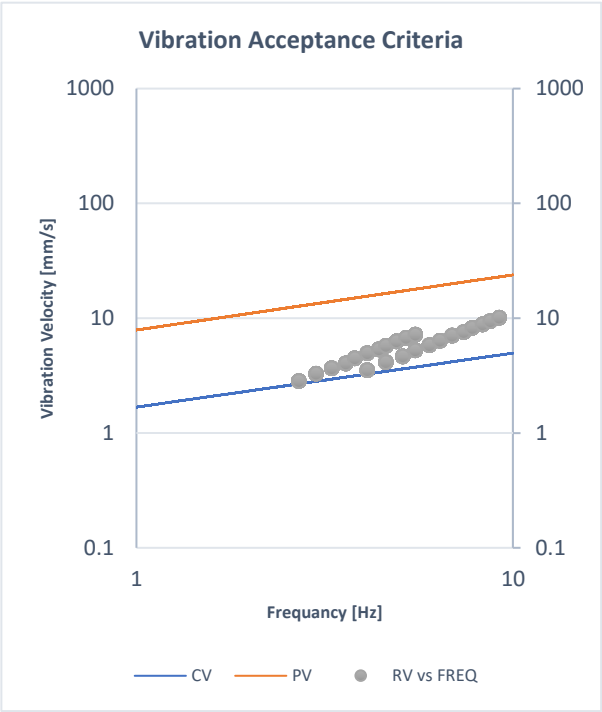


Figure 82. Graph of (CO) category with respect to the VAC lines for sub-model 2.2 (3-Sigma Confidence Results).

### *4.2.3 Sub-model 2.3*

1-sigma results

Similar to the sub-model 2.2, 1600 cases were simulated but 63 cases failed to run by the software due to the low values of rotational and translational support stiffnesses. The remaining 1537 cases were simulated successfully. These results were compared with the VAC to find the vibration levels and they were also compared with the stress curves to find the stress levels. It was found that all the cases are having ok (**O**) levels of vibration and stress. This is similar to the behavior of sub-model 2.2 which also had

the same behavior. The suitability of the VAC, in this case, is 100% at a confidence level of 68.27%. The following Figure 83 shows the graph of the vibration velocity compared to the VAC.

3-Sigma Results

These results were obtained as discussed in earlier sub-models and the same number of cases were considered (1537 cases). After comparing it with the VAC and stress curves all the cases were having ok (O) stress and vibration levels which means that the VAC has suitability of 100% at a confidence level of 99.73%. Figures 84 show the results versus the VAC.

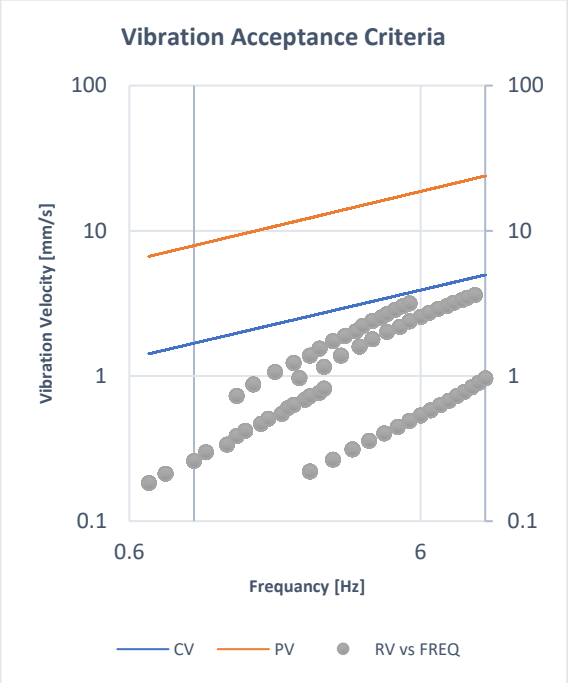


Figure 83. Graph of (OO) category with respect to the VAC lines for sub-model 2.3 (1-Sigma Confidence Results).

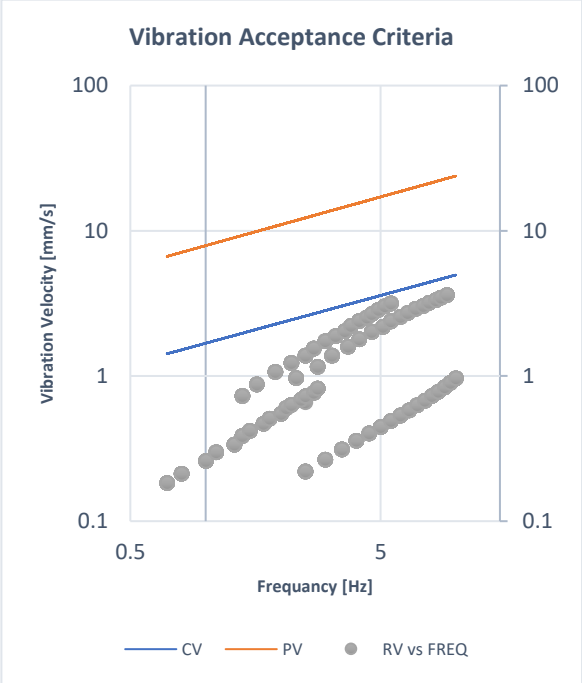


Figure 84. Graph of (OO) category with respect to the VAC lines for sub-model 2.3 (3-Sigma Confidence Results).

*4.2.4 Discussion of model 2*

For this model, 3 different sub-models were investigated to find the effect of the run-pipe length on the suitability of the VAC. The first sub-model has a 0.3-meter-long run-pipe which was excited with 1600 different cases of excitation. The 1-sigma confidence results of this model yielded a 76.5% suitability level, while the 3-sigma results showed only 64.3125%. These results mean that out of 100 vibration velocity measurements on a 0.3-meter run-pipe the VAC correctly judge 76 of the measured reading with a confidence of 68.27% and 64 readings out of the 100 with 99.73% confidence. The second sub-model has a 1-meter-long run-pipe which was also excited with the same 1600 cases of excitation. The suitability level of the VAC for this model was found to be 100% with 68.27% confidence and 64.0625% with a 99.73% confidence. The increase of the length of the run-pipe has increased the suitability level of the VAC from 76.5% to 100% for the 1-Sigma confidence, meaning that the VAC gives the correct vibration level 100 times out of a 100-vibration reading. Meanwhile, the 3-sigma confidence level has not changed much, as it dropped from 65.3125% for sub-model 2.1 to 64.0625% for sub-model 2.2. The third and last sub-model is the 1.5-meter run-pipe sub-model. This sub-model was investigated with the same excitations and the resulting suitability level was obtained as follows. For the 1-sigma confidence, the suitability level was found to be 100%, and the 3-sigma confidence level was also 100%. This model shows the same 1-sigma confidence level compared to sub-model 2.2, but it has an increase of around 24% compared to sub-model 2.1. Interestingly, the 3-sigma confidence for the 2 sub-models is almost the same, but the problem is that the suitability level is only 64%. This means that the VAC will only give a correct judgment of the vibration velocity measurements 64 % of the time. From the above results, it is advised to use the VAC to judge the vibration velocity of a 5-inch run-pipe model when

the span of run-pipes is longer to get higher reliability of the VAC.

## 4.3. Model 3

For this model, 3 sub-models with different lengths of run-pipe were considered for the analysis. The purpose of this variation is to study the effect of the run-pipe length on the suitability of the VAC when judging the vibration levels. Two different types of results were obtained for this model which are the 1 and 3 sigma confidence results. The 1-sigma results provide a confidence level of 68.27% in the judgment of the VAC. Whereas the 3-sigma results provide a 99.73% confidence level as explained in Section 3.1. In the following subsections, the 1 and 3 sigma results are illustrated for the 3 sub-models.

### *4.3.1. Sub-model 3.1*

#### 1-Sigma Results

A total of 1600 cases were simulated for this sub-model. These cases were simulated under different excitations and stiffnesses as mentioned in section 3.5. After running the simulation, the obtained results were compared with the Vibration Acceptance Criteria (VAC) to find the vibration levels resulting from this random vibration analysis. The results were also compared with the stress limits to check the stress levels associated with each case. Ideally the vibration and stress level for each case should match. For instance, if the vibration level is OK then the stress level should be OK as well. To check whether they match or not the cases were categorized based on the vibration and stress levels after they were compared with the vibration and stress curves. The categories are appointed by two letters. The first letter stands for the vibration level, if it is Ok, it is denoted as (O), (C) designates the concern levels, and problem levels are denoted as (P). The second letter represents the stress level, and the letter designation is the same as the vibration level. After comparing all the cases with

the criteria, it was found that a total of 43 cases out of the 1600 cases have (OK) vibration and stress levels. These cases form the first category which is denoted as (OO). The second category (OC) holds 1 case only and the third category (OP) did not have any cases. Furthermore, 73 cases were found to have concern (C) vibration levels. Out of these 73 cases, there are 36 cases with (OK) stress levels and they form the fourth category appointed by (CO). In addition, 14 cases out of the 73 cases have concern (C) stress levels and they form the fifth category which is denoted by (CC). The remaining 23 cases have problem (P) stress levels which form the sixth category appointed by (CP). In addition, 182 cases were found to have problem (P) vibration levels, 15 cases of which have (OK) stress levels and they are the seventh categories which are denoted by (PO). The eighth category has 24 cases that have a concern (C) stress level referred to by (PC), and the last category includes 143 cases with a problem (P) stress level and was denoted by (PP). As for the remaining 1301 cases, it was found that the vibration velocity of the branch tip was matching the vibration velocity of the run-pipe. Hence, at this kind of excitation and supporting stiffnesses, it is highly unlikely for this model to experience any high stresses that might cause fatigue failure. Those 1301 cases were categorized as a No-Risk category and were assigned the letters (NR). Table 18 summarizes all the categories and the number of cases in each category.

Table 18. Classification of Case Categories and The Number of Cases in Each Category for Sub-Model 3.1 (1-Sigma Confidence)

| # | Category | No. of Cases |
|---|---|---|
| 1 | OO | 43 |
| 2 | OC | 1 |
| 3 | OP | 0 |
| 4 | CO | 36 |
| 5 | CC | 14 |
| 6 | CP | 23 |
| 7 | PO | 15 |
| 8 | PC | 24 |
| 9 | PP | 143 |
| 10 | NR | 1301 |
| Total | - | 1600 |

After categorizing the cases as shown above it is noticed that only 182 cases out of the 299 cases are matching. Using the above-illustrated results, it can be shown that the VAC has a suitability of 66.8896%. This suitability level means that the VAC for this model will give correct judgment off the vibration levels almost 67% of the time with a confidence of 68% only.

The following figures 85 to 92 show the above-prescribed categories which are illustrated with respect to the VAC curves. In these graphs, the Orange line (upper line) corresponds to Problem vibration levels, and the blue line (lower line) corresponds to the concern vibration levels. The gray dots are the cases that were described above. In the graphs below the horizontal axis represent the frequency of vibration in (Hz). Where the left vertical axis is the vibration velocity of the VAC in (mm/s). And the right vertical axis is the vibration velocity of the branch-tip in (mm/s). All the axes on the graphs are of a logarithmic scale.

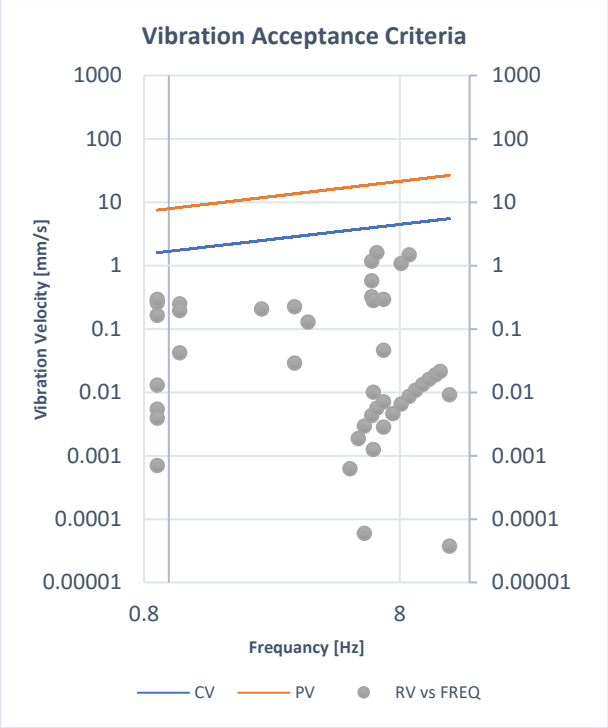


Figure 85. Graph of (OO) category with respect to the VAC lines for sub-model 3.1 (1-Sigma Confidence Results).

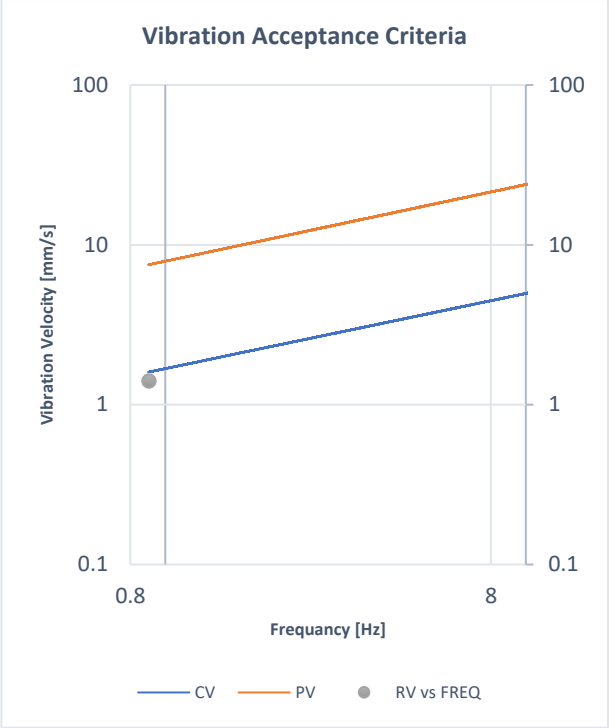


Figure 86. Graph of (OC) category with respect to the VAC lines for sub-model 3.1 (1-Sigma Confidence Results).

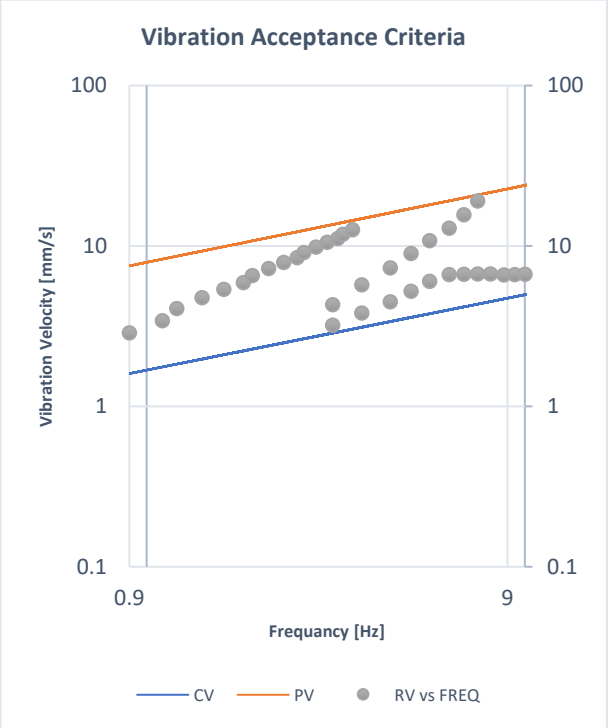


Figure 87. Graph of (CO) category with respect to the VAC lines for sub-model 3.1 (1-Sigma Confidence Results).

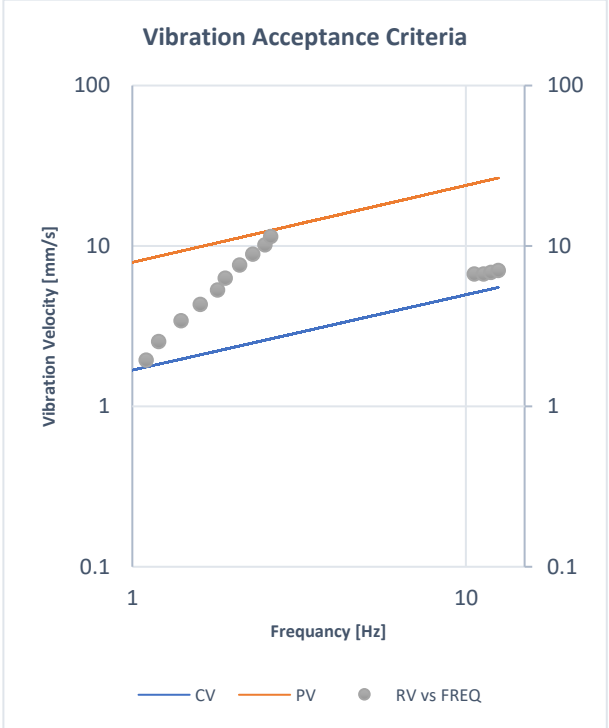


Figure 88. Graph of (CC) category with respect to the VAC lines for sub-model 3.1 (1-Sigma Confidence Results).

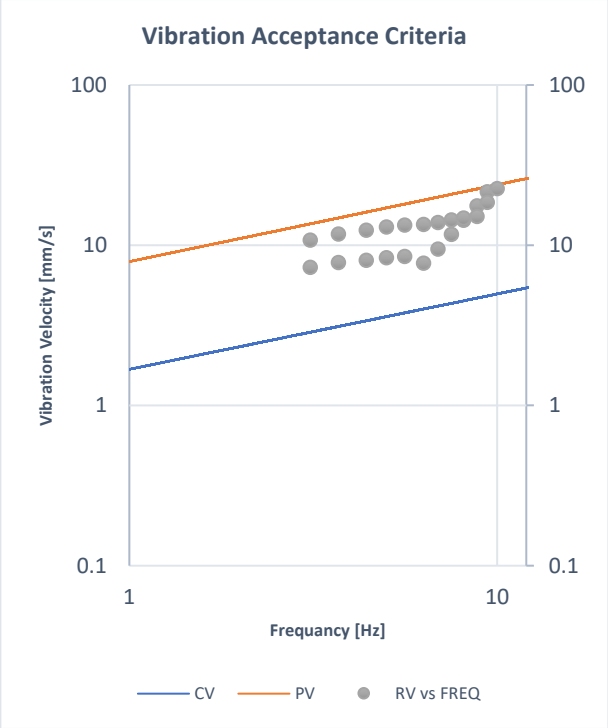


Figure 89. Graph of (CP) category with respect to the VAC lines for sub-model 3.1 (1-Sigma Confidence Results).

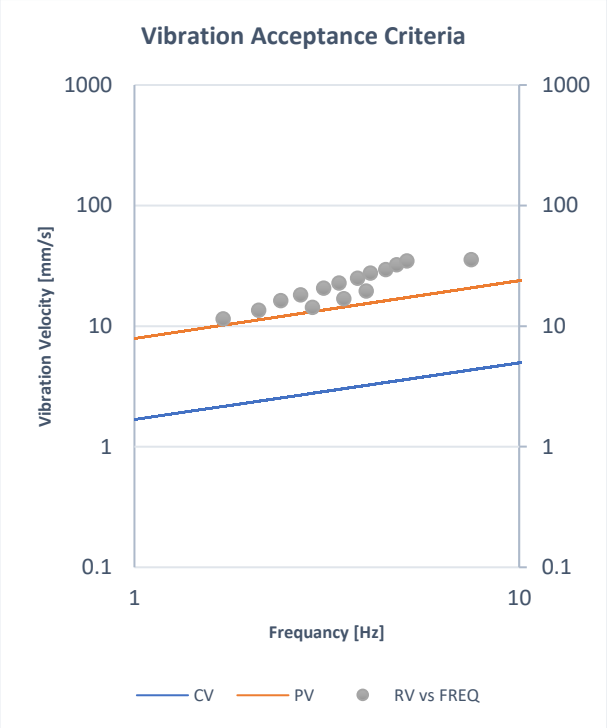


Figure 90. Graph of (PO) category with respect to the VAC lines for sub-model 3.1 (1-Sigma Confidence Results).

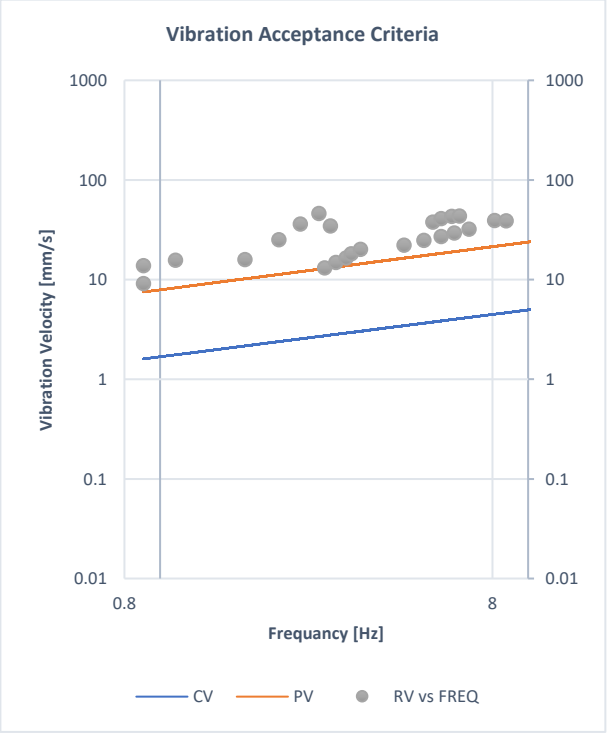


Figure 91. Graph of (PC) category with respect to the VAC lines for sub-model 3.1 (1-Sigma Confidence Results).

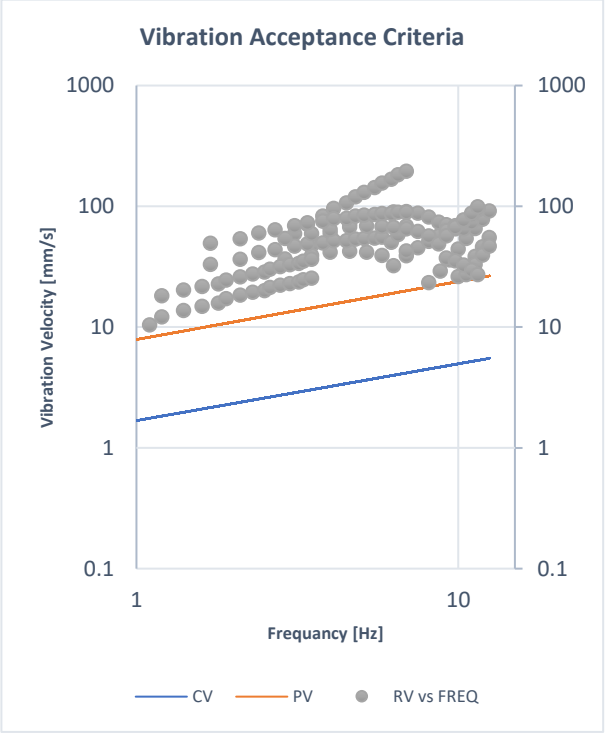


Figure 92. Graph of (PP) category with respect to the VAC lines for sub-model 3.1 (1-Sigma Confidence Results).

3-Sigma Results

The same categorization was done on the 3-sigma results, which were obtained by multiplying the vibration velocity and the stress by a factor of 3. The distribution of the 299 cases in each category has changed and the new distribution of cases is shown in the below table.

From Table 19 it can be shown that the suitability of the VAC in judging the vibration levels have increased and it is now 84.281%. Not only has the suitability of the VAC increased, but the confidence has also increased from 68% for the 1-sigma to 99.73% for the 3-sigma. This means that the VAC almost with 100% confidence correctly judges the vibration levels 84.281% of the time. In other words, if an operator took 100 vibration measurements on a 4-inch, 0.3 m run-pipe and compared it with VAC, 84 of those readings are most likely to be correctly judged by the VAC. The following figures 93- 100 show the 3-sigma results with respect to the VAC.

Table 19. Classification of Case Categories and the Number of Cases in Each Category for Sub-Model 3.1 (3-Sigma Confidence)

| # | Category | No. of Cases |
|---|---|---|
| 1 | OO | 40 |
| 2 | OC | 2 |
| 3 | OP | 0 |
| 4 | CO | 5 |
| 5 | CC | 3 |
| 6 | CP | 10 |
| 7 | PO | 18 |
| 8 | PC | 12 |
| 9 | PP | 209 |
| 10 | NR | 1301 |
| Total | - | 1600 |

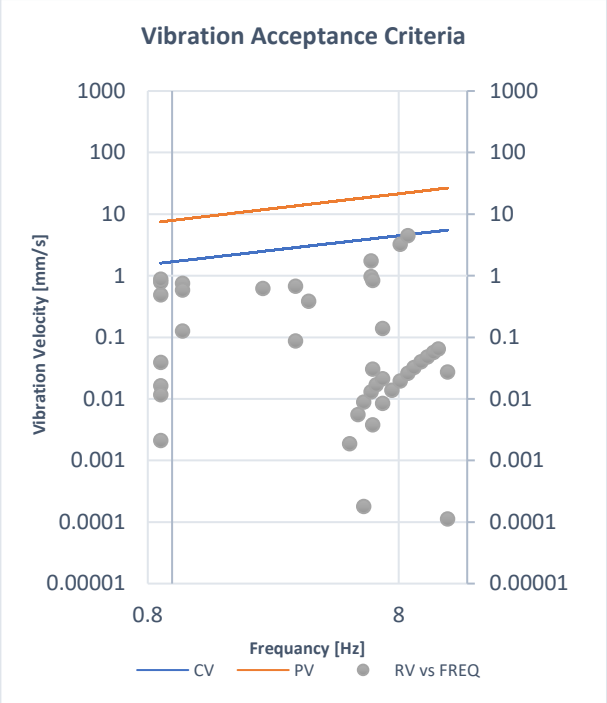


Figure 93. Graph of (OO) category with respect to the VAC lines for sub-model 3.1 (3-Sigma Confidence Results).

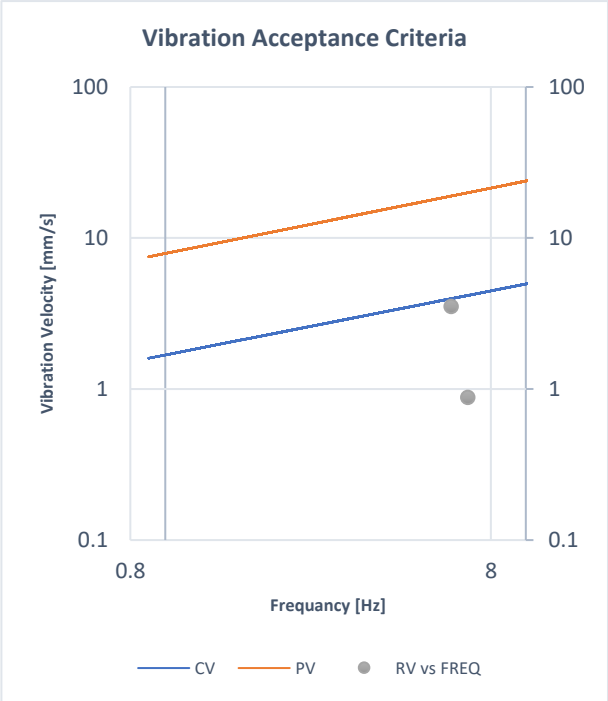


Figure 94. Graph of (OC) category with respect to the VAC lines for sub-model 3.1 (3-Sigma Confidence Results).

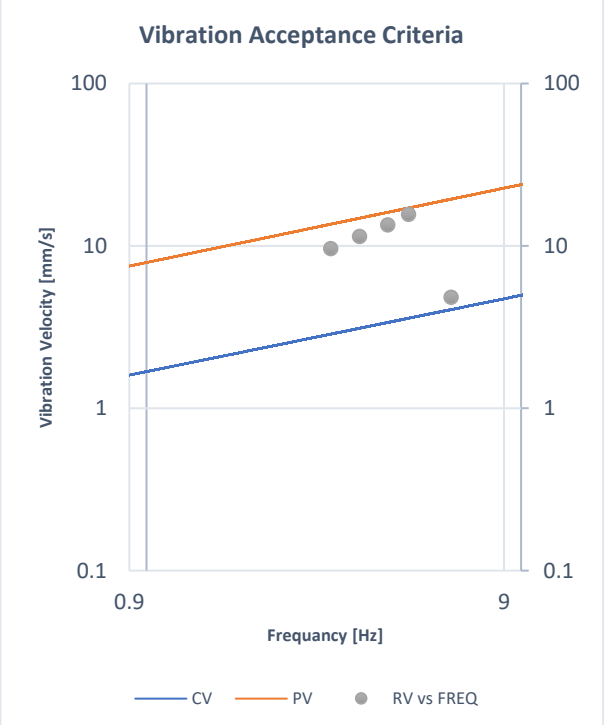


Figure 95. Graph of (CO) category with respect to the VAC lines for sub-model 3.1 (3-Sigma Confidence Results).

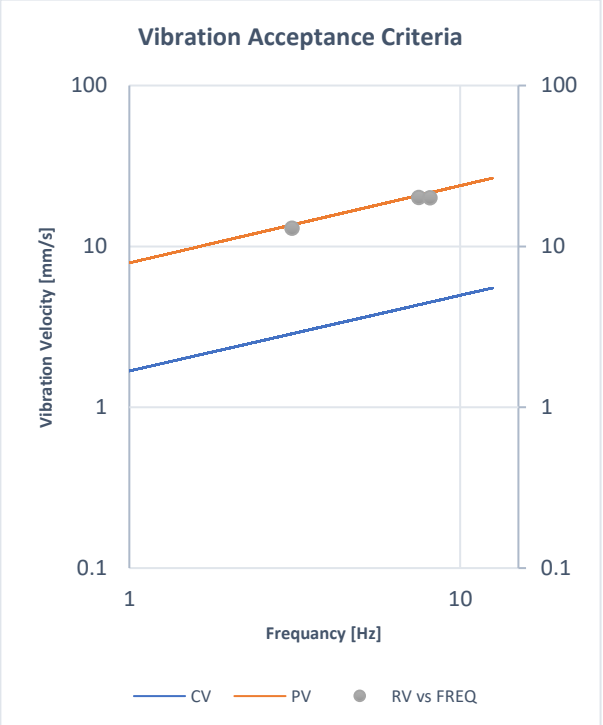


Figure 96. Graph of (CC) category with respect to the VAC lines for sub-model 3.1 (3-Sigma Confidence Results).

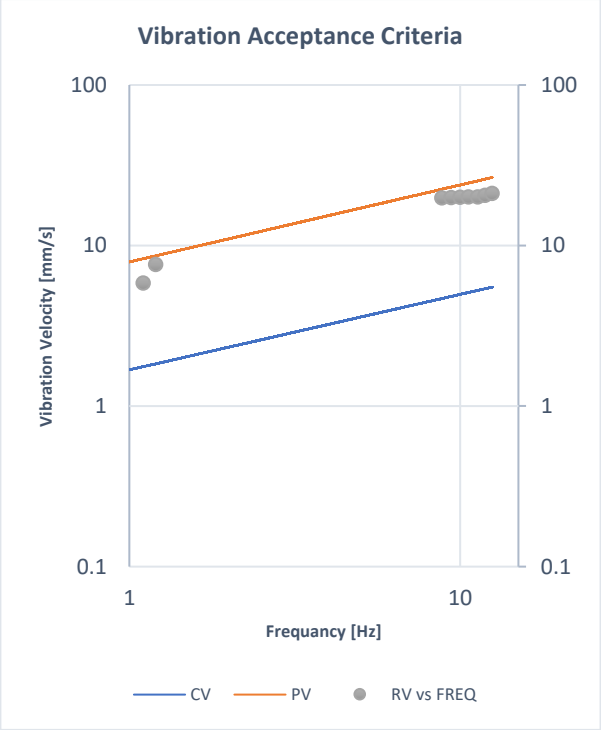


Figure 97. Graph of (CP) category with respect to the VAC lines for sub-model 3.1 (3-Sigma Confidence Results).

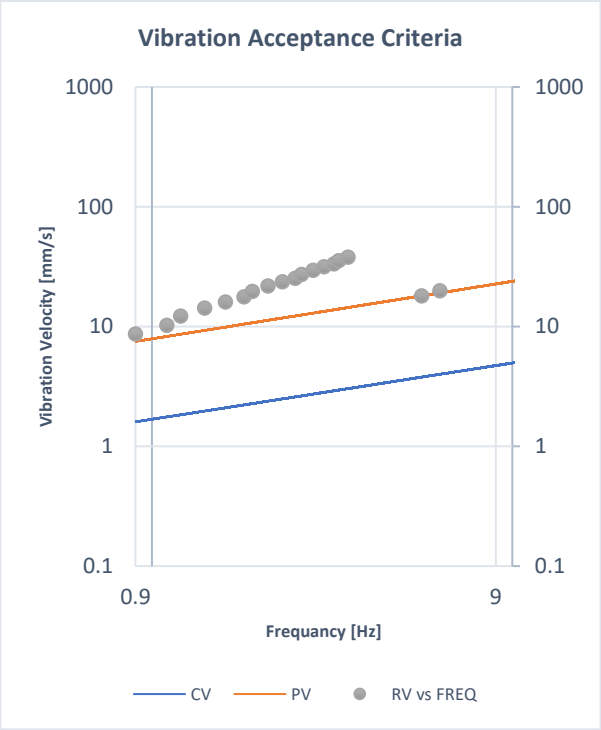


Figure 98. Graph of (PO) category with respect to the VAC lines for sub-model 3.1 (3-Sigma Confidence Results).

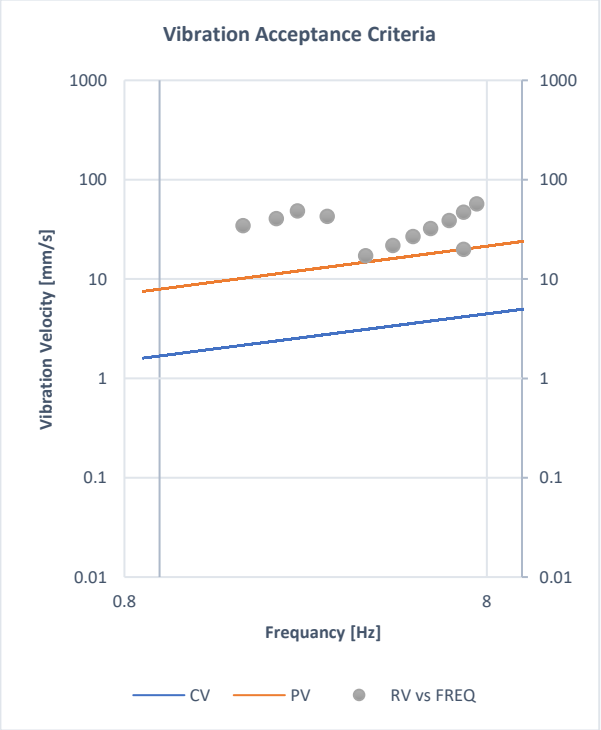


Figure 99. Graph of (PC) category with respect to the VAC lines for sub-model 3.1 (3-Sigma Confidence Results).

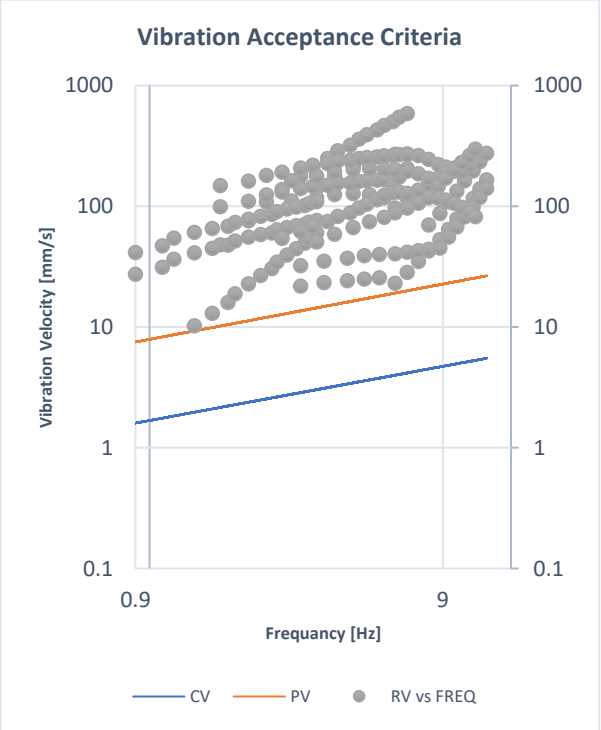


Figure 100. Graph of (PP) category with respect to the VAC lines for sub-model 3.1 (3-Sigma Confidence Results).

*4.3.2. Sub-model 3.2*

1-Sigma Results

For this sub-model, the same 1600 cases were simulated. The results were obtained and compared with the VAC and the stress curves as was done for the earlier model. unlike sub-model 3.1, the branch pipe of this sub-model is vibrating at a different speed from the run pipe at all the 1600 cases. The distribution of the 1600 cases among the categories is as follows. The first category which is (OO) has 900 cases compared to 40 cases in the same category for sub-model 3.1. The second category (OC) has 32 cases which were 2 in sub-model 3.1. Furthermore, the third category (OP) consists of 4 cases that were not present in the earlier sub-model 3.1. The (CO), (CC), and (CP) categories have 268, 57, and 17 cases respectively where sub-model 3.1 had 5, 3, and 1 for the same categories representatively. The categories which have problem vibration levels (PO), (PC), and (PP) has 114, 46, 162 cases correspondingly, where the earlier sub-model 3.1 had 18, 12, 209 cases for the same categories. Table 20 shows a summary of the categories and the number of cases in each category. Using these results, it was found that the VAC suitability is 69.9375% with a confidence level of 68.27% compared to 66.8896% for sub-model 3.1. This 10% increase proves that the suitability of the VAC is sensitive to the change in the run-pipe length. The below-summarized cases in Table 20 are shown in figures 101- 109 with respect to the VAC.

Table 20. Classification of Case Categories and the Number of Cases in Each Category for Sub-Model 3.2 (1-Sigma Confidence)

| # | Category | No. of Cases |
|---|---|---|
| 1 | OO | 900 |
| 2 | OC | 32 |
| 3 | OP | 4 |
| 4 | CO | 268 |
| 5 | CC | 57 |
| 6 | CP | 17 |
| 7 | PO | 114 |
| 8 | PC | 46 |
| 9 | PP | 162 |
| Total | - | 1600 |

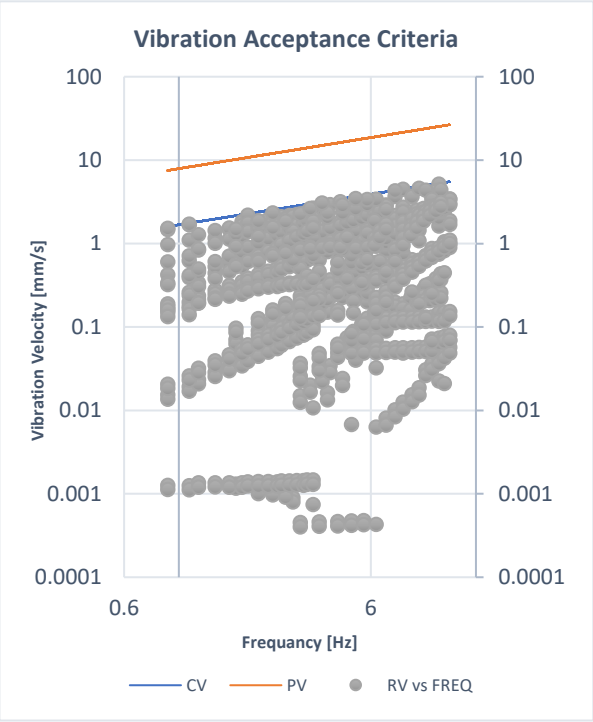


Figure 101. Graph of (OO) category with respect to the vibration acceptance criteria lines for the 4 inches 1-m run pipe model (1-Sigma Results).

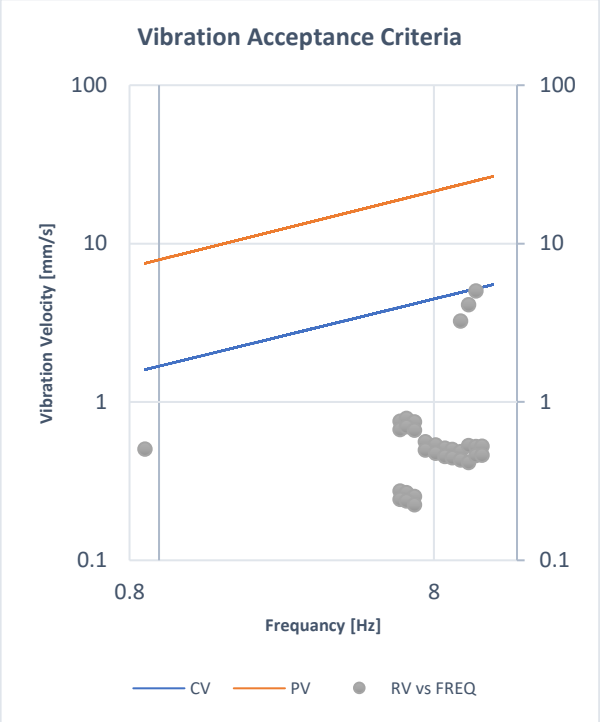


Figure 102. Graph of (OC) category with respect to the vibration acceptance criteria lines for the 4 inches 1-m run pipe model (1-Sigma Results).

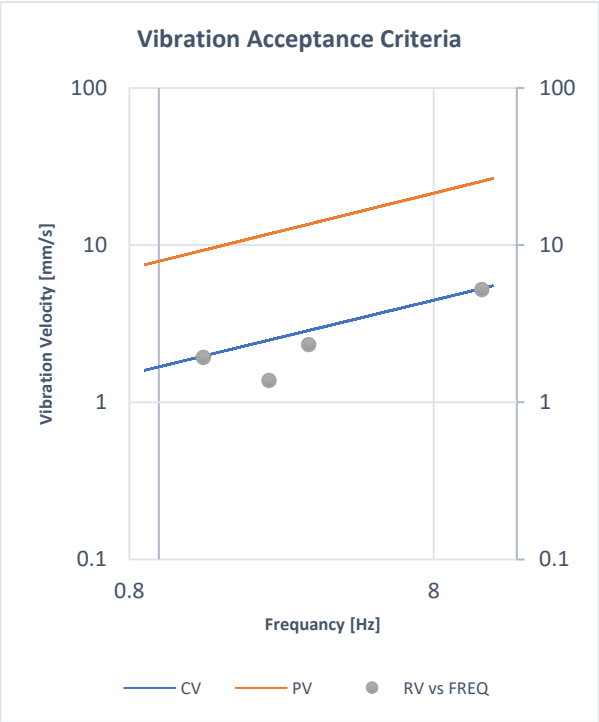


Figure 103. Graph of (OP) category with respect to the VAC lines for sub-model 3.2 (1-Sigma Confidence Results).

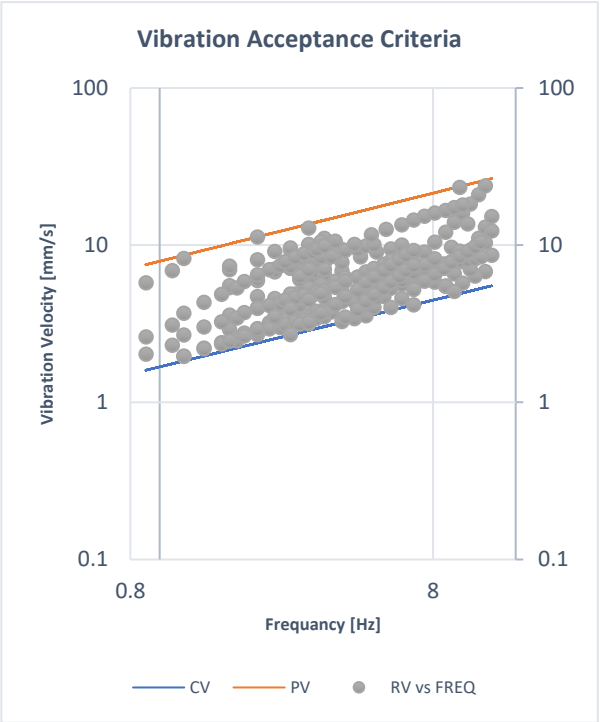


Figure 104. Graph of (CO) category with respect to the VAC lines for sub-model 3.2 (1-Sigma Confidence Results).

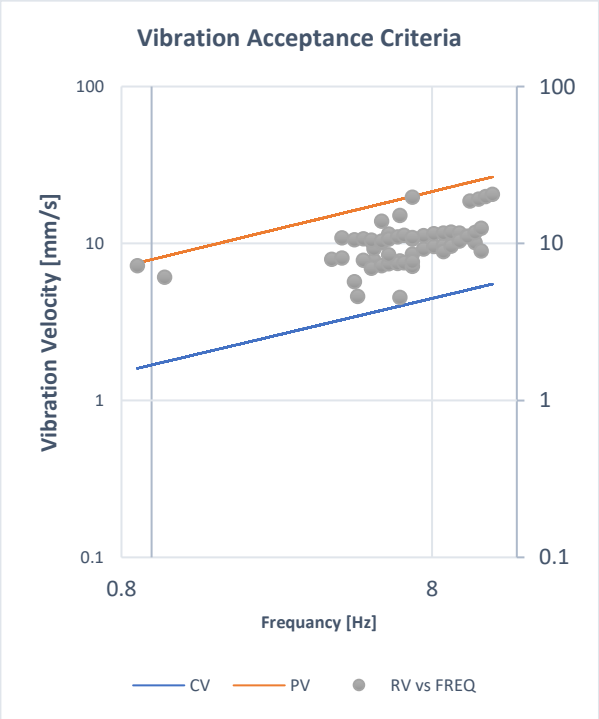


Figure 105. Graph of (CC) category with respect to the VAC lines for sub-model 3.2 (1-Sigma Confidence Results).

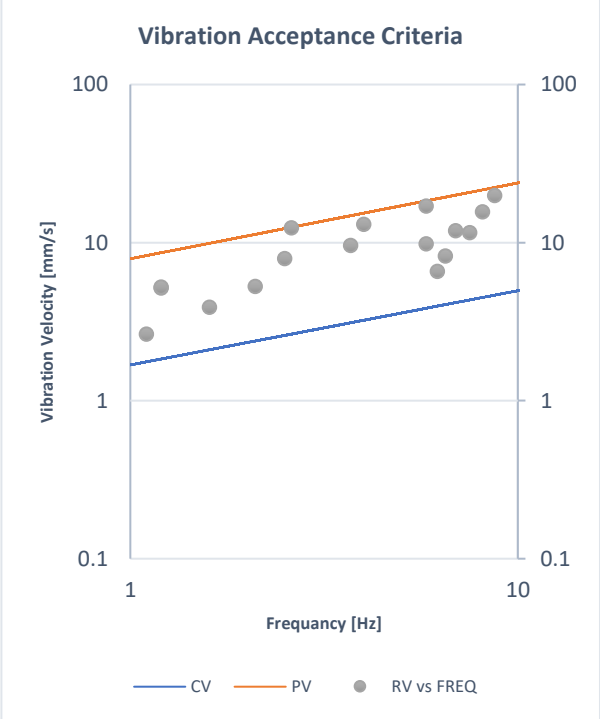


Figure 106. Graph of (CP) category with respect to the VAC lines for sub-model 3.2 (1-Sigma Confidence Results).

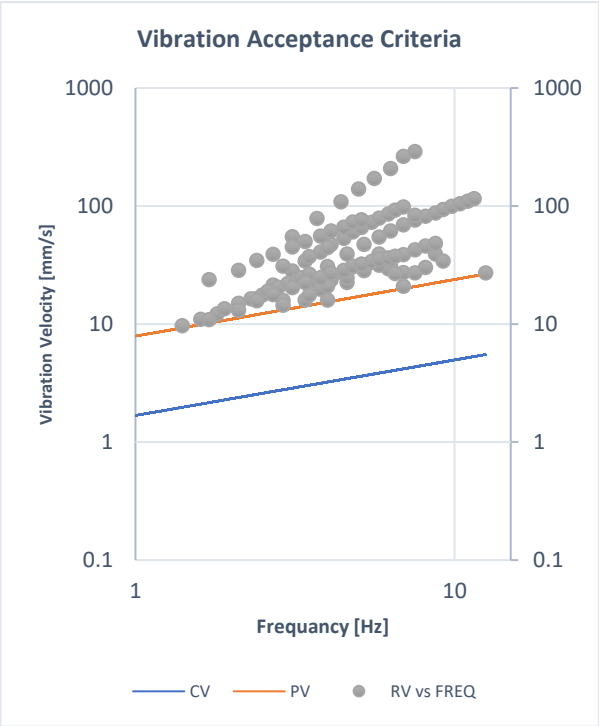


Figure 107. Graph of (PO) category with respect to the VAC lines for sub-model 3.2 (1-Sigma Confidence Results).

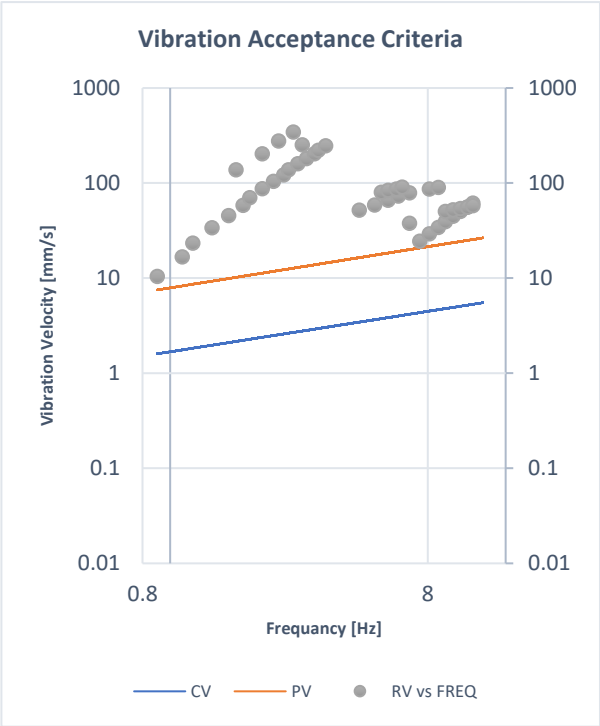


Figure 108. Graph of (PP) category with respect to the VAC lines for sub-model 3.2 (1-Sigma Confidence Results).

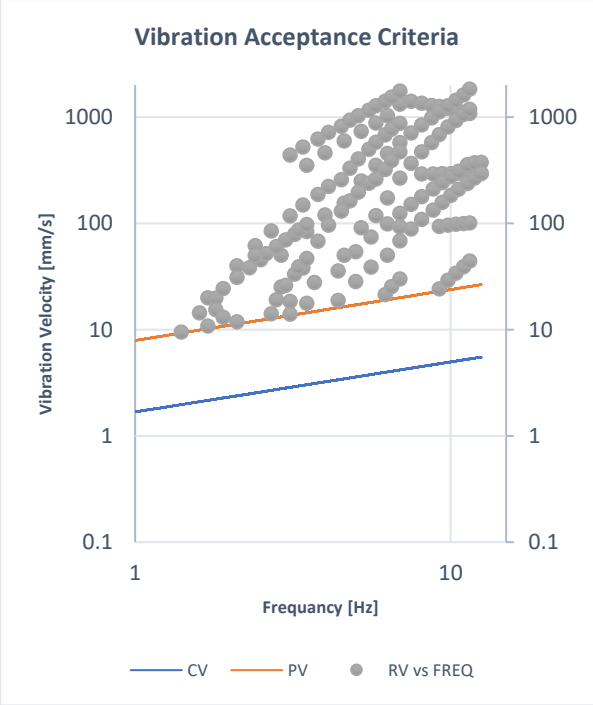


Figure 109. Graph of (PP) category with respect to the VAC lines for sub-model 3.2 (1-Sigma Confidence Results).

3-Sigma Results

The 3-sigma results of this sub-model show similar behavior to the 1-sigma results. For example, the number of cases in the first category (OO) has dropped from 900 cases in the 1-sigma result to 533 cases for the 3-sigma. The classification of the cases among the categories of this sub-model is summarized in Table 21. Using the data in this table the suitability of the VAC was found to be 59.5625% with a confidence of 99.73%. These results show that the VAC only gives a correct judgment of the vibration level 59.5625% of the time. In the following figure 110- 118, the cases of each category are presented with respect to the VAC.

Table 21. Classification of Case Categories and the Number of Cases in Each Category for the Sub-Model 3.2 (3-Sigma Confidence)

| # | Category | No. of Cases |
|---|---|---|
| 1 | OO | 532 |
| 2 | OC | 77 |
| 3 | OP | 67 |
| 4 | CO | 259 |
| 5 | CC | 79 |
| 6 | CP | 29 |
| 7 | PO | 147 |
| 8 | PC | 68 |
| 9 | PP | 342 |
| Total | - | 1600 |

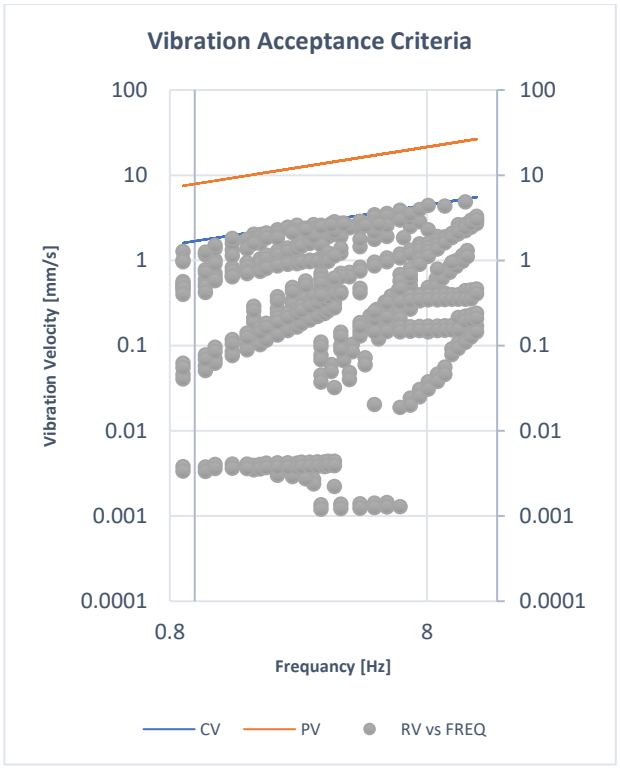


Figure 110. Graph of (OO) category with respect to the VAC lines for sub-model 3.2 (3-Sigma Confidence Results).

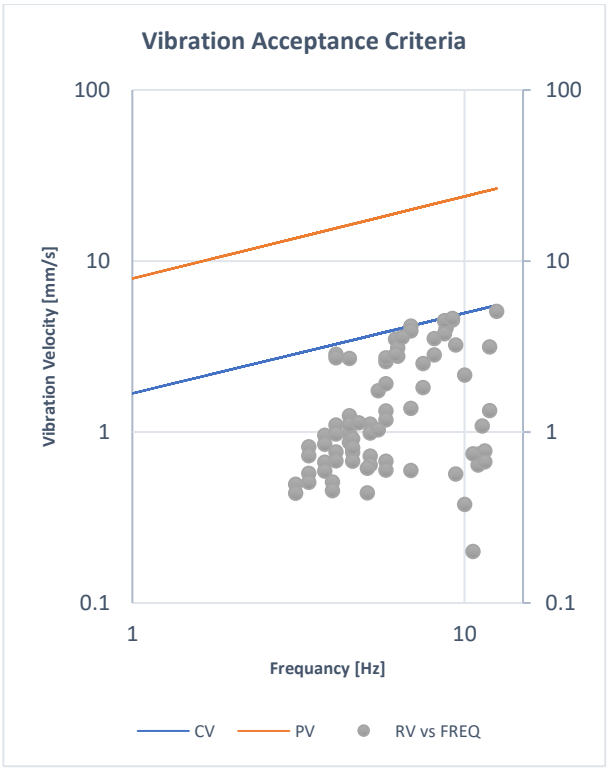


Figure 111. Graph of (OC) category with respect to the VAC lines for sub-model 3.2 (3-Sigma Confidence Results).

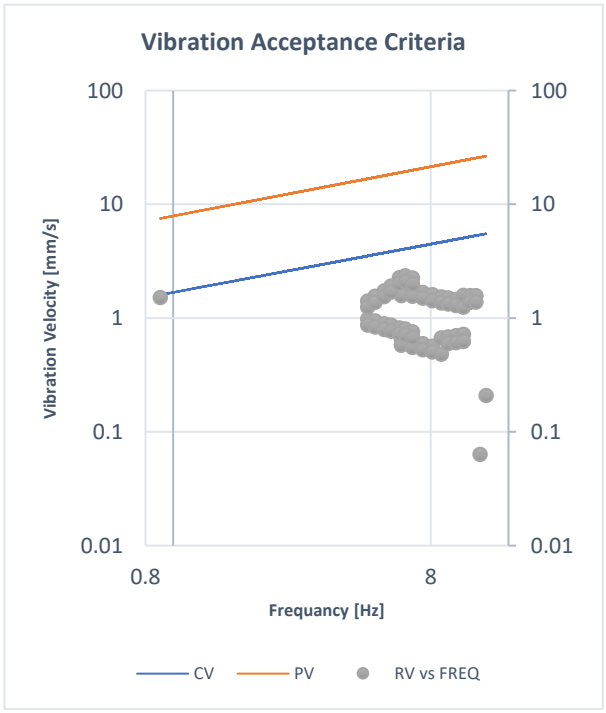


Figure 112. Graph of (OP) category with respect to the VAC lines for sub-model 3.2 (3-Sigma Confidence Results).

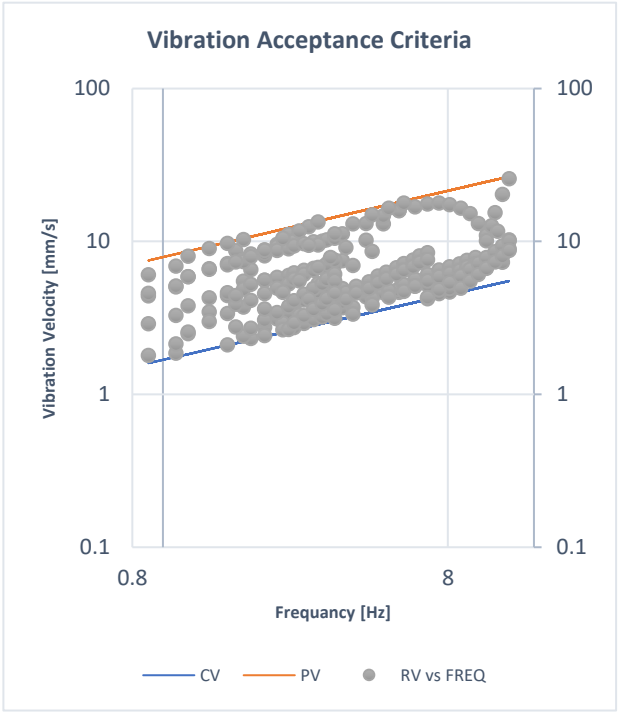


Figure 113. Graph of (CO) category with respect to the VAC lines for sub-model 3.2 (3-Sigma Confidence Results).

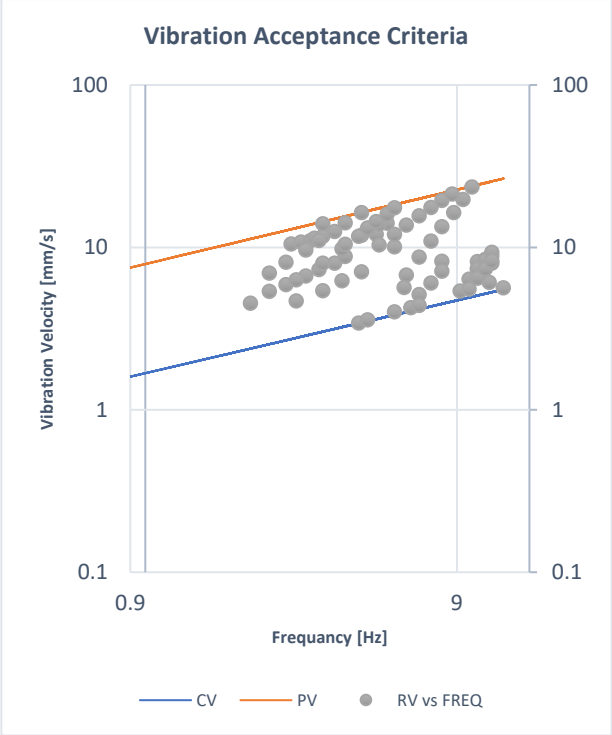


Figure 114. Graph of (CC) category with respect to the VAC lines for sub-model 3.2 (3-Sigma Confidence Results).

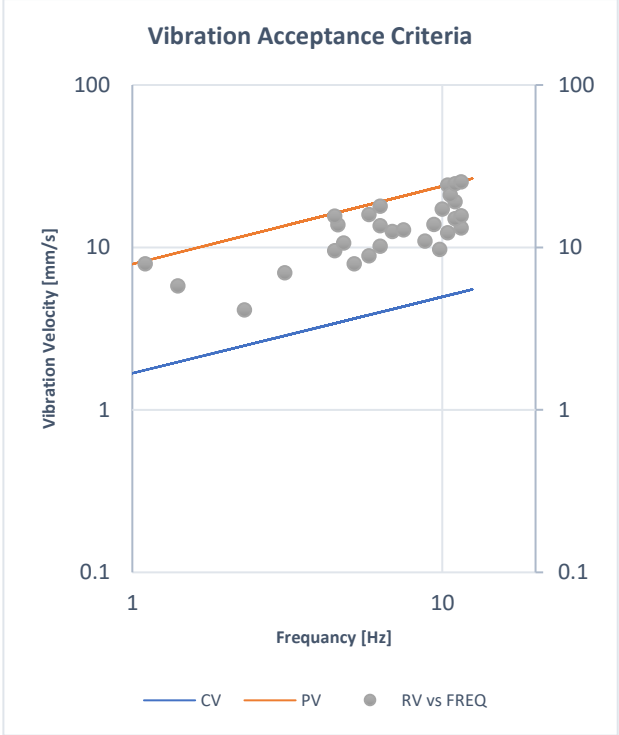


Figure 115. Graph of (CP) category with respect to the VAC lines for sub-model 3.2 (3-Sigma Confidence Results).

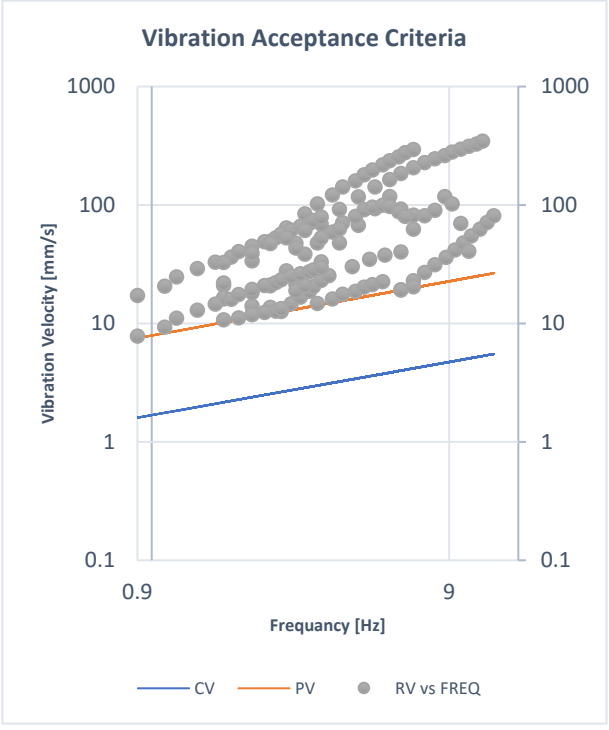


Figure 116. Graph of (PO) category with respect to the VAC lines for sub-model 3.2 (3-Sigma Confidence Results).

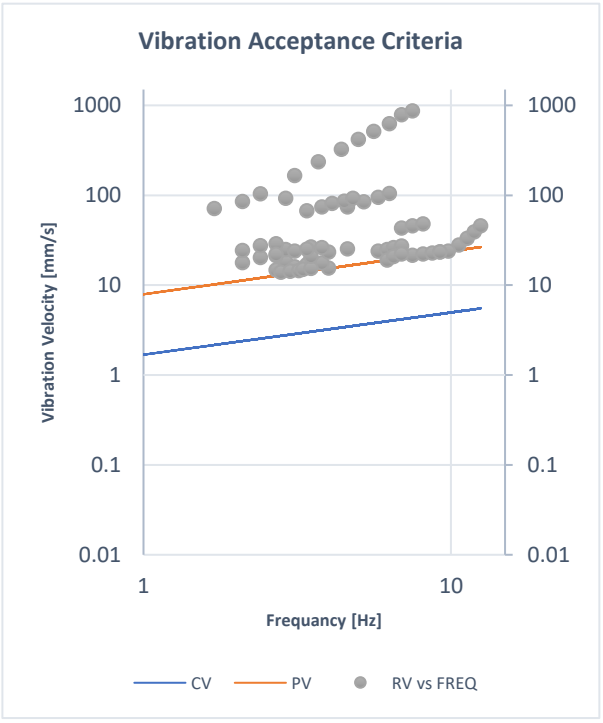


Figure 117. Graph of (PC) category with respect to the VAC lines for sub-model 3.2 (3-Sigma Confidence Results).

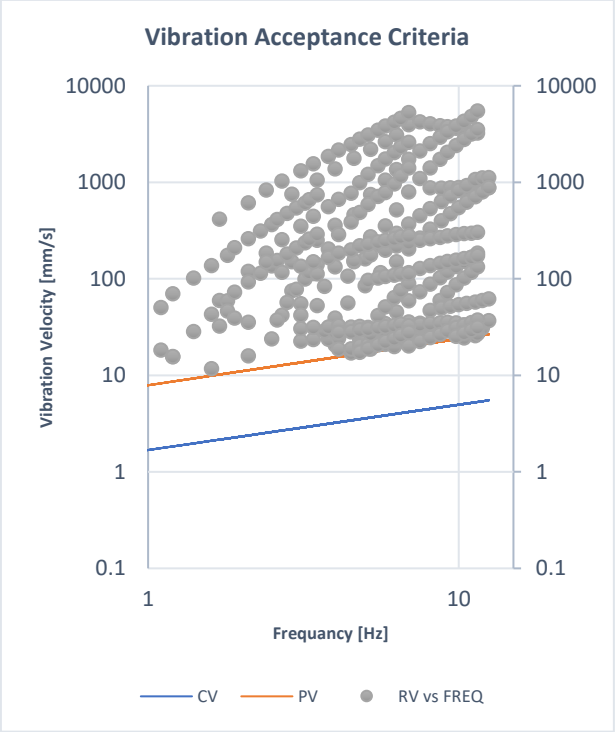


Figure 118. Graph of (PP) category with respect to the VAC lines for sub-model 3.2 (3-Sigma Confidence Results).

### *4.3.3. Sub-model 3.3*

1-sigma results

This sub-model is the last of three with a run-pipe of 4-inches. It was also simulated with the same 1600 cases that were used for the earlier sub-models. Out of these 1600 cases, 63 cases failed to run due to the low support stiffnesses. Like the 2 sub-models before this one has a different classification of cases among the categories. For instance, the first category (OO) has 882 cases, while the (OC) category has 4 cases, and the (OP) category has 4 cases. The number of cases for each of the concern vibration velocity categories (CO), (CC), and (CP) are 307, 26, and 4, respectively. Moreover, the (PO) category holds 101 cases, whilst the (PC) category has 70 cases, and the (PP) categories have 139 cases. These classifications are summarized in Table 22. Using the below-summarized cases the suitability of the VAC was found to be 68.1197% with a

confidence of 68% meaning that the VAC will correctly judge the vibration levels only 68.1197% of the time. Figures 119- 127 present the graphs of each of these categories with respect to the VAC.

Table 22. Classification of Case Categories and the Number of Cases in Each Category for the Sub-Model 3.3 (1-Sigma Confidence)

| # | Category | No. of Cases |
|---|---|---|
| 1 | OO | 882 |
| 2 | OC | 4 |
| 3 | OP | 4 |
| 4 | CO | 307 |
| 5 | CC | 26 |
| 6 | CP | 4 |
| 7 | PO | 101 |
| 8 | PC | 70 |
| 9 | PP | 139 |
| Total | - | 1600 |

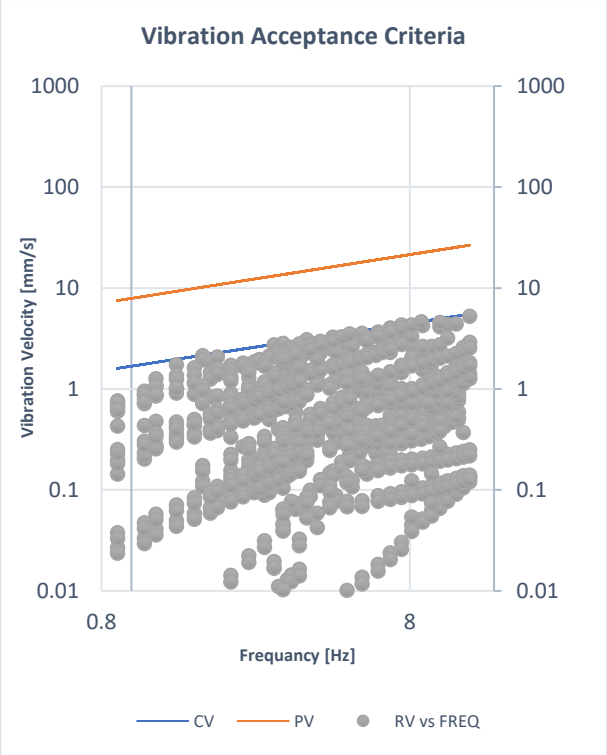


Figure 119. Graph of (OO) category with respect to the VAC lines for sub-model 3.3 (1-Sigma Confidence Results).

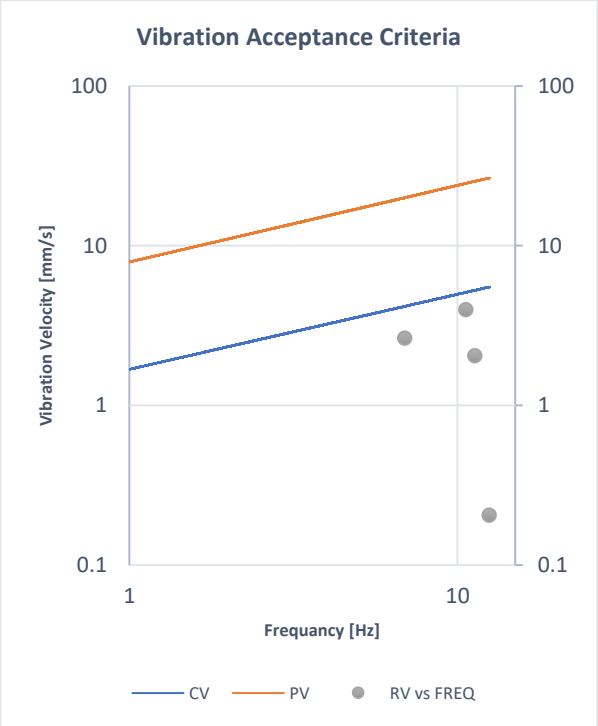


Figure 120. Graph of (OC) category with respect to the VAC lines for sub-model 3.3 (1-Sigma Confidence Results).

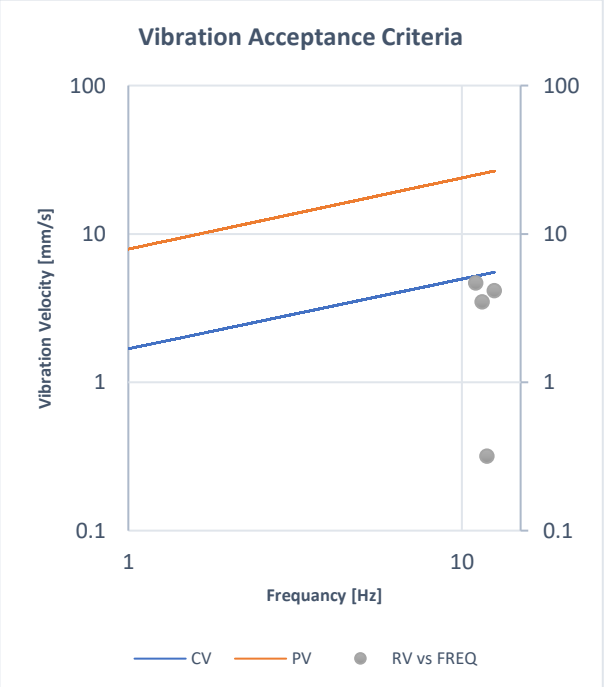


Figure 121. Graph of (OP) category with respect to the VAC lines for sub-model 3.3 (1-Sigma Confidence Results).

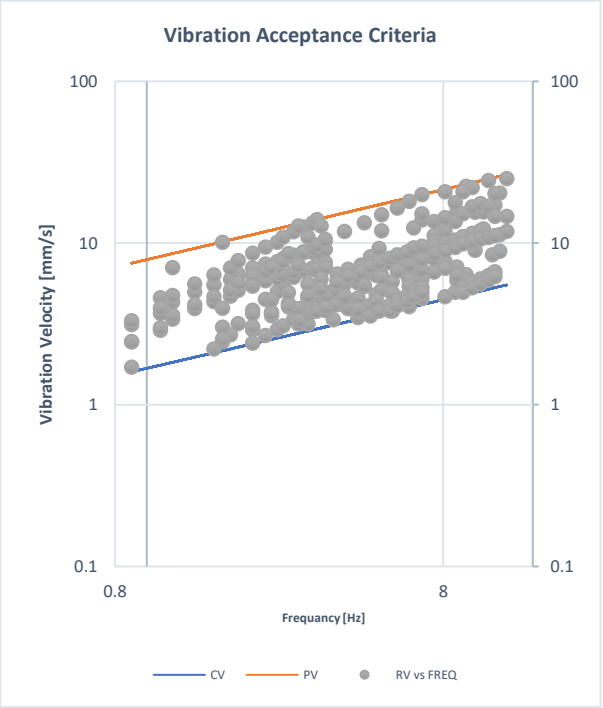


Figure 122. Graph of (CO) category with respect to the VAC lines for sub-model 3.3 (1-Sigma Confidence Results).

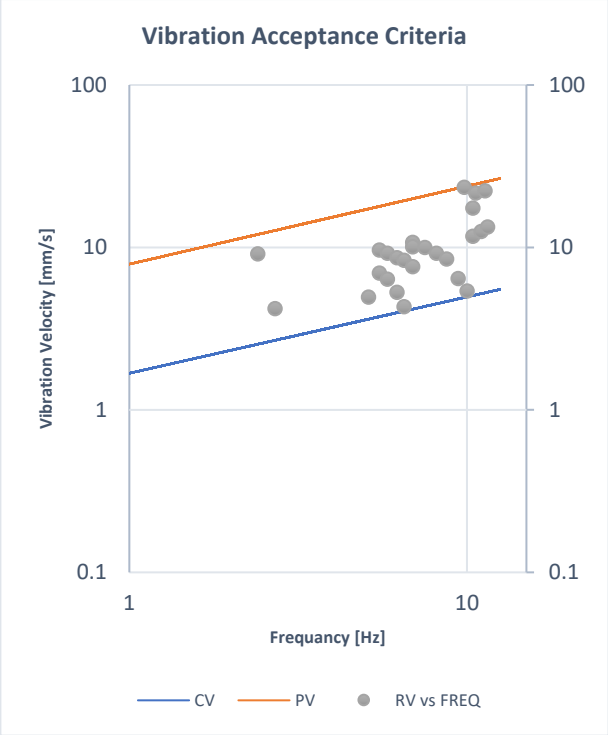


Figure 123. Graph of (CC) category with respect to the VAC lines for sub-model 3.3 (1-Sigma Confidence Results).

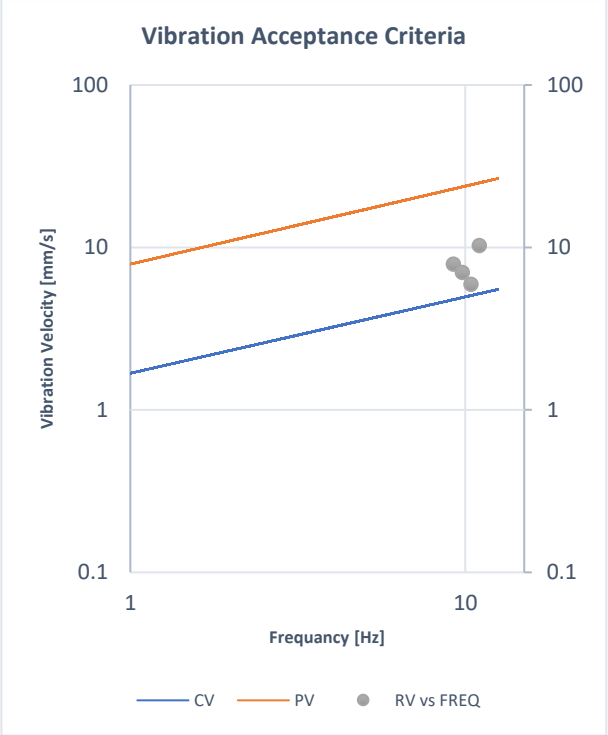


Figure 124. Graph of (CP) category with respect to the VAC lines for sub-model 3.3 (1-Sigma Confidence Results).

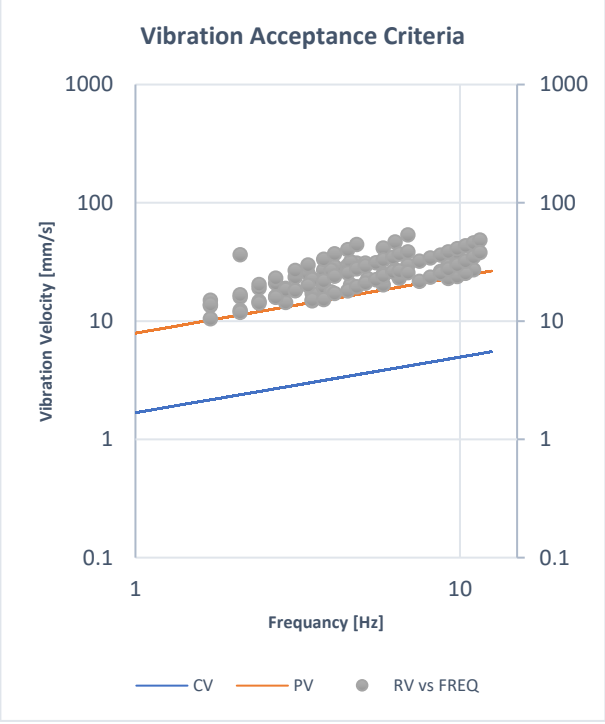


Figure 125. Graph of (PO) category with respect to the VAC lines for sub-model 3.3 (1-Sigma Confidence Results).

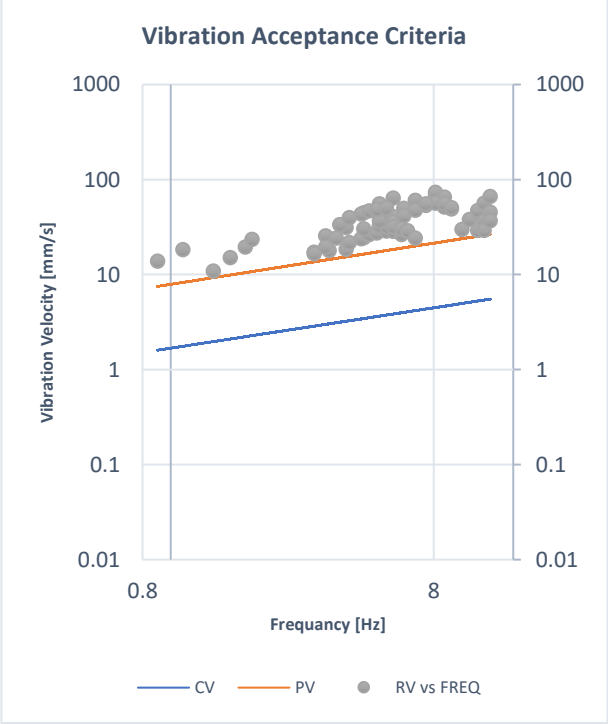


Figure 126. Graph of (PC) category with respect to the VAC lines for sub-model 3.3 (1-Sigma Confidence Results).

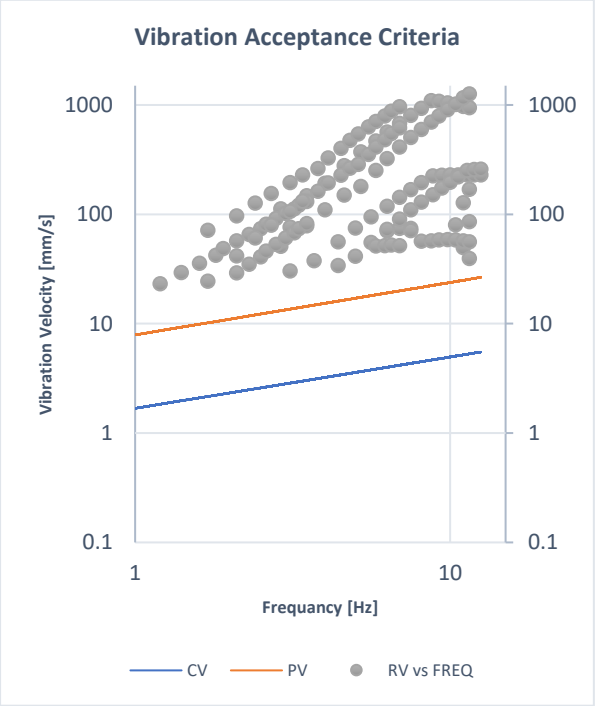


Figure 127. Graph of (PP) category with respect to the VAC lines for sub-model 3.3 (1-Sigma Confidence Results).

3-Sigma Results

The 3-sigma results of this sub-model show similar behavior to the 1-sigma results. For example, the number of cases in the first category (OO) has dropped from 900 cases in the 1-sigma result to 533 cases for the 3-sigma. The classification of the cases among the categories of this sub-model is summarized in Table 23. Using the data in this table the suitability of the VAC was found to be 59.3125% with a confidence of 99.73%. These results show that the VAC only gives a correct judgment of the vibration level 59.3125% of the time. In the following figure 128- 136, the cases of each category are presented with respect to the VAC.

Table 23. Classification of Case Categories and the Number of Cases in Each Category for Sub-Model 3.3 (3-Sigma Confidence)

| # | Category | No. of Cases |
|---|---|---|
| 1 | OO | 608 |
| 2 | OC | 28 |
| 3 | OP | 10 |
| 4 | CO | 297 |
| 5 | CC | 31 |
| 6 | CP | 23 |
| 7 | PO | 145 |
| 8 | PC | 81 |
| 9 | PP | 310 |
| Total | - | 1600 |

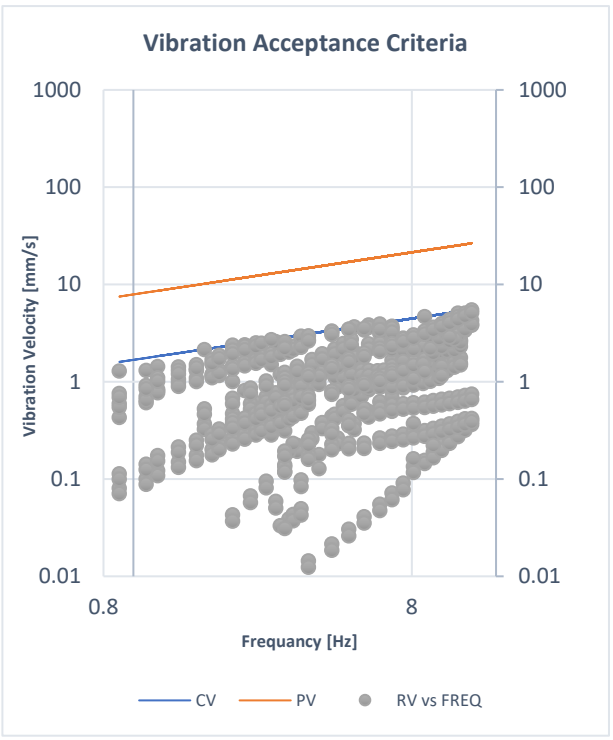


Figure 128. Graph of (OO) category with respect to the VAC lines for sub-model 3.3 (3-Sigma Confidence Results).

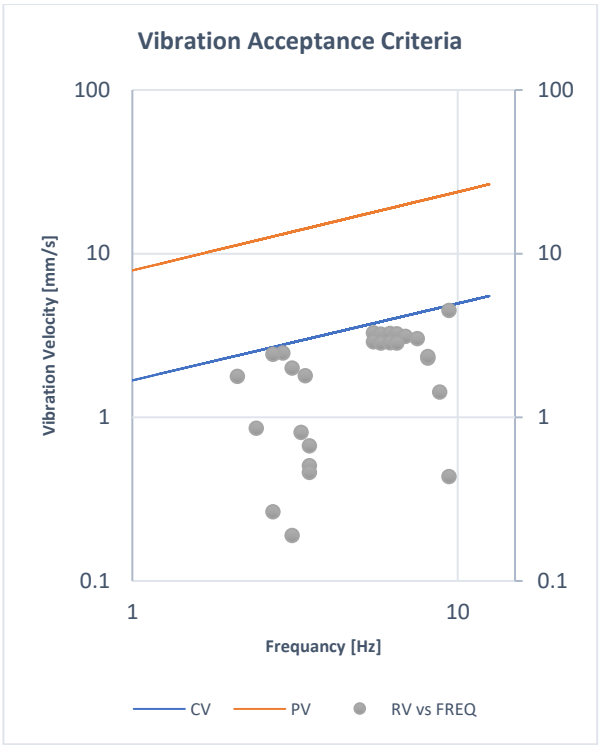


Figure 129. Graph of (OC) category with respect to the VAC lines for sub-model 3.3 (3-Sigma Confidence Results).

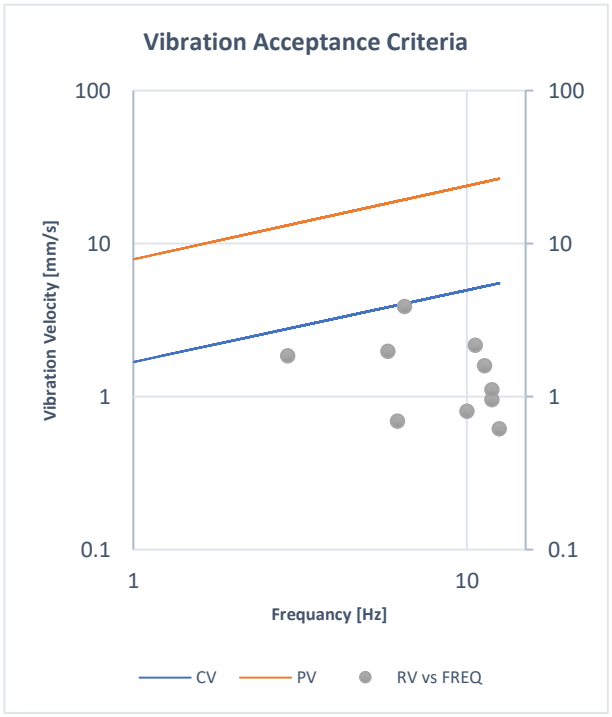


Figure 130. Graph of (OP) category with respect to the VAC lines for sub-model 3.3 (3-Sigma Confidence Results).

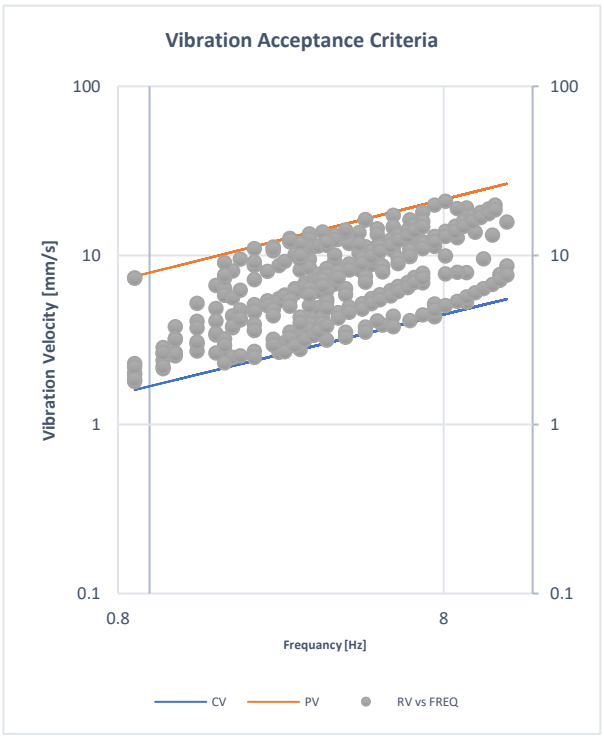


Figure 131. Graph of (CO) category with respect to the VAC lines for sub-model 3.3 (3-Sigma Confidence Results).

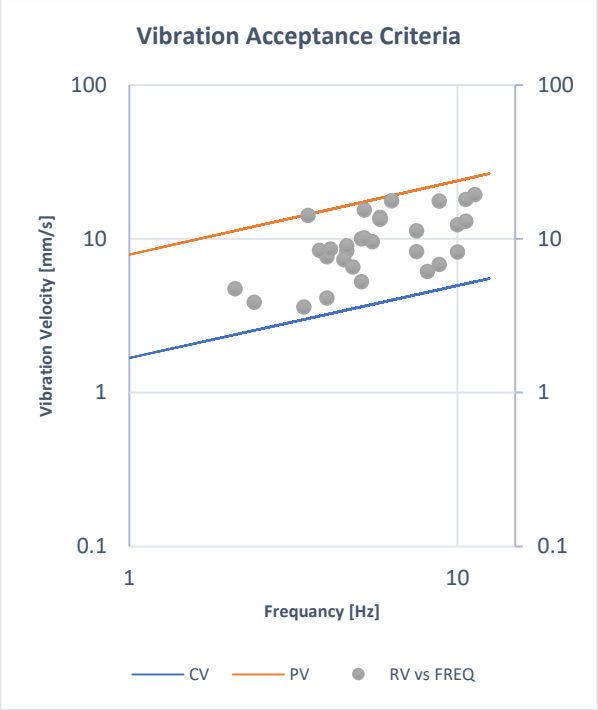


Figure 132. Graph of (CC) category with respect to the VAC lines for sub-model 3.3 (3-Sigma Confidence Results).

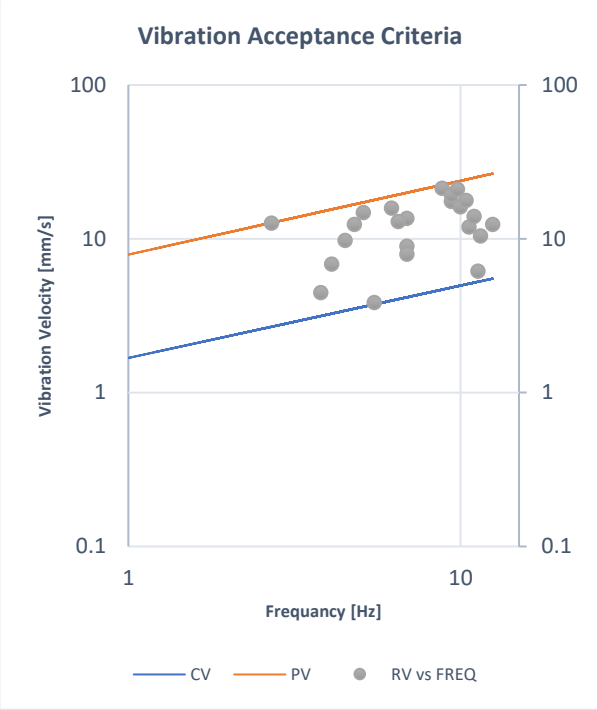


Figure 133. Graph of (CP) category with respect to the VAC lines for sub-model 3.3 (3-Sigma Confidence Results).

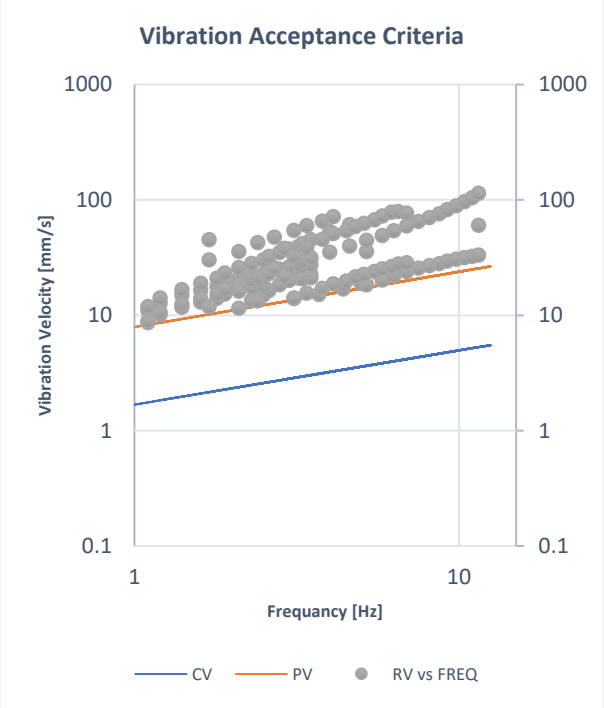


Figure 134. Graph of (PO) category with respect to the VAC lines for sub-model 3.3 (3-Sigma Confidence Results).

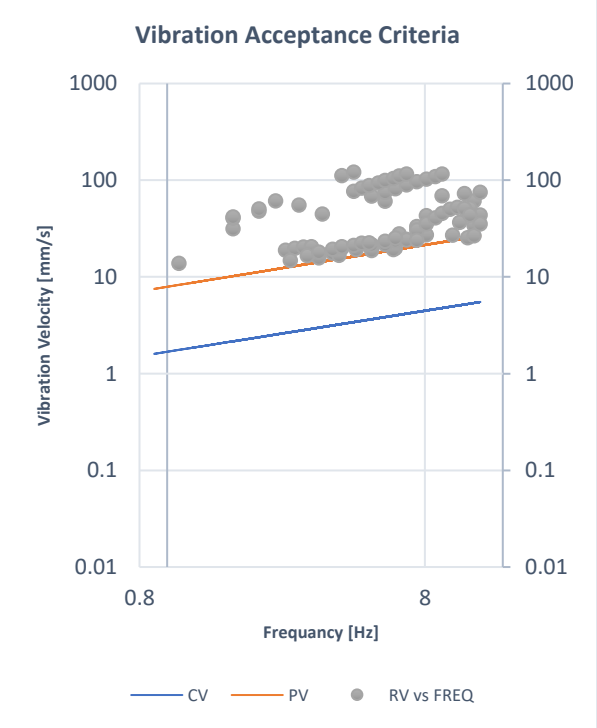


Figure 135. Graph of (PC) category with respect to the VAC lines for sub-model 3.3 (3-Sigma Confidence Results).

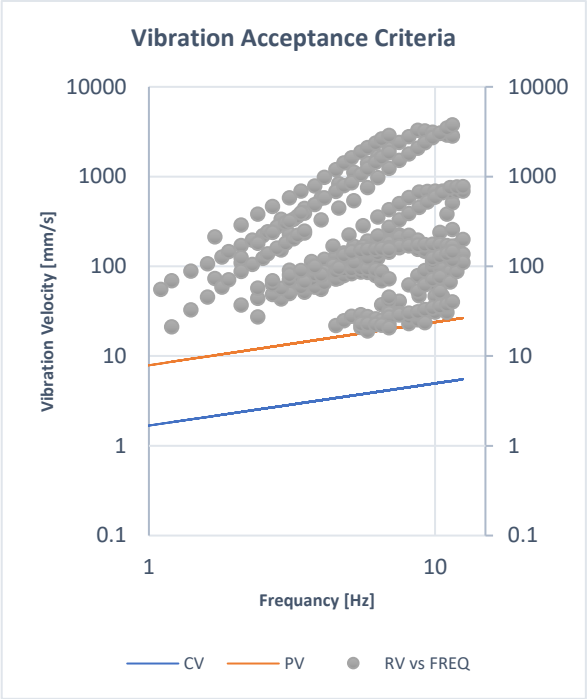


Figure 136. Graph of (PP) category with respect to the VAC lines for sub-model 3.3 (3-Sigma Confidence Results).

### *4.3.4. Discussion of Model 3*

For this model, 3 different sub-models were investigated to find the effect of the run-pipe length on the suitability of the VAC. The first sub-model has a 0.3-meter-long run-pipe which was excited with 1600 different cases of excitation. The 1-sigma confidence results of this sub-model yielded a 66.8896% suitability level, while the 3-sigma results showed an 84.281% suitability level. These results mean that out of 100 vibration velocity measurements on a 4-inch, 0.3-meter run- pipe the VAC will correctly judge almost 67 of the measured reading with a confidence of 68.27% and about 84 readings out of the 100 with 99.73% confidence. The second sub-model has a 1-meter-long run-pipe which was also excited with the same 1600 cases of excitation. The suitability level of the VAC for this model was found to be 69.9375% with 68.27% confidence and 59.5625% with a 99.73% confidence. The increase of the length of the run-pipe has increased the suitability level of the VAC from 66.8896% to 69.9375% for the 1-Sigma

confidence, meaning that the VAC only indicates a correct vibration level and an average of 68 times out of a 100-vibration reading. Meanwhile, the 3-sigma confidence level decreased significantly, as it dropped from 84.281% for sub-model 3.1 to 59.5625% for sub-model 3.2. The third and last sub-model is the 1.5-meter run-pipe sub-model. This model was investigated with the same excitations and the resulting suitability level was obtained as follows. For the 1-sigma confidence, the suitability level was found to be 68.1197%, and the 3-sigma confidence level was 59.3125%. This model shows an increase in the 1-sigma confidence level by about 2% compared to sub-model 3.1 and almost 1% compared to sub-model 3.2. The 3-sigma confidence for this sub-model is almost the same as sub-model 3.2 which is similar behavior to model 1 that had an average of about 65% suitability for its 3 sub-models. The 3-sigma results of sub-model 3.1 are around 20% higher than the 1-sigma result for the same sub-model which is not logical. Having a 3-sigma result which is higher than the 1-sigma result means can be explained by the fact that some of the cases used for the analysis are borderline cases. This means that they were very close to concern or problem vibration lines. Which resulted in many cases changing categories when they were multiplied by 3 to find the 3-sigma results. Considering all the results of the sub-models excluding the 3-sigma results of sub-model 3.1, it can be concluded that the run-pipe length for this model does not affect the suitability of the VAC.

# CHAPTER 5: CONCLUSION

In this thesis, the suitability of the VAC was investigated. This was done using finite element analysis. The suitability was investigated using random vibration analysis. This analysis was conducted on three main models with different run-pipe diameters and these three models had three sub-models with three different lengths. The purpose of this thesis was to investigate the effect of the change in geometry on the suitability of the VAC. By studying the suitability of the VAC and the effect of the run-pipe dimensions the following recommendations are important when assessing the vibration levels in process pipework:

1. It is advised to use the VAC to judge the vibration velocity of a 6-inch run-pipe model when the span of the run-pipe is short to get higher suitability of the VAC.
2. It is advised to use the VAC to judge the vibration velocity of a 5-inch run-pipe model when the span of the run-pipe is long to get higher suitability of the VAC.
3. For a 4-inch run-pipe model, the run-pipe length does not affect the suitability of the VAC.

## Future Work

Further investigations will be conducted in the future to better understand what factors might affect the suitability of the VAC. Following is a list of possible investigations:

1. Investigate more geometrical variations to find their effect on the suitability of the VAC.
2. Conduct statistical analysis to relate the vibration velocity to the stress.
3. Develop a statistical model to predict the stress levels in an SBC using the vibration velocity

# References


[1] Clark, C. (2018, July 3). *What are hydrocarbons?* Retrieved October 29, 2019, from Gulf Coast Environmental Systems (GCES): http://www.gcesystems.com/what-are-hydrocarbons/

[2] Adipah, S. (2019, January 07). Introduction of Petroleum Hydrocarbons Contaminants and its Human Effects. *Journal of Environmental Science and Public Health, 3*(1), 001-009. doi:10.26502/jesph.96120043

[3] *Crude and Petroleum Products*. (2011). Retrieved from U.S. Environmental Protection Agency.

[4] Alonzo, B. (2017, April 25). *The Effects of Pollution on the Body*. Retrieved October 30, 2019, from Sciencing: https://sciencing.com/effects-pollution-body-8792.html

[5] Teixeira, G. D. (2017, May 07). *Fatigue of Metals: Failure and Success.* Retrieved October 31, 2019, from Researchgate: https://www.researchgate.net/publication/316735574_Fatigue_of_Metals_Failure_and_Success

[6] Neuber, H., J.S., B., & Ba, D. W. (1946). *Theory of Notch Stresses; Principles for Exact Stress Calculation.* Ann Arbor, J.W. Edwards.

[7] Taylor, D. (2007). *The Theory of Critical Distances: A New Perspective in Fracture Mechanics.* Elsevier Ltd.

[8] Dowling, N. (2013). *Mechanical Behavior of Materials* (4 ed.). Pearson Education Limited.

[9] *Basics for Fatigue Analysis of Piping System using Caesar II*. (2019, August 06). Retrieved October 31, 2019, from What is Piping: https://www.whatispiping.com/basics-fatigue-analysis

[10] *Overview of Fatigue (Material)*. (n.d.). Retrieved from Inspectioneering: https://inspectioneering.com/tag/fatigue

[11] Howell, D. (2010, August). *A Brief History of Steel Pipe*. Retrieved August 31, 2020, from Pipeline Equities: http://www.pipelineequities.com/A-Brief-History-of-Steel-Pipe.

[12] Fafandjel, N., Rubesa, R., & Simone, W. (2008). New approach for shipyard pipe production line optimization. In *Maritime Industry, Ocean Engineering and Coastal Resources, Volume 1 Maritime Transportation* (pp. 469-476). London: Taylor and Francis / Balkema.

[13] Sölken, W. (n.d.). *Steel Pipe and Manufacturing Processes*. Retrieved September 1, 2020, from Wermac: http://www.wermac.org/pipes/pipemaking.html

[14] *Introduction to Seamless Pipe Manufacturing*. (n.d.). Retrieved September 1, 2020, from The Process Piping: https://www.theprocesspiping.com/introduction-to-seamless-pipe-manufacturing/

[15] *Introduction to Welded Pipe Manufacturing*. (n.d.). Retrieved September 1, 2020, from The Process Piping: https://www.theprocesspiping.com/introduction-to-pipe/

[16] *Codes, Standards, and Recommended Practices*. (n.d.). Retrieved from The Process Piping: https://www.theprocesspiping.com/codes-standards-and-recommended-practices/

[17] *PIPING FATIGUE ANALYSIS*. (n.d.). Retrieved from Kelm Engineering: https://www.kelmengineering.com/analytical-services/piping-fatigue-analysis

[18] *Weldolet, Sockolet, Threadolet*. (2020, August 31). Retrieved from Octal Pipe

Fittings: https://www.octalpipefittings.com/weldolet-sockolet-threadolet/

[19] *Ferrous Alloys- General Steel*. (n.d.). Retrieved from efunda: http://www.efunda.com/

[20] (2020). *ISSF Duplex Stainless Steels.* International Stainless Steel Forum.

[21] *Metals and Alloys*. (2005). Retrieved November 3, 2019, from Engineering ToolBox: https://www.engineeringtoolbox.com

[22] *What's the Difference Between Stainless Steel and Carbon Steel?* (2018, January 31). Retrieved November 12, 2019, from Monroe Engineering: https://monroeengineering.com/blog/whats-the-difference-stainless-steel-vs-carbon-steel/

[23] Leong, D. (2019, April 24). *Carbon Steel vs Stainless Steel*. Retrieved November 3, 2019, from Markforged: https://markforged.com/blog/carbon-steel-vs-stainless-steel/

[24] Palsson, Namurata Sathirachinda ; Kaewkumsai, Siam ; Wongpinkaew, Kosit ; Khonraeng, Witsanupong ;. (2017, Augest 22). Fatigue Failure of Hydrocarbon Piping System. *Journal of Failure Analysis and Prevention*, *17*, 838–847. doi:10.1007/s11668-017-0339-7

[25] Semiga, V. (2016). *Fatigue Considerations for Natural Gas Transmission Pipelines.* BMT FLEET TECHNOLOGY LIMITED. Interstate Natural Gas Association of America.

[26] *Common Causes Of Piping Vibration And Its Effects On Piping Systems*. (n.d.). Retrieved from Rishabh Engineering: https://www.rishabheng.com/blog/causes-and-effects-piping-system-vibration/

[27] WANT2LEARN. (2019, September 11). *Common Causes and Effects of Piping*

*Vibration: A short article*. Retrieved from What is Piping: https://www.whatispiping.com/piping-vibration

[28] Petroleum Safety Authority Norway. (2016, March 15 ). *Investigation of Hydrocarbon Leak on Gudrun on 18 February 2015*. Retrieved from https://www.ptil.no/en/supervision/investigation-reports/2016/statoil---gudrun---investigation-into-hydrocarbon-leak/

[29] Petroleum Safety Authority Norway. (2014, May 15). *Investigation of hydrocarbon leak at the Hammerfest LNG facility in northern Norway on 5 January 2014*. Retrieved from https://www.ptil.no/en/supervision/investigation-reports/2014/statoil---hammerfest-lng---gransking-av-hydrokarbonlekkasje/

[30] Energy Institute. (2008). Guidelines for the Avoidance of Vibration Induced Fatigue Failure in Process Pipework. The UK.

[31] British Standards Institute. (2014). BS7608 Guide to fatigue design and assessment of steel products.

[32] Requirements for preoperational and initial start-up vibration testing of nuclear power plant piping systems. (1983). The United States.

[33] API 618 5th Edition. (2007). *Reciprocating Compressors for Petroleum, Chemical, and Gas Industry Services.* Washington, D.C.: American Petroleum Institute.

[34] Southwest Research Institute. (1986). Pipeline and Compressor Research Council. Controlling the Effects of Pulsations and Fluid Transients in Piping Systems. Southwest Research Institute. Dallas. Retrieved from Southwest Research Institute.

[35] Greenfield, S., & de La Roche, L. (1996). *Introduction to Vibration & Pulsation*

*in Reciprocating Compressors.* Canada.

[36] European Forum Reciprocating Compressors (EFRC). (2009). *Guidelines for Vibrations in Reciprocating Compressor Systems.*

[37] *Controlling the Effects of Pulsations and Fluid Transients in Piping Systems*. (1979). San Antonio, TX: Southwest Research Institute.

[38] Riverin, J. -L., & Pettigrew, M. J. (2007, FEBRUARY ). Vibration Excitation Forces Due to Two-Phase Flow in Piping Elements. *Journal of Pressure Vessel Technology, Vol. 129*(1), 7-13. Retrieved August 27, 2020

[39] Pettigrew, M. J., & Taylor, C. E. (1994, August 1). Two-Phase Flow-Induced Vibration: An Overview (Survey Paper). *Journal of Pressure Vessel Technology, 116*(3), 233-253. Retrieved August 27, 2020

[40] Thomson, W. T., & Dahleh, M. D. (1998). *Theory of Vibration with Applications* (5th ed.). New Jersey.

[41] Bifano, M. F., Breaux, L., Feller, A. J., & Brodzinski, R. (2018). *New Fatigue Screening Criteria for the Fitness-for-Service Assessment of In-Service Process Piping Vibrations*. Retrieved 8 27, 2020, from https://asmedigitalcollection.asme.org/pvp/proceedings/pvp2018/51586/v01at01a002/274302

# APPENDIX A: PIPEWORK STANDARDS

The American Petroleum Institute (API) Standards

API 5L – Specification for Line Pipe

API 6D – Pipeline Valves, End Closures, Connectors, and Swivels

API 6F – Recommended Practice for Fire Test for valves

API 593 – Ductile Iron Plug Valves – Flanged Ends

API 598 – Valve Inspection and Test

API 600 – Steel Gate Valves

API 601 – Metallic Gaskets for Refinery Piping

API 602 – Compact Design Carbon Steel Gate Valves

API 604 – Ductile Iron Gate Valves – Flanged Ends

API 605 – Large Diameter Carbon Steel Flanges

API 607 – Fire Test for Soft Seated Ball Valves

API 609 – Butterfly Valves

API 1104 – Standard for Welding Pipeline and Facilities

The American Iron and Steel Institute (AISI) Standard

AISI 410 – 13% Chromium Alloy Steel

AISI 304 – 18/8 Austenitic Stainless Steel

AISI 316 – 18/8/3 Austenitic Stainless Steel

The American National Standards Institute (ANSI) Standards

ASME B31.1 – Power Piping

ASME B31.2 – Fuel Gas Piping

ASME B31.3 – Process Piping

ASME B31.4 – Pipeline Transportation Systems for Liquid Hydrocarbons and Other Liquids

ASME B31.5 – Refrigeration Piping and Heat Transfer Components

ASME B31.8 – Gas Transmission and Distribution Piping Systems

ASME B31.8S- Managing System Integrity of Gas Pipelines

ASME B31.9 – Building Services Piping

ASME B31.11 – Slurry Transportation Piping Systems

Other major ANSI / ASME Standards refereed for the piping elements are:

ANSI B 1.1 – Unified Inch Screw Threads
ANSI / ASME B 1.20.1 – Pipe threads for general purposes
ANSI / ASME B 16.1 – Cast Iron Pipe Flanges and Flanged Fittings
ANSI / ASME B 16.3 – Malleable Iron Threaded Fittings
ANSI / ASME B 16.4 – Cast Iron Threaded Fittings
ANSI / ASME B 16.5 – Steel Pipe Flanges and Flanged Fittings
ANSI / ASME B 16.9 – Steel Butt Welding Fittings
ANSI / ASME B 16.10 – Face to Face and End to End Dimensions of Valves
ANSI / ASME B 16.11 – Forged Steel Socket Welding and Threaded fittings
ANSI B 16.20 – Metallic Gaskets for Pipe Flanges – ring joint, spiral wound
ANSI / ASME B 16.21 – Non-Metallic Gaskets for Pipe Flanges
ANSI / ASME B 16.25 – Butt Welding Ends
ANSI / ASME B 16.28 – Short Radius Elbows and Returns
ANSI / ASME B 16.34 – Steel Valves, Flanged and butt welding ends
ANSI / ASME B 16.42 – Ductile Iron Pipe Flanges and Flanged Fittings – Class 150# and 300#
ANSI / ASME B 16.47 – Large Diameter Steel Flanges – NPS – 26″ to 60″
ANSI / ASME B 18.2 1 and 2 – Square and Hexagonal head Bolts and Nuts (Inch and mm)
ANSI / ASME B 36.10 – Welded and Seamless Wrought Steel Pipes
ANSI / ASME B 36.19 – Welded and Seamless Austenitic Stainless Steel Pipe
The American Society for Testing and Materials (ASTM) Standards
These consist of 16 sections on definitions and classifications of materials of construction and Test methods. Most of the ASTM Standards are adapted by ASME and are specified in ASME Section II. Section II has four parts.
Part A – Ferrous Materials
Part B – Non-Ferrous Materials
Part C – Welding Materials
Part D – Properties of Materials
American Welding Society (AWS) Standards
These standards provide information on the welding fundamentals, weld design, welder’s training qualifications, testing and inspection of the welds, and guidance on

the application and use of welds. Individual electrode manufacturers have given their brand names for the various electrodes and the same are sold under these names.

American Water Works Association (AWWA) Standards

These standards refer to the piping elements required for low-pressure water services. These are less stringent than other standards. Valves, Flanges, etc., required for large diameter water pipelines are covered under this standard and are refereed rarely by piping engineers.

C-500: Gate Valves for Water and sewage system

C-504: Rubber Seated Butterfly Valves

C-507: Ball Valves 6″ to 48″

C-508: Swing Check Valves 2″ to 24″

C-509: Resilient Seated Gate Valves for water and sewage

C-510: Cast Iron Sluice Gate Valves

The Manufacturers Standardization Society of Valves and Fitting Industry – Standard Practices (MSS-SP) Standards

In addition to the above standards and material codes, there are standard practices followed by manufacturers. These are published as advisory standards and are widely followed. The most common MSS-SP standards referred for piping are

MSS-SP-6: Standard Finishes for contact surface for flanges

MSS-SP-25: Standard marking system for valves, fittings, flanges

MSS-SP-42: Class 150 corrosion-resistant gate, globe, and check valves

MSS-SP-43: Wrought stainless steel butt weld fittings

MSS-SP-56: Pipe hanger supports – Material, design, and manufacture

MSS-SP-61: Pressure testing of valves

MSS-SP-67: Butterfly Valves

MSS-SP-68: High Pressure off seat butterfly valves

MSS-SP-69: Pipe hanger supports – selection and applications

MSS-SP-70: Cast iron gate valves

MSS-SP-71: Cast iron check valves

MSS-SP-72: Ball Valves

MSS-SP-78: Cast iron plug valves

MSS-SP-80: Bronze gate, globe, and check valves

MSS-SP-81: Stainless steel bonnet-less knife gate valves

MSS-SP-83: Pipe unions

MSS-SP-85: Cast iron globe valves

MSS-SP-88: Diaphragm valves

MSS-SP-89: Pipe hangers and supports – fabrication and installation practices

MSS-SP-90: Pipe hangers and supports – guidelines on terminology

MSS-SP-92: MSS valves user guide

MSS-SP-108: Resilient seated eccentric CI plug valves

British Standards

In many instances, it is possible to find a British Standard which may be substituted for American Standards. For example, BS 2080 (British Standard for Face to Face or End to End dimensions of valves) is identical to ANSI/ASME B16.10. Similarly, BS 3799 and ANSI/ASME B 16.11 also compare.

There are certain British Standards referred to by Indian Manufacturers for Piping and Valves. The most commonly referred British Standards in the Piping Industry are :

BS 10: Flanges

BS 806: Pipes and Fittings for Boilers

BS 916: Black Bolts, Nuts, and Screws

BS 970: Steel for Forging, Bars, Rods, valve steel, etc.

BS 1212: Specification for Float Operated Valves

BS 1306: Copper and Copper alloy pressure piping system

BS 1414: Gate Valves for Petroleum Industry

BS 1560: Steel Pipe Flanges

BS 1600: Dimensions of Steel Pipes

BS 1640: Butt-Welding Fittings

BS 1740: Wrought Steel screwed pipe fittings

BS 1868: Steel Check Valves for Petroleum Industry

BS 1873: Steel Globe and Check Valves for Petroleum Industry

BS 1965: Butt-welding pipe fittings

BS 2080: Face to Face / End to End Dimensions of Valves

BS 2598: Glass Pipelines and Fittings

BS 3059: Boiler and Super-heater Tubes

BS 3063: Dimensions of Gaskets for Pipe Flanges

BS 3381: Metallic Spiral Wound Gaskets

BS 3600: Dimensions of Welded and Seamless Pipes and Tubes

BS 3601: C.S. Pipes and Tubes for pressure purposes at room temperature

BS 3602: C.S. Pipes and Tubes for pressure purposes at high temperature

BS 3603: C.S. and Alloy Steel Pipes and Tubes for pressure purposes at low temperature

BS 3604: Alloy Steel Pipes and Tubes for high temperature

BS 3605: SS Pipes and Tubes for pressure purposes

BS 3799: Socket Weld / Screwed Fittings

BS 3974: Pipe hangers, Slides, and Roller type supports

BS 4346: PVC pressure pipe – joints and fittings

BS 4504: Steel, Cast Iron, and Copper alloy fittings

BS 5150: Cast Iron Wedge and Double Disc Gate Valves for general purposes

BS 5151: Cast Iron Gate (parallel slide) Valves for general purposes

BS 5152: Cast Iron Globe and Check Valves for general purposes

BS 5153: Cast Iron Check Valves for general purposes

BS 5154: Copper alloy Globe, Gate, and Check Valves

BS 5155: Cast Iron and Cast Steel Butterfly Valves for general purposes

BS 5156: Diaphragm Valves for general purposes

BS 5157: Steel Gate (parallel slide) Valves for general purposes

BS 5158: Cast Iron and Cast Steel Plug Valves for general purposes

BS 5159: Cast Iron and Cast Steel Ball Valves for general purposes

BS 5160: Flanged Steel Globe and Check Valves for general purposes

BS 5163: Flanged Cast Iron Wedge Gate Valves for general purposes

BS 5351: Steel Ball Valves for Petroleum Industry

BS 5352: Steel Gate, Globe and Check Valves, smaller than 2″ NB

BS 5353: Specifications for Plug Valves

BS 5391: Specifications for ABS pressure pipes

BS 5392: Specifications for ABS fittings

BS 5433: Specifications for underground stop valves for water services

BS 5480: Specifications for GRP pipes and fittings

BS 6364: Specifications for Valves for Cryogenic services

BS 6755: Testing of Valves

BS 6759: Safety Valves

Indian Standards

Bureau of Indian Standards (BIS) has so far not developed an Indian Standard for the

design of Piping Systems. Hence, ANSI Standards ASME 31.1 and 31.3 are widely used for the design. These standards also accept materials covered in other standards. Unlike American Standards, Indian Standards cover dimensions and material specifications under the same standard number. There are no groupings based on a branch of engineering. Some of the most commonly referred Indian Standards by Piping Engineers are :

IS 210: Grey Iron Castings
IS 226: Structural Steel (superseded by IS 2062)
IS 554: Dimensions of Pipe Threads
IS 778: Specification for Copper Alloy Gate, Globe, and Check Valves
IS 780: Specification for Sluice Valves – 50 NB to 300 NB
IS 1239 (Part I and II): Specification for Mild Steel tubes and fittings
IS 1363: Hexagonal Bolts, Screws and Nuts – Grade C
IS 1364: Hexagonal Bolts, Screws and Nuts – Grade A and B
IS 1367: Technical supply conditions for threaded steel fasteners
IS 1536: Centrifugally Cast Iron Pipes
IS 1537: Vertically Cast Iron Pipes
IS 1538: Cast Iron Fittings
IS 1870: Comparison of Indian and Overseas Standards
IS 1879: Malleable Iron Pipe Fittings
IS 1978: Line Pipe
IS 1979: High Test Line Pipe
IS 2002: Steel Plates
IS 2016: Plain Washers
IS 2041: Steel Plates for Pressure Vessels used at moderate and low temperature
IS 2062: Steel for general structural purposes
IS 2379: Color Code for Identification of Pipelines
IS 2712: Compressed Asbestos Fiber Jointing
IS 2825: Code for Unfired Pressure Vessels
IS 2906: Specification for Sluice Valves – 350 NB to 1200 NB
IS 3076: Specification for LDPE Pipes
IS 3114: Code of Practice for laying pipes
IS 3516: Cast Iron flanges and flanged fittings for Petroleum Industry

IS 3589: Seamless or ERW Pipes (150 NB to 2000 NB)

IS 4038: Specifications for Foot Valves

IS 4179: Sizes for pressure vessels and leading dimensions

IS 4853: Radiographic Examination of Butt Weld Joints in pipes

IS 4864 to IS 4870: Shell Flanges for vessels and equipment

IS 4984: Specification for HDPE Pipes

IS 4985: Specification for PVC Pipes

IS 5312: Specification for Check Valves

IS 5572: Classification of Hazardous area for Electrical Installation

IS 5822: Code of practice for laying welded steel pipes

IS 6157: Inspection and Testing of Valve

IS 6286: Seamless and Welded pipes for Subzero temperatures

IS 6392: Steel Pipe Flanges

IS 6630: Seamless alloy steel pipes for high-temperature service

IS 6913: Stainless Steel tubes for the food and beverage industry

IS 7181: Horizontally cast iron pipes

IS 7240: Code of Practice for Cold Insulation

IS 7413: Code of Practice for Hot Insulation

IS 7719: Metallic spiral wound gaskets

IS 7806: Stainless Steel Castings

IS 7899: Alloy Steel castings for pressure services

IS 8008: Specification for molded HDPE Fittings

IS 8360: Specification for fabricated HDPE Fittings

IS 9890: Ball Valves for general purposes

IS 10221: Code of Practice for coating and wrapping of underground MS pipelines

IS 10592: Eyewash and safety showers

IS 10605: Steel Globe Valves for Petroleum Industries

IS 10611: Steel Gate Valves for Petroleum Industries

IS 10711: Size of Drawing Sheets

IS 10805: Foot Valves

IS 10989: Cast / Forged Steel Check Valves for Petroleum Industry

IS 10990: Technical drawings – Simplified representation of pipelines

IS 11790: Code of Practice for preparation of Butt welding ends for valves, flanges, and fittings

IS 11791: Diaphragm Valves for general purposes

IS 11792: Steel Ball Valves for Petroleum Industry

IS 12709: Specifications for GRP pipes

IS 13049: Specifications for Diaphragm type float operated valves

IS 13095: Butterfly Valves

IS 13257: Ring type joint gasket and grooves for flanges

## APPENDIX B: MATLAB CODES USED TO GENERATE PSD CURVES

Model 3 Code:

```
beta=xlsread('Case studies - Copy','D=4',
'B2:B1601');
m1=xlsread('Case studies - Copy','D=4', 'C2:C1601');
m2=xlsread('Case studies - Copy','D=4', 'D2:D1601');
f0bar=xlsread('Case studies - Copy','D=4',
'E2:E1601');
PSD0bar=xlsread('Case studies - Copy','D=4',
'F2:F1601');
rhog=xlsread('Case studies - Copy','D=4',
'H2:H1601');
rhol=xlsread('Case studies - Copy','D=4',
'I2:I1601');
V=xlsread('Case studies - Copy','D=4', 'J2:J1601');
G=xlsread('Case studies - Copy','D=4', 'K2:K1601');
f0=xlsread('Case studies - Copy','D=4', 'L2:L1601');

D=4.026*0.0254;

f = 0.1:0.1:100;
for i = 1 : length(V)
    for j = 1 : length(f)
        fbar(i,j) = f(j)*D/V(i);
            if fbar(i,j) < f0bar(i)
                PSDbar(i,j) =
(PSD0bar(i)/f0bar(i)^m1(i))*fbar(i,j)^m1(i);
            else
                PSDbar(i,j) =
(PSD0bar(i)/f0bar(i)^m2(i))*fbar(i,j)^m2(i);
            end
         PSD(i,j) = PSDbar(i,j)*(G(i)*D)^2;
    end
    [maxPSD,   index] = max(PSD,[],2);
    freq2(i)= f(index(i));
end
loglog(f,PSD(1:end,:))
title('PSD Vs f')
xlabel('f (Hz)')
ylabel('PSD (m^4/s)')
results = PSD;
xlswrite('PSDRESULTS D=4.xlsx',results)
xlswrite('Freq2 D=4.xlsx',freq2)
```

==========

Model 2 Code:

```
beta=xlsread('Case studies - Copy','D=5',
'B2:B1601');
m1=xlsread('Case studies - Copy','D=5', 'C2:C1601');
m2=xlsread('Case studies - Copy','D=5', 'D2:D1601');
f0bar=xlsread('Case studies - Copy','D=5',
'E2:E1601');
PSD0bar=xlsread('Case studies - Copy','D=5',
'F2:F1601');
rhog=xlsread('Case studies - Copy','D=5',
'H2:H1601');
rhol=xlsread('Case studies - Copy','D=5',
'I2:I1601');
V=xlsread('Case studies - Copy','D=5', 'J2:J1601');
G=xlsread('Case studies - Copy','D=5', 'K2:K1601');
f0=xlsread('Case studies - Copy','D=5', 'L2:L1601');

D=5.05*0.0254;

f = 0.1:0.1:100;
for i = 1 : length(V)
    for j = 1 : length(f)
        fbar(i,j) = f(j)*D/V(i);
            if fbar(i,j) < f0bar(i)
                PSDbar(i,j) =
(PSD0bar(i)/f0bar(i)^m1(i))*fbar(i,j)^m1(i);
            else
                PSDbar(i,j) =
(PSD0bar(i)/f0bar(i)^m2(i))*fbar(i,j)^m2(i);
            end
         PSD(i,j) = PSDbar(i,j)*(G(i)*D)^2;
    end
    [maxPSD,   index] = max(PSD,[],2);
    freq2(i)= f(index(i));
end
loglog(f,PSD(1:end,:))
title('PSD Vs f')
xlabel('Frequency')
ylabel('PSD')
```

==========

Model 1 Code:

```
beta=xlsread('Case studies - Copy','D=6',
'B2:B1601');
m1=xlsread('Case studies - Copy','D=6', 'C2:C1601');
m2=xlsread('Case studies - Copy','D=6', 'D2:D1601');
f0bar=xlsread('Case studies - Copy','D=6',
'E2:E1601');
PSD0bar=xlsread('Case studies - Copy','D=6',
'F2:F1601');
rhog=xlsread('Case studies - Copy','D=6',
'H2:H1601');
rhol=xlsread('Case studies - Copy','D=6',
'I2:I1601');
V=xlsread('Case studies - Copy','D=6', 'J2:J1601');
G=xlsread('Case studies - Copy','D=6', 'K2:K1601');
f0=xlsread('Case studies - Copy','D=6', 'L2:L1601');

D=6.065*0.0254;

f = 0.1:0.1:100;
for i = 1 : length(V)
    for j = 1 : length(f)
        fbar(i,j) = f(j)*D/V(i);
            if fbar(i,j) < f0bar(i)
                PSDbar(i,j) =
(PSD0bar(i)/f0bar(i)^m1(i))*fbar(i,j)^m1(i);
            else
                PSDbar(i,j) =
(PSD0bar(i)/f0bar(i)^m2(i))*fbar(i,j)^m2(i);
            end
         PSD(i,j) = PSDbar(i,j)*(G(i)*D)^2;
    end
    [maxPSD,   index] = max(PSD,[],2);
    freq2(i)= f(index(i));
end
loglog(f,PSD(1:end,:))
title('PSD Vs f')
xlabel('f (Hz)')
ylabel('PSD (m^4/s)')
results = PSD;
xlswrite('PSDRESULTS D=6.xlsx',results)
xlswrite('Freq2 D=6.xlsx',freq2)
```

APPENDIX C: SOLIDWORKS MODELS

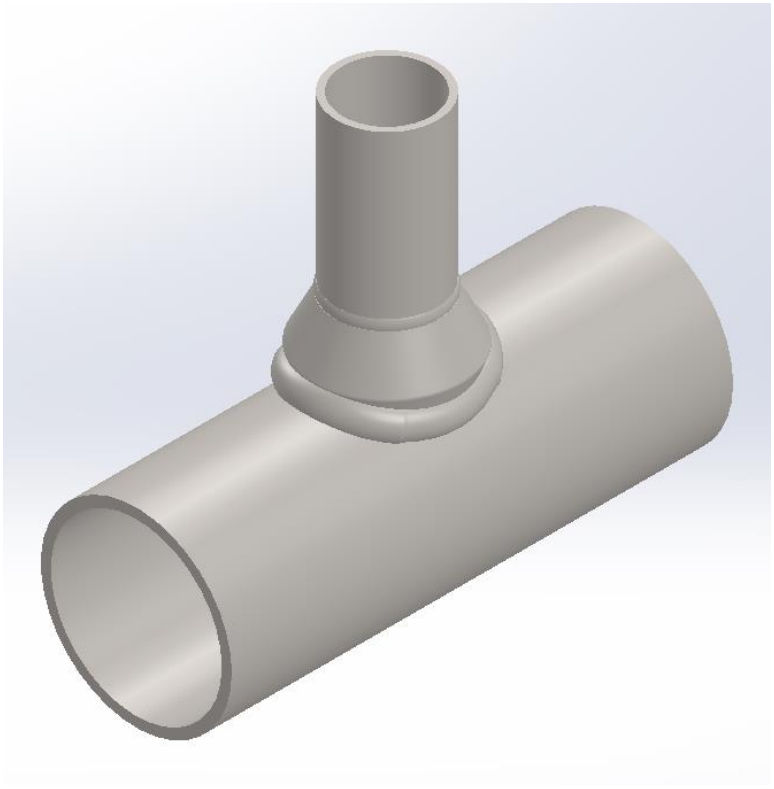

Figure 137. Isometric view of sub-model 3.1

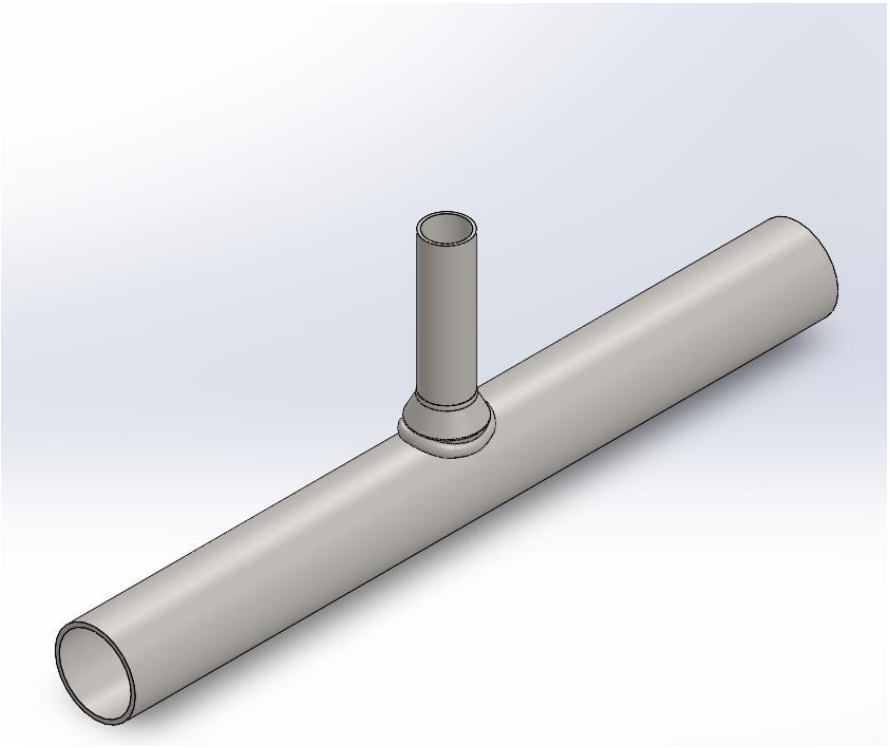

Figure 138. Isometric view of sub-model 3.2

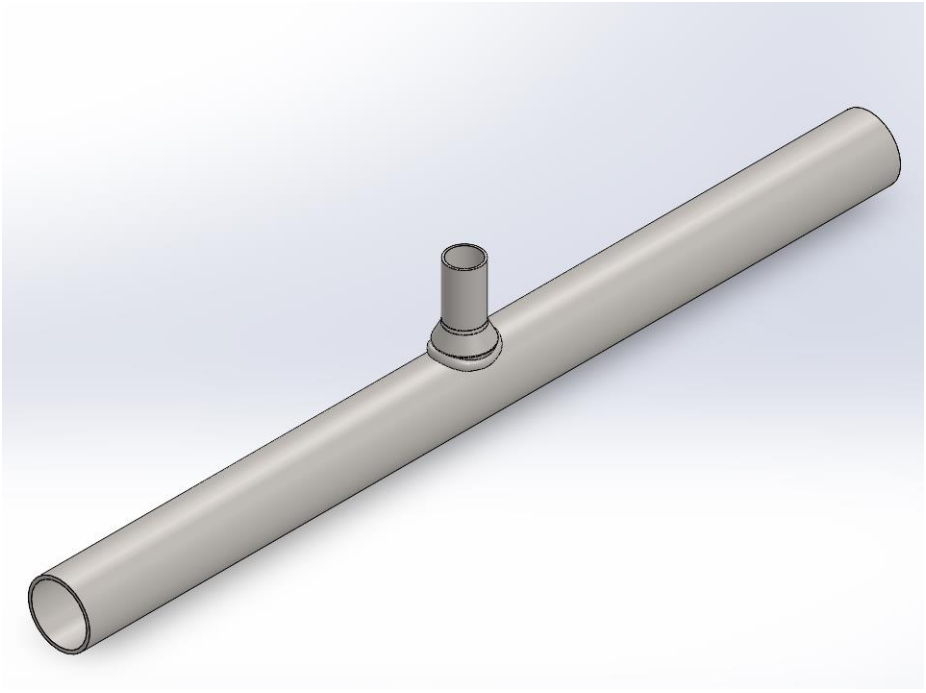

Figure 139. Isometric view of sub-model 3.3

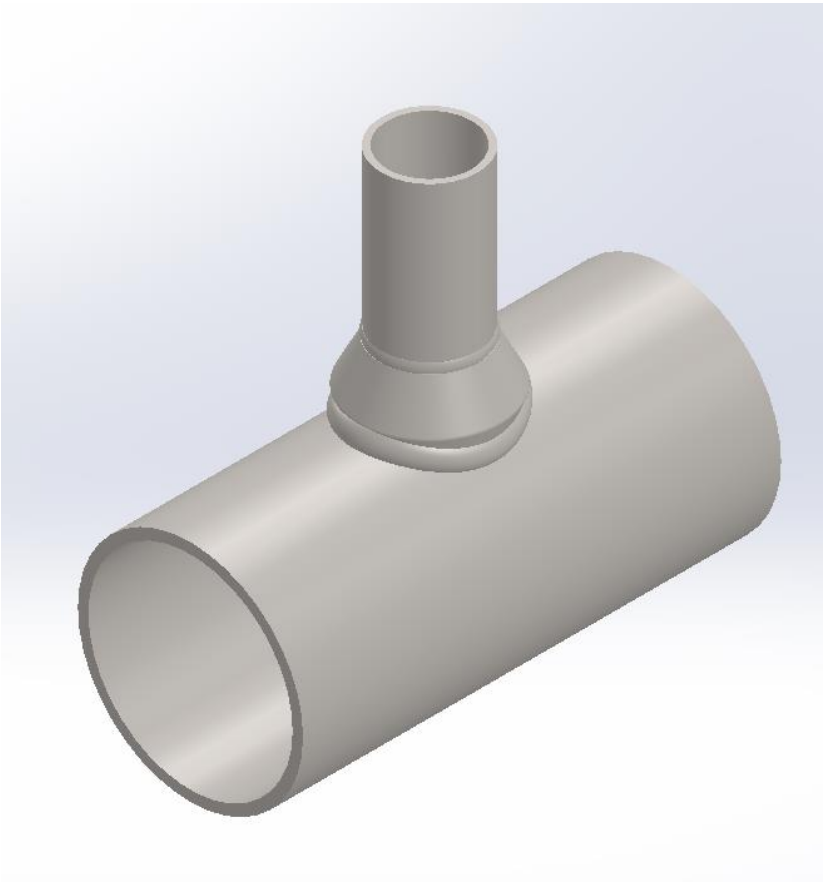

Figure 140. Isometric view of sub-model 2.1

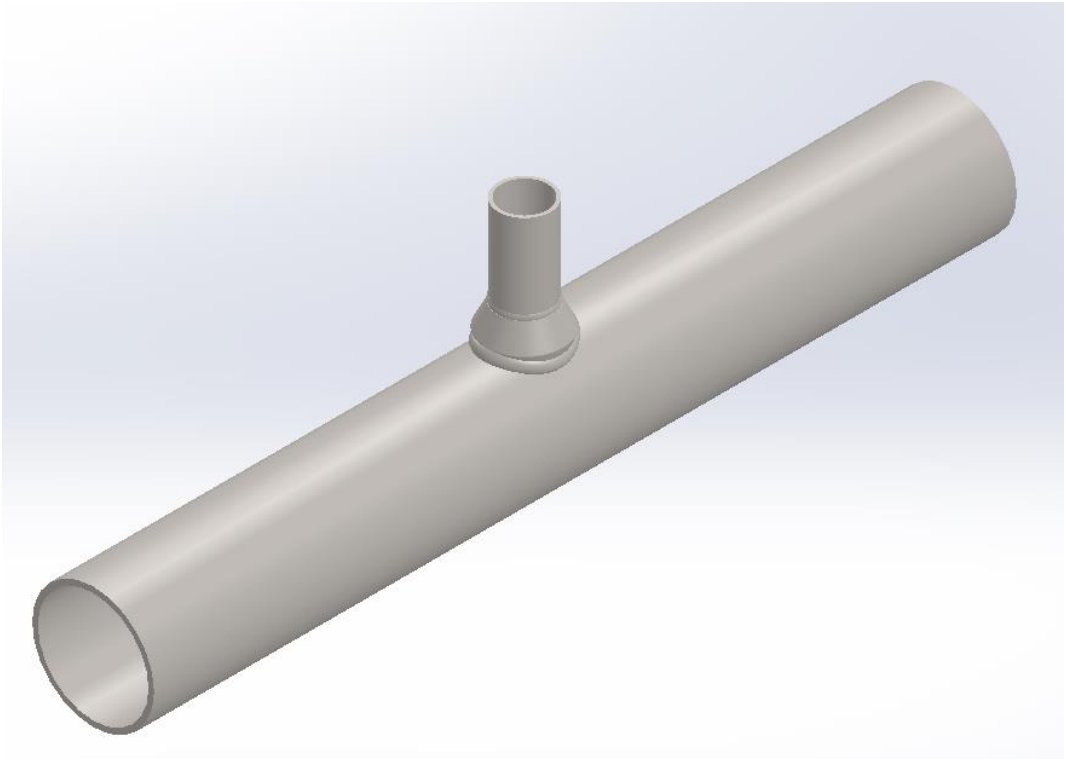

Figure 141. Isometric view of sub-model 2.2

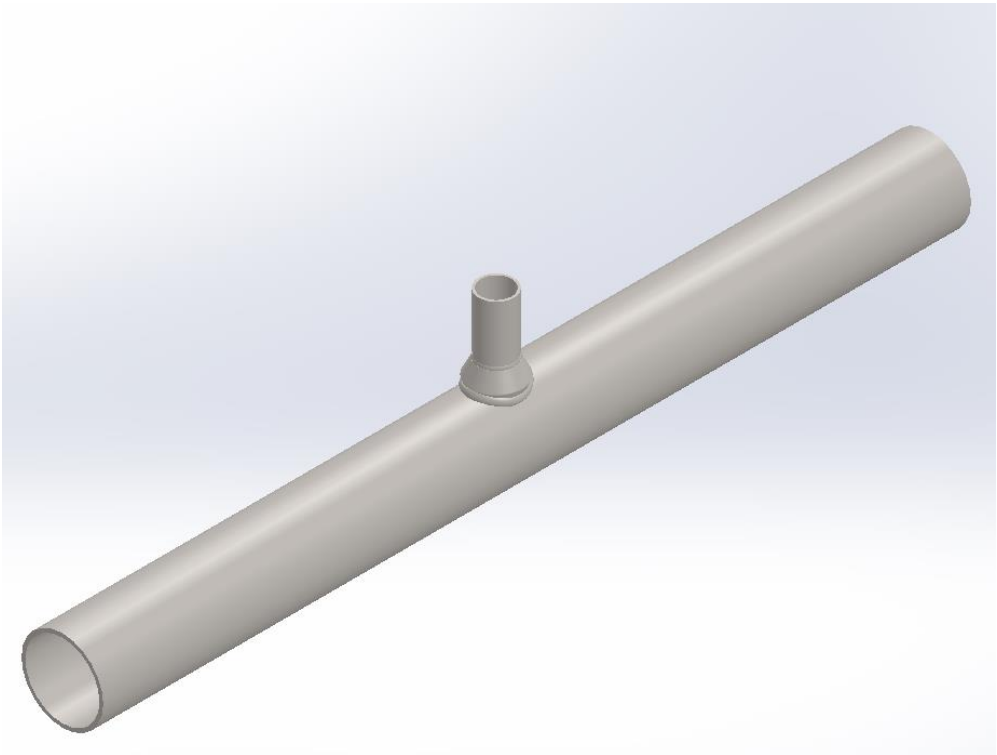

Figure 142. Isometric view of sub-model 2.3

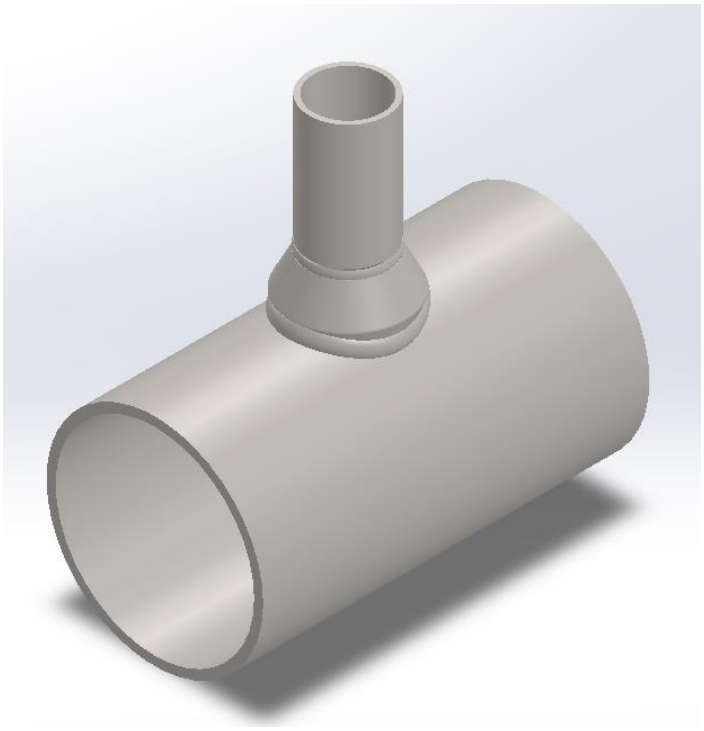

Figure 143. Isometric view of sub-model 1.1

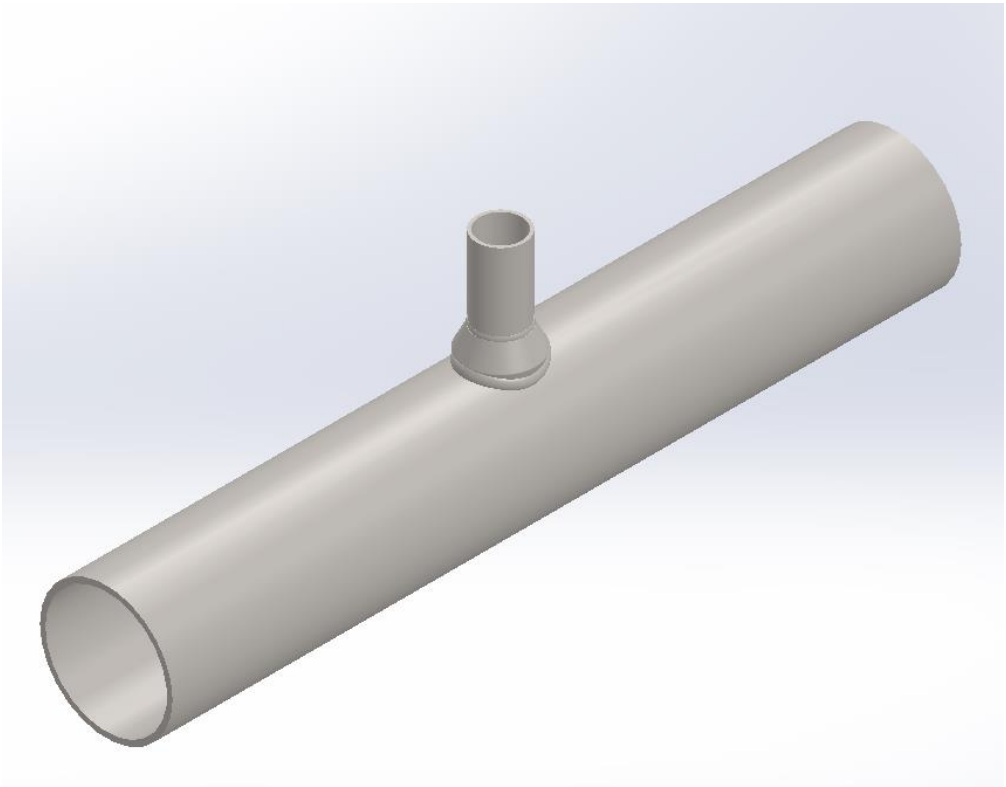

Figure 144. Isometric view of sub-model 1.2

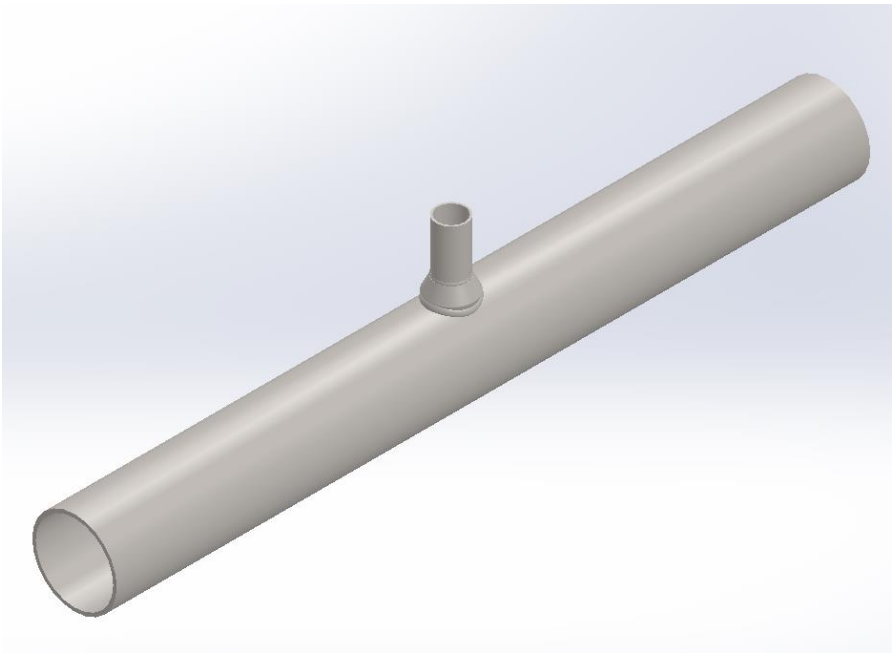

Figure 145. Isometric view of sub-model 1.3

# APPENDIX D: PIPEWORK MANUFACTURING PROCESSES

Steel pipes are long hollow pipes used for various purposes. They are manufactured using two distinct methods that result in either a welded or a seamless pipe. There are three stages in the overall manufacturing process for both methods. In both processes, raw steel is first turned into a more workable shape. Next, the pipe is created on a fabrication line that is continuous or semi-continuous. The pipe is eventually cut and altered to suit customer requirements. In the first half of the 19th century, the advent of rolling mill technology and its growth also kicked off industrial tube and pipe manufacturing [13]. First, rolling sheet strips were formed by funnel arrangements or rolls to form a circular cross-section, and then lap or butt welded at the same temperature (forge welding process). Different processes for seamless tube and pipe production became available by the turn of the century, with manufacturing volumes growing quickly over a relatively short time frame. While additional welding methods were introduced, the continued creation and advancement of seamless techniques resulted in a nearly complete push-out of the welded tube from the market, resulting in a seamless tube and pipe dominating until the Second World War. The results of research into welding technology resulted in an improvement in the fortune of the welded pipe during the subsequent period, resulting in a rise in production and a widespread of various tube welding processes. Currently, nearly two-thirds of the world's steel tubes are welded [13]. However, about a quarter of this number takes the form of so-called large-diameter pipes in sizes other than those economically feasible in the seamless manufacture of the tube and the pipes.

Seamless Tube and Pipe: towards the end of the 19th century, the main seamless production processes of tubes were created. The original various parallel inventions became less distinct with the expiry of patent and proprietary rights and the different

phases of their creation became incorporated into further processes [14]. The state of the art has now advanced to the degree that the following new high-performance processes are preferred:

- With an external diameter range from approximately 21 to 178 mm, the continuous rolling mandrel, and the push bench process Figure 3.
- The Multi Stand Plug-Mill (MPM) is approximately size-free, with a controlled (constricted) floating mandrel bar. External diameter 140 to 406 mm Figure 4.
- The piercing process of the cross roll and pillagers, ranges in the size between about 250 and 660 mm outside diameter.

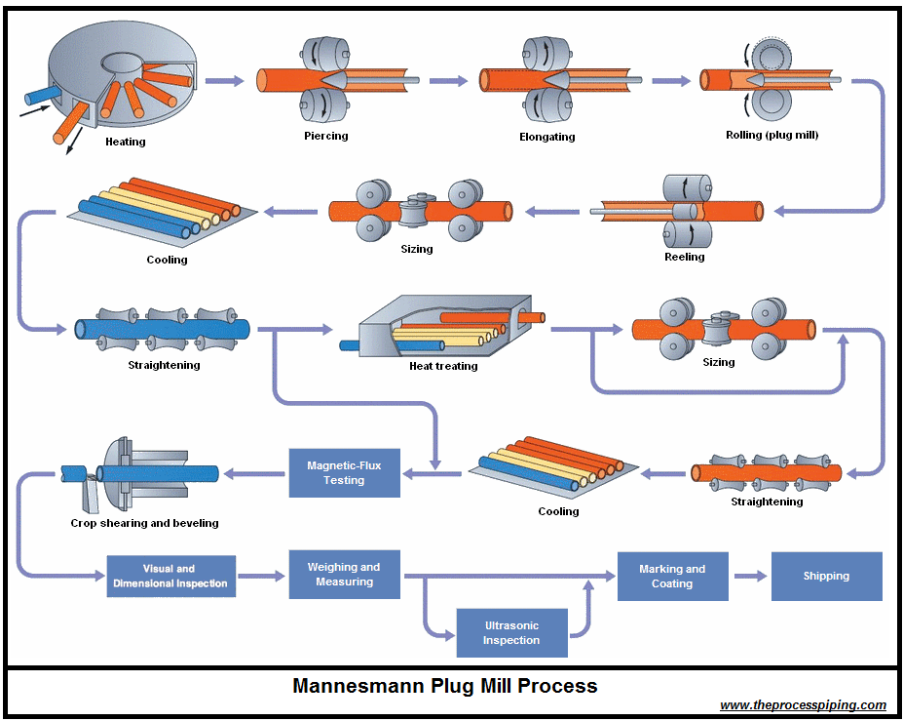


Figure 146. Schematics of Mandrel Mill Process showing the different stages the pipe goes through from heating up to the shipping stage [14].

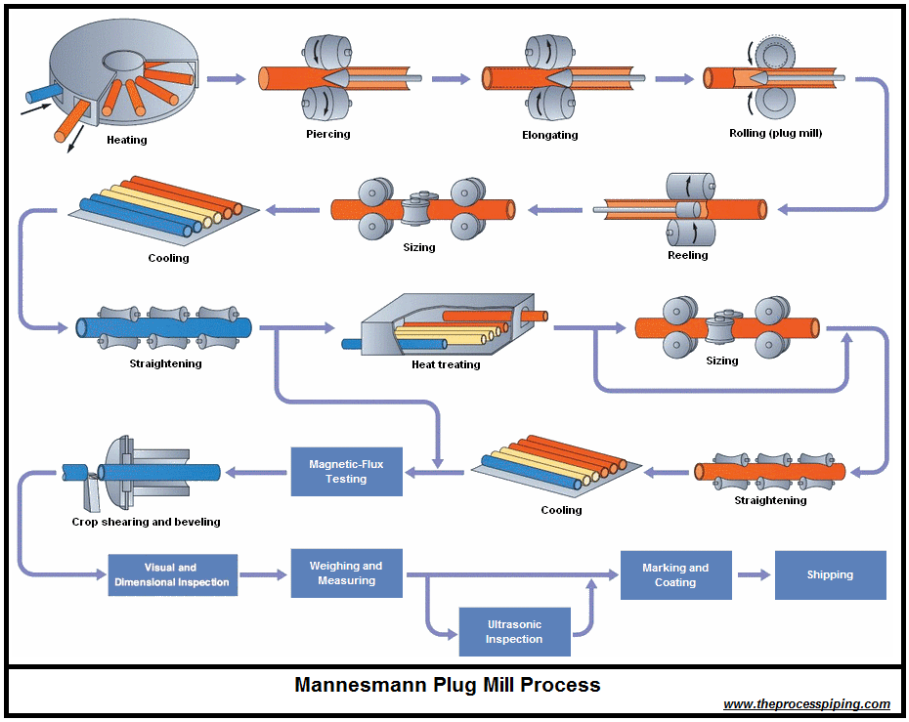


Figure 147. Mannesmann's plug-mill process is somewhat similar to that of Mandrel, with a significant difference in rolling plug-in mounts instead of the Mandrel mill [14].

**Welded Tube and Pipe:** Since the production of strips and plates has been possible, people have always tried to bend the material and to connect it to tubing and pipe production. This led to the development of the oldest process of welding, the forging process, which dates back 150 years. In 1825 a patent was issued for the manufacture of welded pipes to the British ironware dealer James Whitehouse. The process consisted of forging individual sheets of metal across a dip to make an open-seam tube and then heating the edges of the open seam by pressing them mechanically on a drawing bench. The technology has evolved to such an extent that strips can be made and welded in a welding furnace in one pass. This concept of butt-welding coincided with the FretzMoon process, which was conceived by J Moon, and Fretz, in 1931 [15]. The welding lines that use this process still work well today in the production of tubes of approx. 114 mm diameters up to the outside. Apart from this technique of hot-pressure welding, which heats the strip in the furnace at the temperature of the soil, the American E. Thomson has devised several other processes, from 1886 to 1890, which allow the

electric welding process of metals [15]. The basis of this was the property of James P. Joule that causes it to heat up because of its electrical resistance by passing an electric current through a conductor. The following are the various methods involved in welded pipe manufacturing [15].

- Electric Resistance Welding (ERW) Processes: several processes to produce pipes are available with ERW, the two most important ERW types are the High-Frequency Welding process and the Rotary Contact Wheel Welding process.
- Submerged Arc Welding (SAW) Processes: there are two types of (SAW) processes, Spiral Submerged Arc Welding (SSAW) Process and Longitudinal Submerged Arc Welding (LSAW) Process
- Electric Flash Welding Process no longer used as a major process for pipe manufacturing.
- The lap Welding Process is also no longer used as a major process for pipe manufacturing.

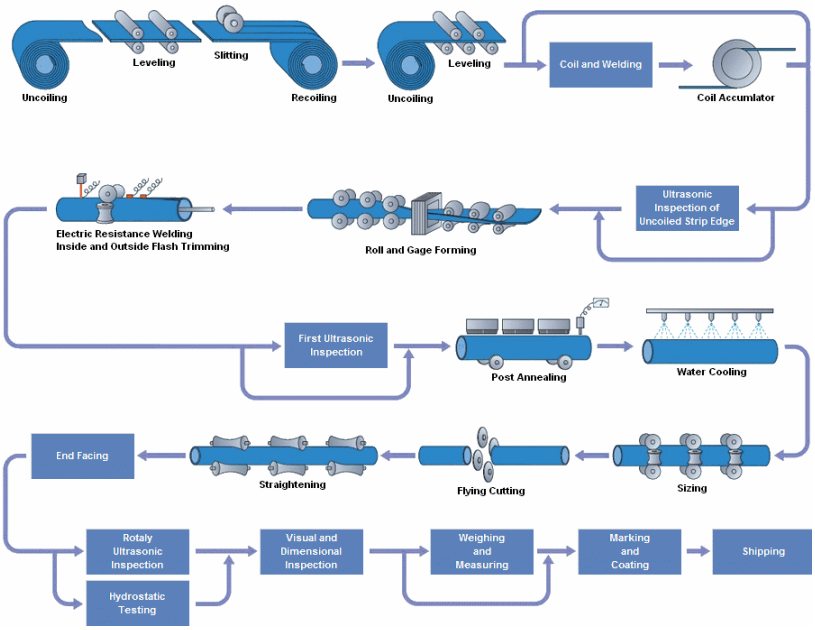


Figure 148. Schematics of the Electric Resistance Welding (ERW) process showing the different stages the pipe goes through [13].